Marine and Petroleum Geology
October 2022, Volume 144, Pages 105820 (30p.)
https://doi.org/10.1016/j.marpetgeo.2022.105820
https://archimer.ifremer.fr/doc/00786/89758/

Crustal structures and salt tectonics on the margins of the western Algerian Basin

Soto Juan I. [1, 2, *], Déverchère Jacques [3], Hudec Michael R. [1], Medaouri Mourad [4], Badji Rabia [4], Gaullier Virginie [5], Leffondré Pierre [3]

[1] Bureau of Economic Geology, Jackson School of Geosciences, The University of Texas at Austin, University Station, Box X, Austin, TX, 78713-8924, USA
[2] On Leave of Absence from, Departamento de Geodinámica, Universidad de Granada, Avenida de Fuente Nueva S/n, 18071, Granada, Spain
[3] Univ Brest, CNRS, Ifremer, Geo-Ocean, F-29280 Plouzane, France
[4] SONATRACH - Division Exploration, Boumerdes, Algeria
[5] Univ Lille, Univ Littoral Côte D'Opale, UMR 8187, LOG, Laboratoire D'Océanologie et de Géosciences, F-59000 Lille, France

* Corresponding author : Juan I. Soto, email address : juan.soto@beg.utexas.edu

jacdev@univ-brest.fr ; michael.hudec@beg.utexas.edu ; mourad.medaouri@sonatrach.dz ; rabia.badji@sonatrach.dz ; virginie.gaullier@univ-lille.fr ; pierre.leffondre@protonmail.com

Abstract :

We present an overview of the crustal architecture of the continental margins of the oceanic Algerian Basin in the westernmost Mediterranean Sea. During the Cenozoic, and with a variable oblique convergence between the African and Eurasian plates during the Cenozoic, the Western Mediterranean Sea has experienced thinning and extension behind a tight orogenic arc formed by the Betics, Rif, and Tell Cordilleras. This study is focused on the structural style affecting the Messinian salt layer, which is mostly restricted to the deep domains of the Algerian Basin, where it is floored by a thin oceanic crust of probable Miocene age.

Using deep-penetrating seismic profiles and wells from offshore western Algeria to southeastern Spain, we have analyzed the crustal structures affecting the domains close to the oceanic-continent transition on the three margins of the western Algerian Basin. Since the Early Miocene, active shortening in the Tell-Atlas domain has accommodated most of the plate convergence in the basin, whereas the Alboran margin in the west and the Iberian margin in the north experienced eastward and southward crustal extension and thinning, respectively, accompanied by volcanism. The Algerian margin in the south shows incipient thrusting of African continental crust over oceanic crust. This shortening occurred since at least the Late Miocene, also promoting decoupling and contraction of the deep, sub-horizontal Messinian salt layer. The salt exhibits diapir squeezing and suprasalt folding, whereas the presalt sequence preserves partially-inverted half-grabens. Salt tectonic processes along the northern and western margins of the Western Mediterranean Basin show contrasting structural styles formed by narrow extensional and transtensional domains with gentle salt anticlines.

This region shows therefore a somewhat unusual salt-tectonic style, departing from the gravity-driven model typical of continental margins that contain an initial continuous, gently-dipping salt layer. In the Algerian Basin, salt is mostly restricted to deep water domain floored by oceanic crust, so it does not participate in significant gravity-driven deformation. Instead, Messinian salt and the suprasalt sequences underwent significant shortening along the southern margin, simultaneous with thick-skinned extension involving the Messinian evaporites in the northern and eastern margins.

Graphical abstract

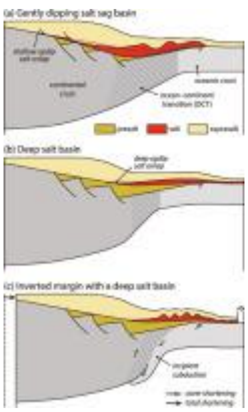

Highlights

► Crustal structure of the W Algerian Basin is reviewed by the first time. ► Seismic interpretation to unravel the crustal structures of the basin and margins. ► How the Messinian salt layer is deformed in the oceanic floor of the basin. ► How the deformation occurring in the margins affected the deep–seated salt layer. ► Restoration to evaluate timing, magnitude, and rate of post-6 Ma deformations.

Keywords : Salt margins, salt folded belts, thick-skinned deformation, crustal extension, tectonic inversion, Messinian, Western Mediterranean, Algerian Basin

1. Introduction

Our study is focused on reviewing the overall structure of the oceanic Algerian (or South Balearic) Basin in the westernmost Mediterranean Sea to provide, for the first time, a comprehensive review of the crustal structure of the basin and its continental margins (Fig. 1). To simplify the terminology for the three margins of the Algerian Basin, we use Algerian margin, Alboran margin, and Iberian margin when referring to the southern, western, and northern margins, respectively. The first two terms refer to the so-called North Algerian (or Algeria) margin and the western transition from the East Alboran Sea to the Algerian Basin.

For some of the basin margins, the overall crustal structure, the main crustal characteristics, and principal stages of the Neogene evolution are very well established. For example, numerous studies document the crustal configuration of the long Algerian margin (reviews by Strzerzynski et al. [2010], Leffondré et al. [2021], and Klingelhoefer et al. [2022]), and many authors have inspected the geophysical characteristics of the continent–ocean transition in the Alboran margin (Comas et al., 1997; Booth-Rea et al., 2007, 2018; Medaouri et al., 2014; Gómez de la Peña et al., 2018, 2020, 2021). In contrast, understanding of the crustal architecture, tectonic structures, and recent evolution in the Iberian margin is poorly established. There are some regional sections (Driussi et al., 2015b; Kumar et al., 2021) and local studies of recent processes affecting the sea-floor and the most recent sediments (Acosta et al., 2001; Lastras et al., 2004, 2006; Camerlenghi et al., 2009). Nevertheless, it remains unknown which structures mainly affect the different segments of the Iberian margin, and some researchers even debate the margins' kinematics. Most authors suggest strike-slip motion (mostly due to right-lateral faulting) for the structures affecting the studied sector of this margin (Mauffret et al., 1992; Camerlenghi et al., 2009; Maillard and Mauffret, 2013; Driussi et al., 2015a; Kumar et al., 2021).

We have conducted the first complete regional synthesis of the western Algerian Basin and its margins by interpreting multi-channel seismic profiles from both industrial and academic sources. Seismic interpretation is based in a revision of the stratigraphic information provided by all the available wells in the region, coming from both African and Iberian offshore areas (Fig. 1). The interpretation of the structural styles and our inferences about the magnitude and timing of the Neogene (mostly Upper Miocene to recent) deformation are integrated into the tectonic scenario of the region, which has also been summarized through review of previous publications in the area.

Our tectonic analysis of the crustal configuration and structure of the western Algerian Basin and its margins also studies how the Messinian evaporites are deformed in the region, a topic that has received little attention to date (e.g., Bellucci et al., 2021). The seismic data we use vary in quality, because we have used vintage commercial seismic reflection profiles on the Iberian margin, a single section on the Alboran margin, and a complete set of commercial and scientific lines on the Algerian margin. Due to this data-quality issue, our study of salt structures, together with the presalt and suprasalt sequences, is necessarily incomplete and of variable precision. In the Algerian margin, for example, we could complete a structural restoration of a selected seismic interpretation. However, our approach to the salt tectonic processes affecting the Alboran and Iberian margins is preliminary and will require future re-evaluation pending on the availability of better and more modern seismic datasets.

The position, geometry, and nature of the Messinian salt layer in the Algerian Basin has been known for many years (e.g., Biju-Duval et al., 1978; Lofi et al., 2018). Nevertheless, researchers debate how evaporite precipitation in the deep basin was connected to the sedimentary systems operating in the surrounding continental platforms during the Messinian Salinity Crisis (MSC) and whether evaporites were also deposited along the costal and continental regions (e.g., Meijer and Krijgsman, 2005; Bache et al., 2009; Garcia-Castellanos et al., 2009; Raad et al., 2021). The Messinian salt was deposited throughout the Mediterranean Basin due to a gradual restriction of water exchange with the Atlantic Ocean in Late Miocene time, and due to a generalized sea level drop and a basin-wide desiccation, according to several authors. Together, these factors led to extreme paleoenvironmental changes during the climax of the MSC (5.97–5.33 Ma) (see reviews by Lofi et al. [2011], Bache et al. [2012], Flecker et al. [2015], Lofi [2018], and Andreetto et al. [2021]). The isolation of the overall Mediterranean Basin during the short MSC (~660 kyr) made possible the deposition of the Messinian salt in the deepwater domains of the basin (e.g., Haq et al., 2020).

Key questions addressed in this contribution include: What is the overall structural configuration of the Algerian Basin and its margins? What is the role played by Neogene crustal thinning and extension versus igneous intrusions and volcanism on the Alboran margin? What is the main structural style of the Iberian margin? Is the Iberian margin affected by strike-slip faulting or by normal faulting? What is the role played by the Messinian salt during the most recent evolution of the basin? What is the magnitude and timing of salt-detached deformation, compared to the presalt? And finally, can we use modern concepts of salt tectonics to unravel these processes and provide a complete view of the western Algerian Basin and its margins?

2. A review of the tectonic setting of the Western Mediterranean

The Algerian Basin and its margins are part of the Gibraltar Arc System (Figs. 1, 2). The Gibraltar Arc System is a tight, Alpine orogenic loop in the westernmost Mediterranean, formed by the mountain belts of the Betic in southern Spain, the Rif in northern Morocco, and the continuation towards the east along the Tell in northern Algeria (Fig. 3) (e.g., Biju-Duval et al., 1978; Bouillin et al., 1986; Comas et al., 1999; Frizon de Lamotte et al., 2000; Chalouan et al., 2008; Leprêtre et al., 2018; Jolivet et al., 2015, 2021a; Haidar et al., 2022). This system embraces the Alboran Basin, which is floored by stretched continental crust, and the oceanic Algerian Basin further to the east. The Alboran Basin constitutes a Mediterranean back-arc-type basin formed by extensional collapse of the Gibraltar Arc (e.g., Dewey et al., 1989; García-Dueñas et al., 1992; Vissers et al., 1995; Platt et al., 1998, 2013). There is a general consensus that the Neogene orogenic processes shaping both the mountain regions and the offshore basins of the Gibraltar Arc System are as follows:

1. Peripheral thrusting imbricating the former South-Iberian and Maghrebian passive margins over the Iberian and African (Hercynian) forelands, respectively (Figs. 3, 4).
2. Westward migration, imbrication, and exhumation of diverse metamorphic continental terranes forming the Alboran Domain or Internal Zones, which extend from the Internal Betics and Rif to the Kabylies in northern Algeria.
3. Thrust-sheet imbrication within the Alboran Domain, forming a progressively tighter orogenic arc as it migrates westward.
4. Simultaneous collapse of the Alboran Domain flooring the thick depocenter of the West Alboran Basin (e.g., Fig. 4).
5. Extreme crustal stretching accompanied by abundant calc-alkaline and tholeiitic (14–6 Ma) to intraplate-type alkali (6.0–0.8 Ma) volcanism flooring the East Alboran Basin (Fig. 3) (e.g., see review by Soto et al., 2008).
6. Oceanic spreading, possibly during the Lower–Middle Miocene, forming the Algerian Basin, well behind the Gibraltar Arc System.

The Algerian Basin is a large, deepwater abyssal plain with a constant depth of about 2600 m (Fig. 1), which is floored by thin (avg. ~5 km) oceanic crust (Hinz, 1973; Gallart et al., 1997;

Sàbat et al., 1997; Driussi et al., 2015b; Kumar et al., 2021). The age of this crust is debatable, assigned to the Oligocene to Lower Miocene (Biju-Duval et al., 1978; Mauffret et al., 1992; Haidar et al., 2022) or Middle Miocene (Rehault et al., 1984; Gueguen et al., 1998; Carminati et al., 2012; Driussi et al., 2015a, 2015b; dal Cin et al., 2016). Nevertheless, all these authors agree that the oceanic crust was completely accreted in the Tortonian time. This crust was formed by very-rapid oceanic accretion (~ 5 $cm \times yr^{-1}$) (Mauffret et al., 2004; Jolivet et al., 2021a; Haidar et al., 2022; Klingelhoefer et al., 2022). The gravity anomaly map in this basin also shows a rather constant value, close to zero, which tends to decrease slightly (-10 to -20 mGal) towards the northern and eastern limits of the oceanic crust (Fig. 2). Conversely, the Algerian margin, with a steep slope and abrupt continental rise, coincides with a west-east elongated domain with negative gravity values (~ -100 to -120 mGal; Fig. 2) (Auzende et al., 1975; Mauffret et al., 2004; Mauffret, 2007; Badji, 2014; Hamai et al., 2015; Leffondré et al., 2021; Klingelhoefer et al., 2022).

In contrast to the eastern Algerian Basin (Bayer et al., 1973; Galdeano and Rossignol, 1977; Schettino and Turco, 2006; Driussi et al., 2015b; Haidar et al., 2022), the available magnetic anomaly data for the western Algerian Basin do not depict a clear pattern of linear features that can be associated with oceanic crust formed along linear segments of oceanic ridges (~ -100 to -120 mGal). Conversely, the reduced-to-pole magnetic data displays irregular patches, with contrasting magnetic anomalies in the oceanic crust, which can be interpreted as scattered volcanic edifices associated with oceanic spreading centers or as post-accretion magmatism related to deep, partial melting of a metasomatized mantle (Medaouri, 2014; Medaouri et al., 2014; Aïdi et al., 2018; Klingelhoefer et al., 2022).

(insert here Fig. 1)

Fig. 1. *Topography of the Western Mediterranean region in the area between south Iberia and northern Africa, including the connection through the Strait of Gibraltar with the Atlantic Ocean in the Gulf of Cádiz. In the Western Mediterranean, the Algerian Basin in particular is bounded by the narrow and steep Algerian margin, the Alboran margin (in the transition to the East Alboran Basin), and the Iberian margin. The Iberian margin in particular contains different segments with varied orientations, like the concave and narrow margin that connects the Almería margin with the west-east oriented Mazarrón Escarpment, and the continuation towards the east along the southern slope of the islands of Ibiza and Mallorca. Elevation data merge information from the General Bathymetric Chart of the Oceans–Bathymetric Compilation Group 2019 (GEBCO, 2019) for the offshore regions with the Global Bathymetry and Topography at 15 ArcSec (SRTM15+, v. 12.1) for the onshore areas (Tozer et al., 2019). Image created using a grid spacing of 1 km and a light source oriented 135°/60° (azimuth and elevation, respectively). Bathymetry contours are every 500 m, and undersea names are according to GEBCO (2019). Seismic lines (gray lines) used in this study come from the ATH database (ATH, 2020) for Spain and from various sources for the Algerian margin (Badji, 2014; Medaouri, 2014; Medaouri et al., 2014; Badji et al., 2015; Klingelhoefer et al., 2022). Thick black lines mark the position of the different figures and the*

interpreted seismic lines shown in Figs. 8–17. Studied wells (Fig. 6) are located in the Alboran margin, the Iberian margin, and the Algerian margin. Inset shows the location of the study area (red rectangle) in the Mediterranean region.

(insert here Fig. 2)

Fig. 2. *Gravity anomaly map of the same area depicted in Fig. 1. Gravity anomaly from satellite altimetry is taken from Sandwell et al. (2013, 2014) (v. 28.1). Image created using a grid spacing of 1 km and a light source oriented 135°/70° (azimuth and elevation, respectively). Main tectonic contacts are taken from Fig. 3. Thick black lines mark the positions of the different figures and the interpreted seismic lines shown in Figs. 8–17. Undersea names and wells are as in Fig. 1. Inset shows the location of the study area (red rectangle) in the Mediterranean region.*

2.1 Crustal structure of the Algerian Basin margins

The Algerian Basin in our study area has three margins with different orientations and different crustal structures (Figs. 1–3). Hereafter, we will use these names to refer to the three margins: (1) the Algerian margin, which is the southern margin of the basin, has a linear trend and a general west-southwest orientation, which has a narrow continental platform (<15 km) and steep slope connecting with the oceanic plain; (2) the Alboran margin, which is the western margin, contains abundant outcropping volcanic edifices; and (3) the Iberian margin, which is the northern part of the basin, is also formed by a series of segments with contrasting orientations, physiography, and (probably) crustal configuration.

2.1.1 Algerian margin

In comparison with the other margins, the Algerian margin is very-well studied, and numerous works document its characteristics such as seafloor features and the general structure of its sedimentary cover (Déverchère et al., 2005; Domzig et al., 2006, 2009; Mauffret, 2007; Strzerzynski et al., 2010; 2021; Medaouri et al., 2012, 2014; Medaouri, 2014; Arab et al., 2016; Leffondré et al., 2021; Haidar et al., 2022), the crustal structure (Leprêtre et al., 2013; Badji, 2014; Badji et al., 2015; Bouyahiaoui et al., 2015; Aïdi et al., 2018; Klingelhoefer et al., 2022), and the recent tectonic processes that explain the distribution and nature of the earthquake activity (Aoudia et al., 2000; Yelles-Chaouche et al., 2006; Kherroubi et al., 2009, 2017; Soumaya et al., 2018; Ousadou and Bezzeghoud, 2019).

For the purposes of this work, the following are the main characteristics of this margin that are especially relevant for our study:

1. The physiography of the basin floor of the Algerian Basin in the vicinity of the continental rise documents the existence of subcropping, elongated (west-southwest–east-northeast and west-east) salt diapirs that deform the seafloor (Fig. 3) (e.g., Domzig et al., 2006; Mauffret, 2007; Obone-Zue-Obame, 2009; Badji et al., 2015; Leffondré et al., 2021).
2. The sedimentary cover of this margin, particularly in the domain of the abyssal plain, contains diapirs involving the Messinian salt, although their three-dimensional geometry and the tectonic processes shaping these structures is still poorly understood (e.g., Bellucci et al., 2021).
3. The age of the sedimentary cover is mostly Messinian to recent, although older Miocene (and possibly Oligocene) sediments have been locally reported in the margin, filling depocenters with an unclear geometry and a debatable timing for their associated rifting events (e.g., Medaouri et al., 2014; Arab et al., 2016; Haidar et al., 2022).
4. The pre-Messinian sequence thickens progressively from the abyssal plain towards the continental rise (e.g., Bellucci et al., 2021; Leffondré et al., 2021).
5. The abyssal plain is floored by oceanic crust that was probably formed during the Miocene (certainly before the Tortonian) (e.g., Mauffret et al., 1992, 2004; Haidar et al., 2022).
6. The crustal structure of the margin contains a narrow, and possibly steep boundary between the continental and oceanic crusts, with an abrupt crustal thinning (within ~80 km) from ~28 to 8 km (Leprêtre et al., 2013; Badji, 2014; Badji et al., 2015; Bouyahiaoui et al., 2015; Klingelhoefer et al., 2022).

(insert here Fig. 3)

Fig. 3. *Tectonic map of the Gibraltar Arc orogen in the Western Mediterranean Sea and the transition to the oceanic domains of the Algerian Basin in the east and the accretionary wedge of the Gulf of Cádiz in the west. Numerous sources are compiled in this map, which is based on the synthesis of Comas et al. (1999), Fernández-Ibañez and Soto (2017), and Flinch and Soto (2017). The map includes results from this study and additional sources of information for the Algerian margin (Domzig et al., 2006, 2009; Medaouri et al., 2014; Leffondré et al., 2021), the Iberian margin, from Almería to Ibiza (Comas et al., 2000, 2006a, 2006b; Woodside et al., 2000; Giaconia et al., 2015), the Alboran Sea (Mazzini et al., 2003; Martínez-García et al., 2011, 2013; Martínez-García, 2012), the Tell (Domzig et al., 2006, 2009; Yelles-Chaouche et al., 2006; Ansberque, 2011; Leprêtre et al., 2018), the Rif (Flinch, 1993, 1996; Chalouan et al., 2008), the Betics (Rodríguez Fernández et al., 2015), and the Gulf of Cádiz (Flinch, 1993; Medialdea et al., 2004, 2009; Zitellini et al., 2009). Mud volcanoes and shale diapirs, together with sub-outcropping salt diapirs (involving the Triassic or the Messinian evaporites) in the offshore areas, are taken from various*

authors (Comas et al., 2003; Sautkin et al., 2003; Somoza et al., 2003, 2012; Talukder et al., 2003; Van Rensbergen et al., 2005; Domzig et al., 2006; Fernández-Puga et al., 2007; Medialdea et al., 2009; Soto et al., 2010, 2012). For the sake of clarity, the Flyschs units in the Tell region include the Tello Nappes (e.g., Leffondré et al., 2021). Approximate distribution of the compressional folded belt in the Algerian Basin is marked with a stippled pattern. Thick black lines mark the position of the different figures and the interpreted seismic lines shown in Figs. 8–17. Undersea names and wells are as in Fig. 1. Abbreviations: AP= Alicante Platform; AR= Alboran Ridge; DP= Djibouti Plateau; EAB= East Alboran Basin; EBE= Émile Baudot Escarpment; IC= Ibiza (Eivissa) Channel; MC= Mallorca Channel; ME= Mazarrón Escarpment; PF= Palomares fault system; WAB= West Alboran Basin; YF= Yusuf fault system.

Several other well-established observations have been made concerning the crust beneath the Algerian Basin. First, the basin has a rather standard and homogenous oceanic crust that is anomalously thin (~5.5 km). According to tomographic inversion models, this oceanic crust has an upper layer with sediments grading downwards to basalts (V_p varies progressively from 4.8 to 6.0 km×s^{-1}) and a lower oceanic layer that is most probably formed of gabbroic rocks rather than by components of serpentinized mantle (V_p increases from 6.1 to 7.2 km×s^{-1}) (e.g., Badji et al., 2015; Bouyahiaoui et al., 2015; Klingelhoefer et al. 2022). Second, the boundary between the oceanic and continental crusts is one of the singularities of this margin, because it is always accompanied by a narrow transition (~5.5 km wide) between them. The wide-angle refraction profiles in this domain, together with tomographic inversion data, show that the crust in the narrow ocean–continent transition (OCT) has sonic velocities intermediate between those of the bounding oceanic and continental crusts. In particular, the OCT has a strong velocity gradient in the upper crust and the deep crust has velocities similar to the lower continental crust (Leprêtre et al., 2013; Badji, 2014; Badji et al., 2015; Bouyahiaoui et al., 2015; Klingelhoefer et al., 2022). Some segments of the Algerian margin even document the existence of a small domain with a relatively thicker oceanic crust (Moho at 12-13 km depth), showing a local thickening of the lower layer of the oceanic crust (e.g., Bouyahiaoui et al., 2015). The narrow ocean-continent boundary has been interpreted as a result of two processes: the occurrence of a general transcurrent plate boundary along this margin (a subduction transform edge propagation–fault [STEP-fault] margin) (Badji, 2014; Medaouri, 2014; Medaouri et al., 2014; Badji et al., 2015; van Hinsbergen et al., 2014; Spakman et al., 2018; Jolivet et al., 2021a, 2021b; Leffondré et al., 2021) and the occurrence of a moderate underthrusting of the Algerian oceanic crust beneath the continental African plate (Auzende et al., 1975; Déverchère et al., 2005; Mauffret, 2007; Leprêtre et al., 2013; Badji et al., 2015; Hamai et al., 2015, 2018; Leffondré et al., 2021).

2.1.2 Alboran margin

The transition of the Algerian Basin to the East Alboran Basin on the Alboran margin coincides with a broad, north–south-trending domain of a thin continental crust (14–10 km thick) with abundant Neogene calc-alkaline and tholeiitic volcanism with isotopic ages ranging from the Serravallian to the Messinian (12–6 Ma), which evolves to intraplate-type alkali basalts of latest Messinian–to–early Pliocene age (6.0–0.8 Ma) (see reviews of Savelli [2002], Duggen et al. [2003, 2004], and Soto et al. [2008]). The abundance of volcanism together with the geophysical properties of this crust, such as high heat flow (Polyak et al., 1996; Poort et al., 2020), high Vp velocities (typically >6.0 and sometimes ranging between 7.1 and 7.3 km×s^{-1}) (Booth-Rea et al., 2007, 2018), and relatively low densities (2,820–2,840 kg×m^{-3}) (Soto et al., 2008), have been used to postulate that the East Alboran Basin is floored by a highly stretched continental crust (Hatzfeld et al., 1978; Comas et al., 1997; Medaouri et al., 2014) or even with a volcanic arc-type continental crust (Booth-Rea et al., 2007, 2018; Gómez de la Peña et al., 2018, 2020, 2021). According to the half-graben geometries identified in the Neogene sedimentary cover (typically <2 km thick, in places <1 km thick) above this crustal domain, workers have suggested that west-east crustal stretching was active there during the Miocene (possibly during the Middle Miocene) (Mauffret et al., 1992; Medaouri et al., 2014). Nevertheless, the magnitude of extension, three-dimensional geometry of the extensional faults, and the exact timing of the rifting and crustal stretching are still not well established.

In addition to the rifting structures, two important crustal-scale (> 180 km long) strike-slip fault systems deform the East Alboran Basin (Fig. 3). One of these systems is the transtensional, right-lateral Yusuf fault, which trends west-northwest and connects two compressional domains, the Alboran Ridge towards the west (Fig. 4) and the Algerian margin towards the southeast (Mauffret et al., 1992; Fernández-Ibáñez et al., 2007; Medaouri et al., 2012; Martínez-García et al., 2013). The other fault system is the Carboneras fault system, which is formed by various transpressional, left-lateral fault segments. These segments trend southwest–northeast and extend from the Djibouti Plateau to the onshore volcanic province of Cabo de Gata (e.g., Gràcia et al., 2006, 2012) to finally connect eastward with the north–south, left-lateral Palomares fault. This latter fault runs subparallel to the coastline, shaping a north–south continental margin in the eastern Betics (Comas et al., 2006a, 2006b; Giaconia et al., 2015). These two crustal-scale strike-slip faults probably have been active since the Middle and Upper Miocene, and according to seismicity, faulting along them continues up to the present (e.g., Mauffret et al., 1992; Fernández-Ibáñez et al., 2007; Medaouri et al., 2012; Gómez de la Peña et al., 2018; Spakman et al., 2018).

(insert here Fig. 4)

Fig. 4. *Cross section from the western Betics and the West and South Alboran Basins to the African foreland (modified from Flinch and Soto, 2017). Crustal thickness is according to Torne et al. (2000) and Soto et al. (2008). Structures in the offshore region are from various sources (Soto et al., 2010; Martínez-García, 2012; Fernández-Ibáñez and Soto, 2017). Location of the section is shown in Figs. 1–3.*

2.1.3 Iberian margin

The Iberian margin is composed of several segments with varied orientations and possibly with different tectonic styles, and contains the eastern continuation of the Betic Cordillera (Fig. 3). From west to east in the study area, this margin is formed by three segments: (1) a narrow north–south segment that includes the Palomares fault system, which we mentioned previously; (2) the steep west–east segment identified along the Mazarrón Escarpment; and (3) the gently dipping continental talus developed south of the Balearic Islands of Ibiza and Mallorca, which contains the southwest–northeast-trending Émile Baudot Escarpment.

The Palomares segment has a very narrow continental platform (<10 km in width) and a steep continental slope that is incised by deep, west–east canyons and some elongated volcanic highs (e.g., the Abubacer and Maimonides Highs; Fig. 1) that are accompanied by local positive gravity anomalies (Fig. 2). The few studies of this margin document the existence of very recent (Pliocene) and seismically active, high-angle, left-lateral strike-slip faults. These faults are similar in orientation, kinematics, and timing to the onshore segment of the Palomares fault system (Fig. 3) (Mauffret et al., 1992; Comas et al., 2000, 2006a, 2006b; Gómez de la Peña et al., 2018). Some studies also document the existence of a moderate compressional deformation associated with the strike-slip faults, developing southwest–northeast volcanic highs and anticlines (e.g., Abubacer High) that affect the thin Pliocene-to-Quaternary cover of this margin (Giaconia et al., 2015). The overall structure of the Palomares segment is interpreted to correspond to a north–south narrow continental margin with active, left-lateral transpressional strike-slip faulting (Comas et al., 2000, 2006b; Fernández-Ibáñez et al., 2007; Giaconia et al., 2015).

The Palomares segment changes abruptly to a narrow, west-trending slope that corresponds to the Mazarrón Escarpment. This segment of the margin is relatively unexplored, and the few studies there reflect the occurrence of massive submarine slides activated by steep, west-trending normal faults (Fig. 3) (Mauffret et al., 1992; Comas et al., 2000; Woodside et al., 2000; Maillard and Mauffret, 2013). The segment also includes an isolated volcanic edifice known as the Águilas Seamount (Fernández Soler et al., 2000), limited by a northwest-trending, high-angle normal fault (the Tiñosa fault), which does not have a significant associated gravity anomaly (Figs. 1–3). The Mazarrón Escarpment constitutes the continental slope of a larger continental platform, which extends southeast and east of Murcia and Alicante. Sufficient geophysical information (seismic profiles and wells) is available to confirm that the Alboran Domain of the eastern Betics continues offshore beneath this continental platform (Fig. 3) (Comas et al., 2000, 2006b; Fernández Soler et al., 2000; Alfaro et al., 2002; Roca et al., 2004; Maillard and Mauffret, 2013; Driussi et al., 2015a, 2015b; Kumar et al., 2021). The height of the Mazarrón Escarpment diminishes eastward, vanishing in an area where we interpret the presence of an embayment of the oceanic crust (at ~lat 37.5°N, long 0.5°E). This embayment forms a northward continuation of the abyssal plain of the Algerian Basin, which connects with the next segment of the margin, which is marked by the Émile Baudot Escarpment.

The easternmost domain of the Iberian margin in the study area contains two continental platforms around the Ibiza and Mallorca islands and exhibits a common gentle continental slope featuring a rugose seafloor with abundant slide scars (Acosta et al., 2001; Lastras et al., 2004, 2006; Camerlenghi et al., 2009) and some isolated volcanic highs near the continental rise (e.g., the Prunes Seamount; Figs. 1, 2). The trend of this segment of the margin is approximately west–east up to the Prunes Seamount, changing progressively to be southwesterly along the Émile Baudot Escarpment. Multiple researchers suggest that the External and Internal domains of the eastern Betics continue eastward, maintaining a west-southwest trend (Sàbat et al., 1997; Alfaro et al., 2002; Lastras et al., 2004; Maillard and Mauffret, 2013; Maillard et al., 2014). The continent–ocean transition (OCT) occurs along a narrow crustal boundary (Sàbat et al., 1997; Roca et al., 2004; Driussi et al., 2015b) that has been interpreted as a transcurrent margin, associated with right-lateral strike-slip faulting (Mauffret et al., 1992, 2004; Camerlenghi et al., 2009; Dal Cin et al., 2016; Jolivet et al., 2021b) that is accompanied by recent volcanic intrusions (Acosta et al., 2001; Maillard and Mauffret, 2013).

Our interpretation of the limit of the oceanic crust in the Algerian Basin is included in Figs. 2 and 3. Three types of observations have been used to map this limit: (1) our interpretation of the crustal structure according to seismic profiles; (2) the fact that most of the diapiric structures affecting a thick Messinian salt layer occur above the oceanic crust (e.g., Biju-Duval et al., 1978; Mauffret et al., 1992, 2004; Comas et al., 1997, 2000, 2006a, 2006b; Camerlenghi et al., 2009; Maillard et al., 2014; Dal Cin et al., 2016; Pellen et al., 2016; Haq et al., 2020; Bellucci et al., 2021), although some authors suggest that salt pinches out above the deeper parts of the adjacent thinned continental crust (Driussi et al., 2015b); and (3) the distribution and magnitude of the gravity anomalies. The northern limit of oceanic crust coincides clearly with a domain where the polarity of the gravity anomaly changes, being positive in the continental domain and moderately negative or zero in the oceanic domain (also in Driussi et al. [2015b]). In contrast, the southern limit of the continental crust, along the Algerian margin, is marked by a narrow negative anomaly (~50–70 mGal) that runs parallel to the continental rise. The origin of this anomaly has been interpreted as the combination of two processes: a larger sedimentary thickness of the pre-Messinian sediments (i.e., a static contribution to the gravity field) and the effects of the incipient subduction of oceanic crust below the overriding continental crust of the African plate (i.e., a dynamic contribution due to flexure of the subducting oceanic crust) (e.g., Leprêtre et al., 2013; Bouyahiaoui et al., 2015; Hamai et al., 2015).

2.2 Plate-tectonic scenario

Numerous authors have reconstructed the relative motions of the bounding plates in the Western Mediterranean Sea. All these studies document that, with respect to a fixed position of the Eurasian plate, the Africa (Nubia) plate migrated towards the east and southeast starting in the Middle Jurassic, changed direction to move towards the east-northeast (~85–80 Ma) and finally towards the north in the Upper Cretaceous (since the Maastrichtian, at 70 Ma). This relative drift of Africa is illustrated in Fig. 5 using the plate reconstruction model of Rosenbaum et al. (2002). To reconstruct the positions of Africa with respect to Eurasia (Fig. 5c) and compute the trajectories of two singular points of the study area (Figs. 5a, 5b), we have used the dataset of these authors and the standard method to reconstruct plate trajectories in a sphere described by many authors (e.g., Le Pichon et al., 1973).

To illustrate the implications of plate motions in the area of interest, we have computed the trajectories followed since 165 Ma (Callovian) of two representative points (Fig. 5c): one is selected to show the motion of the Algerian margin (presently situated at lat 35°N, long 1.5°E), and the other is representative of the final position of the western Betics, particularly the West Alboran Sea (currently situated at lat 36°N, long 4°W). Importantly, the trajectory of the latter point does not reflect orogenic processes like the large allochthonous westward migration of the Alboran Domain nor its Neogene collapse.

(insert here Fig. 5)

Fig. 5. *Relative motion of the African plate with respect to a fixed Eurasia plate, using the plate-tectonic reconstruction of Rosenbaum et al. (2002).* ***(a)*** *Plot with the orientation of the convergence azimuth for the African plate during the past 50 Ma (Ypresian, early Eocene time), computed for two singular points: one in the West Alboran Basin (with a present-day position of lat 36°N, long 4°W; blue curve) and the other in the onshore region of Algerian margin (lat 37.5°N, long 1.5°E; green curve).* ***(b)*** *Plot with the velocity (in mm×yr^{-1}) of the African plate motion for the same points used for (a). Both plots include the present-day conditions for the African plate motion according to current plate-motion models (Nuvel-1A from DeMets et al. [1994] and Deos-2k from Fernandes et al. [2003]). The two components of the overall vector of the plate convergence in the west–east and north–south orientations are also included in the plot, with discontinuous and dotted lines, respectively. Messinian salt precipitation during the MSC (5.97–5.55 Ma; e.g., Andreetto et al. [2021]) is included in both plots for reference.* ***(c)*** *Map representing the relative motion of the African plate with respect to a fixed Eurasian plate and the trajectories from 165 Ma to present (beginning in Callovian, Middle Jurassic time) of the two singular points used to compute plots (a) and (b). The trajectories followed by these two points during the past 50 million years, which are detailed in (a) and (b), are marked with a thicker colored line. The actual boundary between the two plates is omitted for the sake of clarity. Abbreviation: Pl-Q= Pliocene–Quaternary.*

Although other models reconstruct the plate motions of Africa and Eurasia in the Western Mediterranean Sea (Dewey et al., 1989; Srivastava et al., 1990; Roest and Srivastava, 1991; Mazzoli and Helman, 1994; Capitanio and Goes, 2006; Schettino and Turco, 2006, 2009; Handy et al., 2010; Jolivet et al., 2015, 2021; Hosseinpour et al., 2016; Macchiavelli et al., 2017; Romagny et al., 2020; van Hinsbergen et al., 2020; Frasca et al., 2021), researchers have achieved consensus concerning the following important points:

1. During most of the Mesozoic (at least from 180–80 Ma) the motion of Africa with respect to a fixed Eurasia was a continuous drift towards the southeast, maintaining the north–south dimensions of a relatively narrow corridor that represented the western termination of the Tethys Basin.
2. From the latest Cretaceous to the earliest Eocene (80–55 Ma), the African plate changed its trajectory, initiating a northwest–north-northwest-directed convergence with Eurasia.
3. During a short interval in the early Eocene (55–50 Ma), Africa moved suddenly towards the southwest, promoting a moderate stretching of the narrow basin between the two plates.

The post-Eocene evolution of the two plates is of particular interest to our study (Rosenbaum et al., 2002; DeMets et al., 2015; Romagny et al., 2020) because the African plate moved continuously towards the north-northeast from 45 to 25 Ma (from the middle Eocene to the latest Oligocene), with an increasing rate of convergence with Eurasia peaking at 9–12 $mm \times yr^{-1}$ at 25 Ma (Fig. 5b). During the Lower and Middle Miocene (25–15 Ma), an important modification of the plate convergence occurred because Africa moved towards the northeast and west-northwest down to 4 $mm \times yr^{-1}$ (Figs. 5a, 5b). Since then, from the Upper Miocene to the present, the convergence of the African plate was oblique, with an average trend of convergence that evolved from being west-northwesterly in the latest Middle Miocene to northwesterly in the present day (average azimuths 100°–135°), according to the geodetic models of DeMets et al. (1994) and Fernandes et al. (2003), and the GPS determinations of Bougrine et al. (2019).

After the deposition of the Messinian salt (at ~5.5 Ma), the plate convergence rate diminished slightly through time, being at present slightly higher along the Algerian margin than in the West Alboran Basin (5.5 and 4.7 $mm \times yr^{-1}$, respectively) (Fig. 5b). During this recent epoch (<5.5 Ma), a slight change in the convergence vector between the two plates can be interpreted, evolving from north-northwest to northwest convergence (Fig. 5a). The average trends for plate convergence in this period, changed from 127° to ~115° for the point in the West Alboran Basin and from 140° to 130° for the Algerian margin.

3. Dataset and methods

We used a large dataset of commercial and scientific wells and seismic profiles (of about 280 lines, representing a total length of ~ 8,000 km), from both offshore Spain and Algeria (Fig. 1). Wells selected for this study come from two scientific drillings conducted by the Ocean Drilling Program (ODP) in the East Alboran Basin and a commercial well near the basin's northern margin (Comas et al., 1999), six wells on the eastern continental shelf in Spain (south of Valencia to Murcia) (acquired through Archivo Técnico de Hidrocarburos [ATH, 2020]), and three commercial wells along the Algerian margin (Burollet et al., 1978; Medaouri et al., 2012, 2014). We used these wells to produce the correlations between the Algerian Basin margins shown in Fig. 6. These correlations show synthetic stratigraphic sections in the offshore continuation of the eastern Betics (wells Javea-1, Calpe-1, Alicante A-1, and Muchamiel-1; Fig. 6a), the northern East Alboran Basin (well Andalucía A-1 and ODP

Sites 978 and 977; Fig. 6b), and the variation along-strike in the Algerian margin (wells Habibas-1, Arzew-1, and Alger-1; Fig. 6c).

The 2D seismic lines selected to illustrate this work were acquired from a variety of sources. Seismic for the northern margin of the Alboran Basin in Spain were obtained through ATH (2020). For the Algerian margin in the south, we have selected various commercial and scientific lines reproduced in works like Badji (2014), Medaouri (2014), Medaouri et al. (2014), Badji et al. (2015), and Klingelhoefer et al. (2022). The Alboran margin has been studied using one of the deep seismic profiles of Comas et al. (1997), which was later processed and interpreted by Booth-Rea et al. (2007, 2018) and Gómez de la Peña et al. (2018).

Our seismic interpretation had four goals:

1. Characterize the structures involving the Messinian salt using salt tectonic concepts and theory (e.g., Jackson and Hudec, 2017).
2. Reconstruct the geometry of the suprasalt sequences (i.e., Messinian to recent) to evaluate the relationships among deformation, halokinesis, and sedimentation.
3. Where seismic has enough resolution, evaluate the geometry of the presalt sequences and determine the basement-involved structures.
4. Establish the general structural style of the deformation affecting the basement and identify the reflections marking the crust–mantle boundary to compare with other sources of information for this discontinuity.

The correlation of horizons between seismic lines along the Algerian margin was conducted using a dense grid of seismic profiles (Fig. 1). We then used the relatively few intersections between seismic lines from the Iberian and Algerian margins to correlate the horizons from the south to the north. We are conscious of the relatively poor quality of the vintage seismic lines in the Iberian margin, so our interpretations there, particularly those related to salt geometries, should be accepted with caution.

One of the seismic interpretations from the Algerian margin has been converted to depth using the seismic velocities established in the sedimentary cover of the region (Badji et al., 2015; Bouyahiaoui et al., 2015; Klingelhoefer et al., 2022). Details about the depth conversion, as well as the procedure to make the restoration, are provided in Section 6.

4. Seismic stratigraphy

The seismic stratigraphy scheme used for our study follows the stratigraphic framework established by previous workers in the region. For the East Alboran Basin, for example, we use data from Comas et al. (1992, 1997, 1999), Medaouri et al. (2012, 2014), and Gómez de la Peña et al. (2021). Information about the seismic facies of the sedimentary cover along the Iberian margin is taken from Maillard and Mauffret (2013), Maillard et al. (2014), and Giaconia et al. (2015), together with the detailed Messinian stratigraphy established there by Driussi et al. (2015a, 2015b) and Ochoa et al. (2015). The seismic stratigraphy of the Algerian margin follows information provided by Strzerzynski et al. (2010, 2021), Badji (2014), Medaouri (2014), Mihoubi et al. (2014), Badji et al. (2015), Haidar et al. (2022), and Klingelhoefer et al. (2022). In addition, we have made revisions based on information provided from the following wells: Andalucía A-1 and ODP Sites 977 and 977 (with data from Comas et al. [1999]), Javea-1 (Texas Pacific Oil Co., 1977), Calpe-1 (Texas Pacific Oil Co., 1975), Alicante A-1 (Upton and Young, 1984), Muchamiel-1 (ESSO, 1981), Torrevieja Marino C-1 (ENIEPSA, 1979), Habibas-1 (Medaouri et al., 2012, 2014; Medaouri, 2014), and Alger-1 and Arzew-1 (Burollet et al., 1978). In wells Calpe-1 and Muchamiel-1, we also used the detailed revision of the Upper Miocene sequences conducted by Ochoa et al. (2015).

The stratigraphic correlation that we established among the three margins of the Algerian Basin according to well information is presented in Fig. 6.

All the aforementioned information was extrapolated and tied to the studied seismic profiles, resulting in a seismic stratigraphy scheme that is illustrated in Fig. 7. The seismic facies along the continental rise of the Algerian Basin are shown in Figs. 7a and 7b using a seismic window from the Algerian margin. The domain of the basin floored by oceanic crust is exemplified in Figs. 7c and 7d.

(insert here Fig. 6)

Fig. 6. *Well correlation in the study area along the three margins of the Algerian Basin:* ***(a)*** *a north–south transect (wells Javea-1, Calpe-1, Alicante A-1, and Muchamiel-1) in the Iberian margin, documenting the offshore continuation of the eastern Betics;* ***(b)*** *a northwest–southeast transect (wells Andalucía A-1, ODP Site 978, and ODP Site 977) in the East Alboran Basin towards the Algerian Basin; and* ***(c)*** *west-southwest–earth-northeast transect (wells Habibas-1, Arzew-1, and Alger-1) along strike of the Algerian margin. The diagram shows the correlation for the base of the Pliocene–Quaternary section (the Messinian or M unconformity) as well as the position and nature of the Messinian sequences, differentiating the occurrence of evaporite-dominated (in red; distinguishing when gypsum or anhydrite are the more abundant minerals) and mud-dominated sequences (in light yellow). Inset shows the correlation lines of the three transects, using wells (black dots) as they are located in Fig. 1. Distance between wells is shown between the lithological columns. Stratigraphic and paleontological information in these wells is extracted from: Comas et*

al. (1999) (well Andalucía A-1 and OPD Sites 978 and 977); Medaouri et al. (2012, 2014) (well Habibas-1); Burollet et al. (1978) (wells Arzew-1 and Alger-1); Texas Pacific Oil Co. (1977) (well Javea-1); Texas Pacific Oil Co. (1975) and Ochoa et al. (2015) (Calpe-1); Upton and Young (1984) (well Alicante A-1); and ESSO (1981) and Ochoa et al. (2015) (well Muchamiel-1). Approximate boundary positions are marked with discontinuous lines. Abbreviations: LU= Lower Messinian series; UU= Upper Messinian series.

The Pliocene–Quaternary section thickens towards the center of the Algerian Basin. On the Algerian margin, these series also thickens towards the East Alboran Sea; i.e., towards the west-southwest (cf. change from Arzew-1 to Habibas-1 wells in Fig. 6c). We have interpreted three seismic units within the Pliocene-Quaternary sequence, bounded by unconformities.

The Pliocene–Quaternary sequence lies above a Mediterranean Basin–wide regional unconformity known as the “M reflector” (e.g., Hsü et al., 1977; Biju-Duval et al., 1978; Ryan and Cita, 1978). Below this unconformity, the sedimentary section consists of a Miocene sequence of variable thickness, being up to 1.1 km thick in the shallow portion of the Algerian margin and 2.4 and 2.6 km thick in the continental platforms of the northern and southern East Alboran Basin, respectively (according to data from wells Andalucía A-1 and Habibas-1). The offshore continuation of the External Betics along the Iberian margin consists of a variable sequence of Upper Miocene, fine-grained detritic sediments (with a maximum thickness of 0.95 km in the well Calpe-1) above Jurassic–Paleogene limestones and Triassic evaporites (Fig. 6).

In the shallow portion of the studied margins, the Messinian sequence locally comprises reef buildups, but is characterized in most places by marls, calcareous claystones, and fine-grained siltstones with intercalations of gypsum and eventually anhydrite that becomes more abundant basinward (e.g., wells Calpe-1, Muchamiel-1, and Alger-1; Burollet et al., 1978; Martínez del Olmo, 2011a; Ochoa et al., 2015; Raad et al., 2021). The Messinian evaporite sequence is formed by gypsum-rich marls that grade downward to anhydrite-rich marls and clays (e.g., well Arzew-1). This gypsum-rich sequence in the Iberian margin is referred to as the bedded units (BU) (Lofi et al., 2011a, 2011b; Maillard et al., 2014; Driussi et al., 2015a, 2015b; Ochoa et al., 2015; Raad et al., 2021), which are commonly correlated by these authors with the primary lower gypsum (PLG) unit, with an estimated age of 5.971–5.61 Ma, formed during Stage 1 of the MSC (e.g., Andreetto et al., 2021).

None of the available wells in the area cut the Messinian salt (mostly halite, but possibly also with other evaporites like gypsum and anhydrite) sequence that was deposited in the deepest portion of the basin, flooring the abyssal plain of the Algerian Basin (e.g., Biju-Duval et al., 1978; Mauffret et al., 1992, 2004; Driussi et al., 2015b; Gorini et al., 2015; Dal Cin et al., 2016; Lofi et al., 2018; Haq et al., 2020), which is commonly referred as the mobile unit (MU) (Lofi et al., 2011a, 2011b; Lofi, 2018).

For the Messinian series, we have distinguished the salt layer (equivalent to the MU unit) and two subunits within the Upper Messinian sequence; the so-called UU unit ("Unité Supérieur Messinienne" or "Evaporites supérieures") (*sensu* Lofi et al., 2011a, 2011b; Lofi, 2018; Leroux et al., 2019; Andreetto et al., 2021). The salt unit has semitransparent seismic facies with some scarce discontinuous and strong positive reflections that suggest the existence of other evaporites or lithologies in addition to pure halite (e.g., Raad et al., 2021). The base of the salt corresponds to a weak reflection with a higher amplitude towards the basin margins (e.g., Fig. 7a). The UU unit is represented by layered seismic facies with a pair of strong positive reflections at the top. We have differentiated two seismic units within the UU, an upper UU unit (UU2) with strong parallel reflections and a lower UU unit (UU1) with weak parallel reflections and some patches of transparent seismic facies (in line with a comparable differentiation made in other Messinian deep basins in the Western Mediterranean Sea; e.g., Obone-Zue-Obame et al. [2011], Geletti et al. [2014], and Dal Cin et al. [2016]).

Some wells document also the occurrence of thin intervals of anhydrite and gypsum within the uppermost Tortonian sediments (e.g., wells Alicante A-1 and Alger-1). This evidence may relate to observations in some of the onshore basins in Algeria (e.g., Chlef Basin) and southeastern Iberia (Bajo Segura Basin), showing local deposition of evaporites during the late Tortonian Age (e.g., Krijgsman et al., 2000; Rouchy et al., 2007; Ortí et al., 2014; García-Veigas et al., 2020). Nevertheless, recent studies in some of the offshore wells (Muchamiel-1 and Calpe-1) suggest that all the evaporites (gypsum) can be assigned to the PLG unit of the MSC (Martínez del Olmo, 2011b; Ochoa et al., 2015). In spite of this debate, our summary in Fig. 6 reproduces the available paleontological data, suggesting local deposition of evaporites (with gypsum and anhydrite) in the shallow basins of the Algerian Basin margins during the uppermost Tortonian Age.

The presalt sedimentary sequence is locally identified along the Algerian margin and the Alboran margin, either below the Messinian series (Fig. 7) or under the regional unconformity marked by the strong M reflector, which has associated deep erosion (e.g., Soto et al., 2010; Estrada et al., 2011; Garcia-Castellanos and Villaseñor, 2011; Just et al., 2011; Martínez del Olmo, 2011a, 2011b; Martínez-García et al., 2011, 2013; Do Couto et al., 2016; Booth-Rea et al., 2018) and local deposition of conglomerate deposits around emergent basement highs (e.g., ODP Site 977; Comas et al., 1999). The distribution of the seismic dataset makes it impossible to establish a precise lateral correlation of the presalt sequence age. Our interpretation of the age of this sequence incorporates the information provided from the available wells in the region (Fig. 6). Based on this information, we assume that the presalt sequences in the Algerian Basin margins are of Middle Miocene–Tortonian age. Some of these sequences could locally include Lower Miocene sediments, as has been suggested further to the east in the Algerian margin (e.g., Medaouri et al., 2014; Arab et al., 2016; Haidar et al., 2022).

(insert here Fig. 7)

Fig. 7. *Seismic examples and interpretation illustrating the different seismic units and regional reflections differentiated in this study.* ***(a)*** *Seismic window in the continental rise of the Algerian margin.* ***(b)*** *Seismic interpretation of (a).* ***(c)*** *Seismic window in the oceanic domain of the Algerian Basin.* ***(d)*** *Seismic interpretation of (c). Three Messinian sequences are distinguished in this work, following Lofi et al. (2011a, 2011b) and Lofi (2018), where UU refers to the "Unité Supérieur Messinienne" of these authors (Table 1). Discontinuous lines mark internal reflections within the differentiated seismic units and uncertain seismic reflectors. Double arrows correspond to positively inverted normal faults, with the open arrow indicating the sense of displacement of the previous normal fault. Locations of the seismic windows are detailed in Fig. 17.*

In summary, we have used the following age boundaries for the seismic units (Table 1): (1) top of the Late Pliocene unit: 3.6 Ma; (2) intra-Pliocene discontinuity: ~4.0 Ma; (3) top of the UU2 unit: 5.33 Ma; (4) top of the UU1 unit: ~5.42 Ma; (5) top and base of salt: 5.55 and ~6 Ma (5.971 Ma), respectively; and (6) presalt sequences, containing Middle Miocene–Tortonian sediments (up to ~7.5 Ma). The age we use for the Messinian units follows the regional stratigraphy established in the Mediterranean Basin for the MSC (Krijgsman et al., 1999, 2018; Lofi et al., 2011a, 2011b; Bache et al., 2012; Roveri et al., 2014, 2019; Lofi, 2018; Leroux et al., 2019; Andreetto et al., 2021). For the age of the base of salt, we have preferred to use 6.0 Ma (according to 5.971 Ma), instead of 5.6 Ma (Meilijson et al., 2019). So, we assume that salt deposition (precipitation) occurred in the Algerian Basin from the beginning of the MSC. This excludes a more complex scenario of sedimentation of presalt Messinian sediments in which other evaporites (selenite), euxinic shales, and dolostones would correspond with the lower evaporites (LU) unit (MSC Stage 1, *sensu*, e.g., Roveri et al. [2014]). This assumption also has been followed by previous studies in the area (e.g., Bouyahiaoui et al., 2015; Dale et al., 2021).

			Porosity [2]			
Units	Age (Ma) [1]	Lithology	ϕ_0	c (km^{-1})	V_p ($m \times s^{-1}$)	ρ ($kg \times m^{-3}$)
Sea water	0	-	0	0	1500	1030
Quaternary	0	shale	0.53	0.56	1900	2720
Upper Pliocene	3.60	shale	0.45	0.56	2100	2720
Lower Pliocene	4.00	sand	0.40	0.56	2200	2650
UU2 (Mess.)	5.33	shale [3]	0.38	0.56	2500	2720
UU1 (Mess.)	5.42	silt [3]	0.36	0.56	2750 [4]	2680
Messinian salt	5.55	salt	0	0	4500 [5]	2200 [6]
Presalt	~7.50 [7]	silt	0.56	0.39	3500 [8]	2680
Continental crust [9]	28	-	0	0	6500	2820
Oceanic crust [10]	35	-	0	0	7000	2890

Notes:

(1) Age for the top of the unit. See text for sources.
(2) Using Sclater and Christie (1980).
(3) Approximate lithologies used for backstripping analysis (see note [2]).
(4) Some studies suggest V_p values in the UU unit of up to 3100 (Dal Cin et al., 2016), 3300 (Dale et al., 2021), 3400 (Bouyahiaoui et al., 2015) or 3600 $m \times s^{-1}$ (Leffondré et al., 2021).
(5) Sonic velocities in the Messinian salt are quite variable, varying from 4200 to 5100 $m \times s^{-1}$ (Montadert et al., 1978; Dal Cin et al., 2016; Dale et al., 2021), although some authors infer lower velocities of 3800–4030 $m \times s^{-1}$ (Bouyahiaoui et al., 2015; Haq et al., 2020; Leffondré et al., 2021).
(6) Close to the average density of 2130 $kg \times sm^{-3}$ estimated by Dale et al. (2021).
(7) Assuming the occurrence of late Tortonian sediments below the MSC series.
(8) The deepest sediments in the Algerian margin could have velocities of 4800 $m \times s^{-1}$ (Bouyahiaoui et al., 2015; Klingelhoefer et al., 2022).
(9) Properties according to Christensen and Mooney (1995) and the average density established in the region by Soto et al. (2008).
(10) Properties according to Carlson and Raskin (1984). Measured sonic velocities in the Algerian margin are slightly lower, ~6750 $m \times s^{-1}$ (e.g., Klingelhoefer et al., 2022).

Table 1. *Characteristics of the different seismic units of this study and values used to conduct the restoration (Fig. 18):*

5. Structural interpretation of the seismic profiles

Our interpretation of the general structure of the Algerian Basin margins is presented through selected profiles that illustrate the structural configuration of the Iberian margin in the north (Figs. 8-10), the Alboran margin in the west (Figs. 11-13a), and the structure of the Algerian margin in the south (Figs. 13c-17). All seismic profiles are in two-way time (TWT) and were acquired at different times (from the 1970s to the 2010s) using diverse sources and processed with different workflows.

5.1 Seismic sections along the Iberian margin

The structure of the Iberian margin is shown through two northwest–southeast dip lines (Figs. 8, 9) and a cross-cutting, west-southwest–east-northeast strike line (Fig. 10).

The configuration of the margin from the southernmost domain of the Gulf of Valencia and the Ibiza Channel, across the continental slope containing the Provençaux Bank, and finally the abyssal plain of the Algerian Basin, is shown in Fig. 8. A parallel section from the continental platform east of Alicante and across the slope, situated just east of the Mazarrón Escarpment, is shown in Fig. 9. In these sections, we interpret the general structure of the offshore continuation of the External Betics as a series of NW–directed stacked thrust sheets imbricating the Mesozoic cover (similar to Sàbat et al. [1997], Roca et al. [2004], Maillard and Mauffret [2013] and Driussi et al. [2015a, 2015b]), which are later inverted as low-angle normal faults (Fig. 8b). The same style of extensional tectonics is seen along the offshore continuation of the Internal Betics (or Alboran Domain). Severe extension is seen in both crustal domains through rotated blocks limited by extensional faults that extend downward, probably merging along the middle (and possibly the lower) continental crust. Some of the rotated fault blocks support half-grabens filled by Messinian sediments (BU or PLG units of the MSC that we simplify, correlating them with the UU2) and Pliocene to recent sequences (e.g., half-grabens of the El Cid, Elche, and Formentera Basins in Fig. 8b and of San Pedro and Cogedor basins in Fig. 9b). Although these extensional faults could have a lateral component of displacement, we interpret that the large size of these listric faults is more in agreement with a main downdip displacement. This interpretation contrasts with the strike-slip (right-lateral) motion suggested by other authors for the continent–oceanic boundary in this portion of the margin (e.g., Mauffret et al., 1992; Camerlenghi et al., 2009; Maillard and Mauffret, 2013; Driussi et al., 2015b).

(insert here Fig. 8. Landscape orientation of the page)

Fig. 8. (a) *Northwest–southeast seismic section and* ***(b)*** *interpretation of the line MEDS-29 (seismic line from ATH [2020]) across the offshore continuation of the eastern Betics, showing the structure of the Iberian margin and the northern sector of the Algerian Basin. Notice the occurrence of various perched Messinian half-grabens, bounded by crustal-scale listric normal faults, developed behind the orogenic, thrust front of the External Betic Cordillera, and the occurrence of high-extensional riders and low-angle detachment faults thinning the offshore continuation of the Alboran Domain (Internal Betics) near the transition to the oceanic crust of the Algerian Basin. Seismic units and symbols are detailed in Figs. 7 and 14 and Table 1. Location of the seismic profile and wells used to tie the interpretation are shown in Figs. 1–3. Volcanic edifices (vr) have been found locally along the Émile Baudot Escarpment (Mauffret et al., 1992; Acosta et al., 2001; Camerlenghi et al., 2009; Maillard and Mauffret, 2013; Driussi et al., 2015b).*

(insert here Fig. 9. Landscape orientation of the page)

Fig. 9. (a) *Northwest–southeast seismic line and* ***(b)*** *interpretation of the line MEDS-31 (seismic line from ATH [2020]) across the Iberian margin and the northern sector of the Algerian Basin, showing also the offshore continuation of the Internal Betics in this margin. It is interpreted various perched Messinian half-grabens bounded by crustal-scale listric normal faults thinning the Alboran Domain (Internal Betics) near the transition to the oceanic crust of the Algerian Basin.*

Seismic units and symbols are detailed in Figs. 7 and 14 and Table 1. Location of the seismic profile and well used to tie the interpretation is shown in Figs. 1–3.

(insert here Fig. 10. Landscape orientation of the page)

Fig. 10. (a) *Southwest–northeast seismic line and* ***(b)*** *interpretation of the line MEDS-7D (seismic line from ATH [2020]) along the continental rise of the Iberian margin. In this strike section, we interpret the occurrence of various perched Messinian half-grabens bounded by crustal-scale listric normal faults, which promote a severe thinning of the offshore continuation of the Alboran Domain (Internal Betics) near the transition to the oceanic crust of the Algerian Basin. Notice the occurrence also of various presalt half-grabens. Seismic units and symbols are detailed in Figs. 7 and 14 and Table 1. Location of the seismic profile is shown in Figs. 1–3.*

Our interpretation of the seismic profiles, which is tied by wells like Calpe-1, Muchamiel-1, and Torrevieja Marino-1, indicates that crustal extension, rotated fault blocks, and half-graben formation has continued after the Messinian (Figs. 8b, 9b). The presalt sequences seem also to be bounded by these extensional faults, which is consistent with the formation of a highly stretched continental crust in the transition to oceanic crust (Fig. 10b). Salt deposition occurred during the Messinian Age only at the base of the continental slope and above the thin oceanic crust of the Algerian Basin (total thickness, including the sedimentary sequence, of ~2.2 s TWT).

The geometry of the presalt half-grabens also suggests that crustal stretching has occurred since the Tortonian and possibly during the Middle Miocene (e.g., Mauffret et al., 1992). The position and geometry of the upper Messinian sequences (UU2), filling half-grabens that are progressively higher towards the north (Raad et al., 2021), show that crustal stretching during Messinian time was also accompanied by tectonic uplift and deep erosion (Just et al., 2011). This inference agrees with detailed studies of the Messinian series conducted in this margin, suggesting the occurrence during the MSC of various intermediate, perched basins situated at different depths, connecting the peripheral onshore basins with the deep salt basin (Rouchy and Caruso, 2006; Ryan, 2008; Maillard and Mauffret, 2013; Maillard et al., 2014; Driussi et al., 2015a; Raad et al., 2021).

At the base of the continental slope, the Messinian salt pinches out against the gently dipping top of the basement, corresponding to the highly stretched continental crust of the Internal Betics (or Alboran Domain). With respect to the salt structures, we cannot interpret their geometries with confidence due to the low quality of these commercial seismic profiles. The data suggest the occurrence of broad diapiric culminations and salt-cored anticlines, possibly with some salt-pillow geometries. Some of the geometries seem to indicate the existence of local diapirs discordant with the two UU sub-units and the lower Pliocene sequences (e.g., Figs. 8b, 9b). Suprasalt sequences seem to thin progressively towards the anticline crests, documenting growth since the deposition of the salt layer, and continuing through Pliocene–Quaternary time. Away from diapir highs and anticline culminations, the salt layer has a rather constant thickness of 0.2–0.27 s TWT above the top of the oceanic crust (~450–610 m using an average velocity of 4,500 m×s^{-1}; Table 1).

Our interpretation of the crustal thickness and the location of the continent–ocean boundary, which could correspond with a narrow and sub-vertical contact, agrees with other geophysical observations and models of this margin (Gallart et al., 1997; Sàbat et al., 1997; Vidal et al., 1998; Roca et al., 2004; Maillard and Mauffret, 2013; Driussi et al., 2015b; Kumar et al., 2021).

5.2 Seismic section across the Alboran margin

The structural configuration of the Alboran margin has been inspected through a single seismic section that is part of the ESCI-ALB 2C deep-seismic profile (using data from Comas et al. [1997] and Booth-Rea et al. [2007, 2018]). This portion of the seismic line shows the transition from the relatively thicker continental crust of the East Alboran Basin to the oceanic crust of the Algerian Basin (Fig. 11a). The transition between the two domains includes abundant volcanic edifices (Comas et al., 2000, 2006a, 2006b; Gómez de la Peña et al., 2018).

Our interpretation of the deep structure of the margin, shown in Fig. 11b, suggests a progressive eastward thinning of the thin continental crust of the East Alboran Basin (with a Moho depth shallowing from 7.5 s to 6.75 s TWT in about 70 km of horizontal distance). Structures associated with crustal thinning involve basinward-dipping low-angle extensional faults that describe extensional horses and rotated fault blocks with lenses of possibly upper-crustal rocks, lying along the deep crust and close to the Moho boundary. The transition to oceanic crust is interpreted to occur through a crustal neck (*sensu* Péron-Pinvidic and Manatschal, 2009; Chenin et al., 2018). Deep seismic tomography also suggests that the continent–oceanic boundary coincides with this narrow crustal neck and that crustal thinning is also produced by progressive thinning of the ductile deep crust (e.g., Booth-Rea et al., 2007, 2018; Gómez de la Peña et al., 2020).

The seismic image of the pre-Messinian sequences shows abundant lateral diffractions and seismic noise. In spite of that, we are confident on the existence of a thin remnant of the presalt sequence filling the stretched continental crust (in the crustal neck), and the western domain of the oceanic crust with onlap geometries. If this geometry is confirmed by future seismic observations, it would suggest that crustal stretching occurred on this margin during the Middle Miocene, evolving to a final sag-basin geometry just before the MSC.

Salt structures are better imaged here than on the Iberian margin, and occur in two domains. A thin, perched salt basin is observed in the west, where the base of salt dips to the east. Most structures are low-relief salt pillows, although we do interpret one salt roller. Growth of these pillows is dated by progressive thinning of the two UU subunits over the crests of the structures.

One of the open salt pillows lies above a basement step, and shortening of this salt structure is shown by progressive thinning of the two UU subunits toward the crest, which is accompanied by basinward thrusting of the salt roof (Fig. 12b). These geometries suggest the existence of a linked kinematic system resulting in local thrusting above salt highs. The existence of salt-detached extension at the updip end of the line also suggests the existence of some downdip gliding of the suprasalt series above the thinned continental crust. Thinning of Early Pliocene units towards the west indicates that the eastward regional dip existed at that time (i.e., from 5.5 to 4.0 Ma). Shortening in the UU sequence above salt pillows suggests that this dip may have been in existence at that time as well, and that downslope gliding began shortly after salt deposition. Shortening at the downdip end of this system may also have caused some of the growth of the salt pillows.

(insert here Fig. 11. Landscape orientation of the page to reproduce the illustration and its maximum size)

Fig. 11. ***(a)*** *West-southwest–east-northeast seismic line and* ***(b)*** *interpretation of the line ESCI-ALB 2C (seismic line from Comas et al. [1997] and Booth-Rea et al. [2007]) illustrating the Alboran margin. Seismic units and symbols are detailed in Figs. 7 and 14 and Table 1. The continent–oceanic boundary is suggested according to the tomography model created by Gómez de la Peña et al. (2020) using wide-angle seismic data. Location of the seismic profile is shown in Figs. 1–3. Red rectangles mark the position of the seismic windows shown in Figs. 12 and 13.*

The second domain of salt structures is further to the east, in the oceanic Algerian Basin. Here, we interpret the occurrence of salt pillows and diapirs (Figs. 13a, 13b). The existence of isopachous prekinematic sediments over the crests of some pillows in this seismic line, should be taken with care as it is oriented almost normal to the regional shortening direction.

Nevertheless, shortening is suggested by some of the diapirs exhibiting arched roofs or being pinched off to form disconnected teardrops with sub-vertical secondary welds (Figs. 13a, 13b). Thickness variations in the UU sequences over pillow crests and against the flanks of diapirs are probably apparent due to the orientation of the seismic line. Shortening then began in Pliocene time, as indicated by pinchout of Pliocene units over the crests of many diapirs and pillows.

(insert here Fig. 12)

Fig. 12. (a) *Seismic example and* ***(b)*** *and interpretation of the salt structures in the updip domain of the salt basin in the Alboran margin. Seismic units and symbols are detailed in Fig. 7 and Table 1. Various lenticular bodies with possible channel deposits within the Lower Pliocene unit are also differentiated in (b). The structure of the presalt sequences and the approximate position of the top of basement is included with dotted lines. Location of the seismic window is detailed in Fig. 11.*

From these observations, we conclude that salt was slightly thicker on the oceanic (eastern) side of this margin (≤0.20 s TWT; i.e., ~400–450 m) and that a moderate basinward (eastward) tilting began immediately after the deposition of the Messinian salt and continued throughout the Pliocene Epoch (Fig. 12). This tilting then caused: a progressive thinning of the Pliocene and the UU2 units towards the west and a modest eastward gliding of the suprasalt section. However, this modest gliding is unlikely to have caused the more intense shortening we observe on the eastern end of the seismic line. Instead, below we will suggest that the shortening is probably caused by deformation originating along the Algerian margin (Figs. 13a, 13b).

(insert here Fig. 13)

Fig. 13. (a) *Seismic examples and* ***(b)*** *interpretation of the salt structures in the compressional domain of the Algerian Basin, which is associated to active compression along the Algerian margin. Seismic units and symbols are detailed in Fig. 7 and Table 1. Presalt structures have been omitted for the sake of simplicity. Locations of the seismic windows are detailed in Figs. 11 and 14.*

5.3 Seismic sections along the Algerian margin

The structure of the Algerian margin is shown using four high-quality seismic profiles. All northwest-trending seismic profiles have been interpreted by previous authors, and abundant information is available concerning the geophysical properties of the crust and the nature and position of the continent–ocean boundary (Leprêtre et al., 2013; Badji et al., 2015; Bouyahiaoui et al., 2015; Aïdi et al., 2018; Klingelhoefer et al., 2022). Our interpretations include these aspects of the geology, but salt structures are here explored for the first time using modern salt tectonic principles (Figs. 13–17). A similar approach has been also used recently in the eastern domain of this margin using seismic data and analogue modeling (e.g., Travan et al., 2021).

The Algerian margin has a narrow OCT domain, showing an abrupt change from a uniformly-thick oceanic crust (~3 s TWT thickness with ~2 s TWT of sediments, equal to ~3.5–5.25 km of crystalline oceanic crust with ~2.7–3.0 km of sediments using average velocities of 7,000 and 2,700 m×s^{-1}, respectively; Table 1) to a relatively thick continental crust that thins smoothly basinward. In most areas, excluding the water column, the continental crust thins basinward from 8 s to 4.5 s TWT, including a sedimentary column of ~1–2 s TWT (i.e., from ~27–28 km to ~16–18 km, using an average velocity of 6,500 and 2,700 m×s^{-1}, respectively; Table 1) in about 50–55 km, which represents a general dip for the Moho boundary of about 7° or 8° towards the south (some refraction studies reconstruct local dips of up ~45°, e.g., Badji et al. [2015]). Deep seismic experiments and tomographic models show a narrow OCT that occurs in a margin-parallel band situated in the abyssal plain around 20–25 km north of the base of the continental rise.

The oceanic crust in this sector of the Algerian Basin is immediately overlain by a presalt sequence that locally fills half-grabens thickening into high-angle, basinward normal faults (e.g., Fig. 15b). The exact age and nature of the presalt sediments is unknown, although well information from the continental shelf and regional interpretation of the age of the oceanic crust suggest that they correspond to layered, fine-grained detritic sediments of Middle (and possibly Lower?) Miocene to Tortonian age (Fig. 6) (Medaouri et al., 2014; Badji et al., 2015; Haidar et al., 2022). The presalt sequence thickens towards the base of the Algerian continental slope (i.e., southward), as it was also suggested in previous studies of the margin (e.g., Mauffret, 2007; Arab et al., 2016; Leffondré et al., 2022). This sequence achieves a maximum thickness (0.4–0.5 s TWT; equal to ~0.9–1.1 km) in the OCT region (Figs. 14b, 15b and 16b; see recent reviews by Haidar et al. [2022] and Klingelhoefer et al. [2022]). Beneath the continental slope, the presalt sequence thins progressively southward on top of the continental basement and could be deformed above a basement step formed by a deep, north-directed reverse fault (Fig. 17b; in agreement with many previous studies, e.g., Déverchère et al. [2005], Mauffret [2007], Kherroubi et al. [2009, 2017], Leffondré et al. [2021], and Strzerzynski et al. [2021]). Although we do not have direct evidence on the nature of these sequences, regional information suggest that they could be pelagic marly sequences with some interbedded sandstones and limestone layers of Langhian(?) to Tortonian age (Fig. 6c; Burollet et al., 1978; Medaouri et al., 2014; Arab et al., 2016).

The Messinian series are highly deformed on this margin, with structures ranging from diapirs and salt-cored folds near the base of the slope to gentle salt-cored folds further out in the basin. The basinward decrease in salt-structure amplitude and structural height, suggests that the salt was thickest near the base of the slope and thinned basinward (Figs. 14b, 17b).

Salt onlaps against the base of the slope, and the overlying postsalt sequence onlap progressively further up the continental basement of the margin. However, the margin also contains local perched, upper Messinian basins in the shelf areas (e.g., Figs. 14b–16b).

(insert here Fig. 14)

Fig. 14. (a) *Northwest–southeast seismic section and* ***(b)*** *interpretation of the line ALWG02-169 (seismic line from Badji [2014]) illustrating the structure of the Algerian margin and the narrow transition to the Algerian Basin. Notice the basinward decrease in the height of the salt structures, and how they change progressively from salt pillow, salt walls and diapirs, to smooth, detached salt anticlines with roof thrusting. It is interpreted a presalt trough with a maximum thickness situated above the OCT region. Seismic units and symbols are detailed in Fig. 7 and Table 1. The continent–oceanic boundary is taken from wide-angle refraction and deep seismic reflection tomography studies (Badji et al., 2015). Location of the seismic profile and well used to tie the interpretation is shown in Figs. 1–3. Red rectangle marks the position of the seismic window shown in Fig. 13.*

(insert here Fig. 15)

Fig. 15. (a) *Northwest–southeast seismic section and* ***(b)*** *interpretation of the line SPI-02 (seismic line from Badji et al. [2015]) illustrating the structure of the Algerian margin and the narrow transition to the Algerian Basin. Salt structures are here seen clearly detached along the salt base, with a proximal salt roller, followed basinward by the salt wall of the Ameur diapir. Above the oceanic crust the salt anticlines are probably deformed by low-angle thrusts forming allochthonous salt sheets. We also suggest the occurrence of squeezed salt diapirs with an upper bulb and a narrow sub-vertical feeder. The presalt series show a similar geometry to the one seen in Fig. 14. Seismic units and symbols are detailed in Fig. 7 and Table 1. The continent–oceanic boundary is taken from wide-angle refraction and deep seismic reflection tomography studies (Badji et al., 2015). Location of the seismic profile is shown in Figs. 1–3.*

(insert here Fig. 16)

Fig. 16. (a) *Northwest–southeast seismic section and* ***(b)*** *interpretation of the line ALWG02-165 (seismic line from Badji [2014]) illustrating the structure of the Algerian margin and the narrow transition to the Algerian Basin. In this section, the updip salt pinchout is deformed by a buried thrust involving the basement. Above the OCT region is observed a symmetric, detached salt anticline (with a geometry that resembles a "Napoleon chat"). Some of the salt diapirs are probably thrusted basinward above the UU1 series (e.g., in the Ameur diapir). The presalt sequences have again their maximum thickness in the OCT region. We interpret also the occurrence of some high-angle normal faults affecting the oceanic crust and the presalt sequences. Seismic units and symbols are detailed in Fig. 7 and Table 1. The continent–oceanic boundary is*

taken from wide-angle refraction and deep-seismic reflection tomography studies (Badji et al., 2015). Location of the seismic profile is shown in Figs. 1–3.

(insert here Fig. 17. Landscape orientation of the page to reproduce the illustration and its maximum size)

Fig. 17. (a) *Northwest–southeast seismic section and* ***(b)*** *interpretation of the line SPI-04 (seismic line from Badji et al [2015]) illustrating the structure of the Algerian margin and the narrow transition to the Algerian Basin. In this case, the marginal domain of the salt basin with the salt pinchout and associated salt rollers, is clearly deformed by the buried thrust, which produces basement overthrusting above the presalt sequences and a differential uplift and tilt of the suprasalt section above the thrust hangingwall. The geometry of the suprasalt series above the OCT resembles an expulsion rollover, with an asymmetric Pliocene infill, tilted basinward by simultaneous salt evacuation forming finally a primary salt weld. Basinward there is broad domain of salt diapirs (~25 km) with multiple evidence of contractional deformation, forming pinched-off diapirs, thrust secondary welds, and possibly detached upper salt bulbs. A basinward decrease in the height of the salt structures is clearly evidenced, due possibly to a local thinning of the Messinian source layer. The oceanic crust is here deformed by diverse high-angle normal faults, which bound asymmetric presalt half-grabens. Seismic units and symbols are detailed in Figs. 7 and 14 and Table 1. The continent-oceanic boundary is taken from wide-angle refraction and deep-seismic reflection tomography studies (Badji et al., 2015). Location of the seismic profile is shown in Figs. 1–3. Red rectangles mark the positions of the seismic windows shown in Fig. 7.*

Both the UU1 and the UU2 sequences thin against the diapirs and over the crest of the pillows and salt anticlines (Figs. 13c, 13d). These observations document growth of salt structures during UU time. There are no diagnostic criteria to indicate whether this growth was purely halokinetic (by active diapirism) or compressional (a problem that was also discussed in other areas of the Mediterranean Sea by Gaullier et al. [2014]). However, there are a number of clearly imaged thrust geometries with Pliocene growth (Figs 13c, 13d). In addition, many pillows and diapirs show significant roof uplift during the Pliocene (Figs. 14–17). Together, these observations provide clear evidence for shortening during the Pliocene. This history is similar to the one that we inferred for the structures shown in the eastern end of Fig. 11, suggesting that the compressional deformation there was part of the same fold belt that we see along the Algerian margin (see stippled area in Fig. 3 for map distribution of the belt).

Our seismic interpretation shows only minor extension at the landward end of the salt basin (also identified by Bellucci et al. [2021]), which occurred during the late Messinian (mostly coinciding with the deposition of the UU2 unit) and continued through the Pliocene Epoch (Fig. 7b). The absence of major extension at the landward end of the system is consistent with the restriction of salt to the deep basin. Because the salt layer exhibits little structural relief, little driving force existed for gravity-driven translation.

This extension is clearly of insufficient magnitude to have caused all of the Pliocene–Quaternary shortening affecting the salt structures of the margin. If the shortening was not produced by a salt-detached, gravity-driven system, what caused it?

We see that the base of the Messinian series is clearly uplifted and deformed by basement-involved thrusts that imbricate the continental crust over the oceanic domain (Figs. 7b, 17b; also identified by Mauffret [2007]). This basement shortening in combination with the well-documented basinward tilt and uplift of the margin (Hamai et al., 2015, 2018; Recanati et al., 2019) suggests that basement shortening could be the cause of the salt deformation observed along the Algerian margin of the basin. If so, salt-detached shortening is related to convergence between the African and Eurasian plates. This convergence has been ongoing throughout the Cenozoic Epoch (Fig. 5), so it seems likely that salt-detached shortening did not suddenly begin in the Pliocene. We therefore hypothesize that growth of salt structures during UU deposition was also related to shortening, although we cannot prove this. We investigate this hypothesis in the next section through structural restoration of a selected section across the margin.

6. Cross section restoration in the Algerian margin

We have selected a representative section of the Algerian margin on which to conduct a sequential restoration to explore the hypothesis that suprasalt shortening has been ongoing since the end of salt deposition (Fig. 14b). This section contains a good representation of both the style of the salt structures and a relatively simple presalt configuration. Our restoration of the section starts with a depth conversion of the seismic interpretation using constant-layer properties and the average sonic velocities computed using well-logging information from wells (Table 1). We have also corrected the pull-up effects seen locally at the salt base below the higher salt structures (cf. dotted lines in Fig. 18a). Restoration follows the standard process used to balance salt-bearing cross sections, as summarized by Rowan and Ratliff (2012) and Jackson and Hudec (2017). Restoration was conducted with MOVE software (v. 2018) using a successive decompaction of the sedimentary sequences assuming a local (Airy) isostasy model and ignoring global variations of the sea level. Lithological parameters are from Sclater and Christie (1980) (Table 1). Folds are restored using flexural slip (consistent with our hypothesis that they formed by shortening), whereas high-angle and low-angle faults are restored assuming fault-parallel slip and simple shearing, respectively. Parameters used for depth conversion and layer decompaction are detailed in Table 1.

The results of the restoration are presented graphically in Fig. 18. Values of the incremental and total shortening are also summarized in Table 2. We have also computed the average deformation rate for every interval using the incremental shortening measured for the base of the unit and the time interval of the seismic unit (Table 2).

We make several assumptions in the restoration: (1) all units on the basin floor were deposited horizontally; (2) the pinch-out of the salt layer at the base of the continental slope is fixed (circled number 1 in Figs. 18e, 18f); (3) in the case of exposed salt structures, salt diapirs exhibit a reasonable minimum width (circled number 2 in Figs. 18d, 18e); and (4) shortening is accommodated on different structures in the suprasalt and subsalt sequences. Because salt-detached extension is insufficient to drive the shortening observed on the basin floor, basement shortening is required to balance the section. This basement shortening was accomplished on a gently dipping detachment surface situated in the deep continental crust of the margin. The location and geometry of this thrust is tentative, because it is derived from the line-balancing technique used for the restoration. Notably, our restoration reconstructs only the latest evolution of the Algerian margin, since the early stages of the MSC (early Messinian to recent time).

Our restoration indicates that the original geometries of the stratigraphic units in the margin are as follows:

1. The presalt unit (Tortonian and possible older strata) was deposited in an asymmetric trough, with the thickest accumulations just above the transition from oceanic to continental crust (the OCT), thinning landward and basinward (circled number 3 in Figs. 18f, 18g).
2. Originally, the salt layer had a maximum thickness of 1.5 km close to the landward limit of the oceanic crust, pinching out landward on top of the presalt sequences (circled number 4 in Fig. 18f). The exact position of the salt pinchout should be taken with care, as we cannot ruled out the existence of salt dissolution, particularly in the landward limit of the Messinian basin (e.g., Kirkham et al., 2020).
3. The UU1 unit (5.55–5.42 Ma) was deposited forming small minibasins and troughs between small salt structures (Figs. 13c, 13d and circled number 5 in Fig. 18e).
4. Minibasins subsidence is also recorded by the UU2 unit, although this unit covers most of the salt structures (circled number 6 in Fig. 18d), thus indicating a progressive reduction of salt flow during this epoch (5.42–5.33 Ma). These geometries can be

formed either by passive diapirism with local salt withdrawal forming local minibasins or by moderate shortening.

5. Pliocene and Quaternary units (<5.33 Ma) show a general basinward thinning of the sequences, although they developed a thick depocenter at the continent–ocean boundary, with an internal asymmetric geometry (circled number 7 in Figs. 18a–18c) that documents the basinward evacuation of the salt layer.

The main tectonic findings of the restoration are these:

1. Suprasalt shortening in the deepwater part of the margin was caused by over-thrusting of the continental crust above the oceanic domain.
2. Basement-involved thrusting (thick-skinned tectonics) is also associated with the inversion of the presalt half-graben situated above the OCT (circled number 8 in Figs. 18b–18e). The main fault limiting this half-graben was probably active during Tortonian and earliest Messinian presalt deposition (circled number 9 in Figs. 18f, 18g).
3. This inverted fault propagated upward to connect with the base of salt. This surface acted as a major detachment surface, so that the shortening was then accommodated by formation of salt-cored buckle folds and minor salt-detached thrusts (circled numbers 10-14 in Figs. 18b–18e).
4. Suprasalt shortening was most intense during Pliocene to recent times, with late Messinian shortening producing only folding.
5. Extensional deformation in the cover is insignificant and is restricted to the landward salt pinch-out. A few listric faults detach onto the salt layer, forming small salt rollers. The base of the salt is here uplifted and tilted basinward due to the overthrusting of continental crust over oceanic crust. The activity of these salt rollers seems to be restricted to deposition of the UU2 unit to the Upper Pliocene (i.e., 5.33 to ~3.6 Ma) (circled number 15 in Figs. 18b–18d).

Contractional deformation on the Algerian margin has the following characteristics (Table 2):

1. Continuous contraction since the deposition of the Messinian salt (6–5.55 Ma) arising from the continuous African-Eurasian plate convergence (Fig. 5); the section records a total shortening of 1.15 km.
2. Shortening continued immediately after salt deposition and during the late Messinian age, achieving a maximum rate of deformation during the sedimentation of the two UU units, with a peak of 4.67 $mm \times yr^{-1}$ at 5.33–5.42 Ma (coinciding with deposition

of UU2 unit). The shortening magnitudes estimated for UU should be taken with some care because our approach for the restoration does not differentiated between pure shortening (conducted through layer folding and thrusting) and minibasin sinking with vertical differential subsidence (linked to halokinetic deformations and salt withdrawal).

3. Shortening decreases abruptly and monotonically from the Lower Pliocene time onward (~0.1 mm×yr^{-1} during the Pliocene Epoch and <0.003 mm×yr^{-1} during the Quaternary Period), accompanying the progressive uplift and basinward tilt of the continental margin.

(insert here Fig. 18, occupying the complete page)

Fig. 18. *Sequential restoration of the section shown in Fig. 14, documenting the structure of the Algerian margin.* ***(a)*** *Depth converted section;* ***(b)*** *restoration for the Late Pliocene (3.6 Ma);* ***(c)*** *restoration for the Early Pliocene (~4 Ma);* ***(d)*** *restoration for the UU2 unit (Messinian, 5.33 Ma);* ***(e)*** *restoration for the UU1 unit (Messinian, ~5.42 Ma);* ***(f)*** *restoration for the top of the Messinian salt (Messinian, 5.55 Ma); and* ***(g)*** *restoration for the base of the Messinian salt (possibly at 5.97 Ma). Seismic units are detailed in Fig. 7 and Table 1. Details of the restoration, the depth conversion, and an explanation of the circled numbers are provided in the text. Red and blue numbers mark observations about the stratigraphy of the units and the tectonic processes, respectively, as detailed in the text. Approximate correction of the pull-up effects observed below major salt structures is marked with dotted lines in (a). Uncertain elements of the restorations (b–g) are marked with discontinuous lines. Numerical results of the restoration are summarized in Table 2.*

Since the deposition of the Messinian salt, the overall plate-tectonic scenario consists in an oblique (northwest) convergence of the African (Nubia) plate. On the Algerian margin, we estimate that the average rate of convergence during the MSC was ~6.5 mm×yr^{-1} (corresponding to a north–south convergence of ~4.5 mm×yr^{-1}; Fig. 6b), diminishing to ~5.5 mm×yr^{-1} at present. These values are close to the shortening rates measured in our restoration for the postsalt MSC epoch (3.6–4.7 mm×yr^{-1}) and also follow the magnitudes inferred for the Pliocene–Quaternary period (≤0.12 mm×yr^{-1}; Table 2). This decrease of the shortening rate also matches the previous observations made at the Algerian margin toe, where only a limited tectonic shortening affecting the seafloor has been reported (Domzig et al., 2009; Medaouri et al., 2014; Leffondré et al., 2021).

We suggest, then, that most (if not all) of the plate convergence in this margin was accommodated by basement overthrusting and suprasalt shortening, with a deformation that accompanied the MSC and continued through the Pliocene and decreasing to almost zero during the Quaternary.

Units	Age (Ma) (1)	Shortening (m)		Deformation rate ($mm \times yr^{-1}$) (2)
		Incremental	Total	
Quaternary	0	-	-	<0.003
Upper Pliocene	3.60	~10	10	0.12
Lower Pliocene	4.00	50	60	0.06
UU2 (Mess.)	5.33	80	140	4.67
UU1 (Mess.)	5.42	420	560	3.55
Messinian salt	5.55	461	1021	0.30 (2.52) (3)
Base of salt	5.97 (5.60) (3)	126	1147	

Notes:
(1) Age for the top of the unit (Table 1), except for (3).
(2) Computed using the incremental shortening and the time interval corresponding to the deposition of the unit.
(3) First age considers that salt deposition initiated with the MSC. Value in parenthesis is taken assuming that there is a presalt Messinian sequence, the LU unit (i.e., including the MSC Stage 1). See text for discussion.

Table 2. *Estimated shortening of the Algerian margin according to the restoration shown in Fig. 18:*

7. Tectonic summary and salt-tectonic implications

The varied structure of the Algerian Basin margins in the Western Mediterranean Sea is illustrated with two regional sections that contain a simplified version of our seismic interpretation (Fig. 19). One of the main simplifications in these regional sections is that we simplify the two UU subunits into a single unit. Fig. 19a joins the interpretations in Figs. 9 and 17 to show a continuous north–south section from the Algerian margin to the Iberian margin in the central domain of the study sector of the Algerian Basin. The western domain of the basin is illustrated in Fig. 19b, connecting two highly oblique sections: one west–east across the Alboran margin (Fig. 11) and the other north–south across the westernmost sector of the Algerian margin (Fig. 14). To further support the regional analysis of the basin, we have generated depth conversions of these sections (Fig. 20). These depth sections schematize the salt structures and incorporate results from other geophysical studies that document the position of the crust–mantle boundary and provide information about the depths of the main stratigraphic discontinuities, like top of basement, base of salt, and thickness of the suprasalt layer. Results from gravity models and data from seismic refraction and tomography have been included in these sections, coming from studies on the Algerian margin (Badji et al., 2015; Klingelhoefer et al., 2022), the East Alboran Basin (Booth-Rea et al., 2018; Gómez de la Peña et al., 2020), and the Iberian margin (Hinz, 1973; Gallart et al., 1997; Sàbat et al., 1997; Driussi et al., 2015b; Kumar et al., 2021).

Sections in Figs. 19 and 20 necessarily do not capture the possible component of lateral-motion component along faults and even along the continent–oceanic boundary but summarize the main results of our study. The complete view of the Algerian Basin, from the African to the Iberian margins, makes possible the extraction of the following summary remarks.

The Algerian margin contains a narrow OCT domain accompanied by a steep geometry of Moho discontinuity. In addition, this margin shows multiple evidence for shortening since the Middle Miocene that continues to the present (according to the seismicity, e.g., Aoudia et al. [2000], Yelles-Chaouche et al. [2006], Kherroubi et al. [2009, 2017], and Soumaya et al. [2018]). Our observations are summarized as follows (Figs. 19, 20):

(insert here Fig. 19. Landscape orientation of the page to reproduce the illustration and its maximum size)

Fig. 19. *Sections (in TWT) of the Algerian Basin and its margins merging a simplified version of seismic interpretations.* ***(a)*** *North–south section from version from the Algerian margin to the Iberian margin containing the offshore continuation of the Internal Betics (Alboran Domain) (Figs. 9b, 17b).* ***(b)*** *Composite section in the westernmost Algerian Basin, showing the west–east section in the Alboran margin and the north–south structure of western Algerian margin (Figs. 11b, 14b). Double arrows correspond to positively inverted normal faults, with the open arrow indicating the sense of displacement of the previous normal fault. Locations of the profiles are shown in Figs. 1–3.*

(insert here Fig. 20. Landscape orientation of the page to reproduce the illustration and its maximum size)

Fig. 20. *Synthetic depth sections of the Algerian Basin and its margins, emphasizing the salt structures.* ***(a)*** *North–south section from version from the Algerian margin to the Iberian margin (according to Fig. 19a).* ***(b)*** *Composite section in the westernmost Algerian Basin, showing the west–east section of the Alboran margin joined with a north–south section across the western Algerian margin (according to Fig. 19b). Approximate depth conversion of the sedimentary sequences is generated using average velocities for seismic units (Table 1) and information provided by diverse tomographic studies in the Algerian margin (particularly Badji et al. [2015] and Klingelhoefer et al. [2022]), the Alboran margin (using Booth-Rea et al. [2018] and Gómez de la Peña et al. [2020]), and the Iberian margin (according to Driussi et al. [2015b] and Kumar et al. [2021]). Thick arrows mark the plate convergence imposed by the northwest convergence of the African plate, occurring since the Miocene Epoch (Fig. 5), and the inferred basement uplift and tilting of the North African margin. Locations of the profiles are shown in Figs. 1–3.*

1. The presalt series (Middle Miocene to Tortonian time) is deposited in inverted half-grabens that are thickest near the OCT (continent–ocean transition). These presalt

basins can be interpreted as flexural forebulge basins (Leprêtre et al., 2013; Hamai et al., 2015; Leffondré et al., 2021) formed in response to the northward thrusting of African crust over the oceanic crust of the Algerian Basin.

2. Inversion of these presalt basins is accomplished by basement folding and inversion of pre-existing normal faults.
3. Margin uplift accompanied basement-involved shortening, as is expressed by a moderate basinward tilting of the salt and cover at the landward end of the basin.
4. Moderate basinward gliding and extension of the cover is accomplished through salt rollers and rafts, in a narrow distal domain of the continental basement.
5. Shortening linked to basement shortening forms a wide salt-detached fold belt in the oceanic domain and leads to formation of salt-cored folds, pinched-off diapirs, and some associated salt thrusts. Shortened salt diapirs are preferentially located near the OCT. All these structures are detached along the base of the salt and were mostly formed by early contraction synchronous with the sedimentation of the UU unit (5.55–5.33 Ma, with a rate of shortening of 3.6–4.7 $mm \times yr^{-1}$), continuing with a moderate to low rate of shortening up to the present (from 4 Ma at a rate of $\leq$0.1 $mm \times yr^{-1}$) (Fig. 18, Table 2).

The structure of the western and northern margins of the Algerian Basin contains marked differences from the Algerian margin because crustal thinning and extension is the dominant structural style in both cases. The Alboran margin in the west has the following characteristics (Figs. 19b, 20b):

1. A progressive eastward thinning of the continental crust (the Moho discontinuity rises from 12 to 10 km depth in about 80 or 90 km), which has abundant intrusions of volcanic rocks.
2. The OCT is marked by a crustal neck (Fig. 11b).
3. Crustal thinning and eastward extension are accomplished by low-angle faulting, which forms extensional duplexes and a series of presalt half-grabens. The age of the infilling sediments is uncertain, but on the basis of regional considerations and the available information from nearby wells (Fig. 6), we suggest that most of the crustal thinning and necking occurred during Middle to Upper (pre-MSC) Miocene time.
4. The MSC series dips gently basinward, showing an opposite (westward) progressive thinning of the salt and the UU unit.

5. Subsidence of the oceanic domain with respect to the buoyant continental crust of the East Alboran Basin since the MSC is expressed by progressive basinward thickening of the Pliocene–Quaternary strata and the UU units and by salt gliding towards the oceanic domain.

The Iberian margin has been explored here through several vintage seismic profiles (Figs. 8–10). In spite of the relatively low quality of the seismic data and the locations of sparse number of available wells on the platform, we suggest that this margin has the following characteristics (Figs. 19a, 20a):

1. The margin platform, and the transition to the north to the Valencia Trough (Fig. 8), is deformed by gently south-dipping thrusts and open, west–southwest-trending folds that document compression in the offshore continuation of the orogenic front of the Betics (Alfaro et al., 2002; Maillard and Mauffret, 2013).
2. The continental crust gently thins towards the Algerian Basin. Crustal extension is seen as rotated crustal blocks limited by south-dipping listric faults that affect the offshore continuation of the Internal Betics (Alboran Domain) and part of the External Betics domain.
3. These faults define perched half-grabens that are filled by asymmetric wedges of Messinian–Quaternary-age, and possibly Tortonian-age sediments (Figs. 9b–11b). Although the age of the Messinian sequences in these perched basins is under debate (see discussion in Driussi et al. [2015a], Ochoa et al. [2015], and Raad et al. [2021]), and some of the sequences (particularly towards the east, near the island of Mallorca) might even have a thin salt layer (Maillard et al., 2014; Driussi et al., 2015a; Raad et al., 2021), we are inclined to assign them to the UU unit. Given that interpretation, we conclude that crustal thinning and extension on this margin has occurred from late MSC time (5.33 Ma) to the present, on the basis of minor crustal extension also documented on this margin in the form of high-angle faults that have been active from Pliocene to recent time (Acosta et al., 2001; Camerlenghi et al., 2009; Just et al., 2011; Maillard and Mauffret, 2013; Driussi et al., 2015a; Ochoa et al., 2015).
4. Salt structures consist of gentle pillows and smooth salt-cored anticlines developed in the oceanic domain. The salt layer pinches out landward at the base of the continental slope and is overlain by progressive landward thinning and onlap of the UU units (Figs. 8b, 9b). The salt at the base of the margin appears to be deformed into salt-cored folds, but the data are too poor to infer their timing or genesis with confidence.

In the Algerian Basin, we suggest that a deepwater salt-cored folded belt is developed on the Algerian margin, where the Messinian salt was originally thicker (Fig. 20). The northward convergence of the African plate during the Neogene and Quaternary Periods in the Western Mediterranean Sea (Fig. 5) caused basement-involved thrusting along the Algerian margin, which linked to the salt detachment to form the fold belt. This shortening also caused limited inversion of the presalt (Middle Miocene–Tortonian) “foredeep” flexural basin. In contrast, the northern and western margins of the Algerian Basin were differentially stretched by extensional faulting, causing moderate downslope (eastward) gliding of the MSC series in the transition to the Alboran margin and creating a series of perched, Messinian half-grabens on the Iberian margin. Both margins of the Algerian Basin document a long-lived history of Miocene crustal extension and differential subsidence that continues to the present.

One intriguing possibility for the salt-detached folds observed at the downdip end of the Iberian margin is that they are compressional structures marking the extreme distal end of the fold belt formed at the Algerian margin. We cannot disprove this, although the fact that a wide swath of undeformed strata lies between the Algerian and Iberian margins implies and argument against such interpretation.

Salt layers are well known to be important controls on the structural styles of passive margins. In addition to serving as effective decoupling levels between the salt and the overlying sequences, on many margins, gravity instability of the suprasalt cover generates a combination of updip and thin-skinned extension linked to downdip detached shortening in a deepwater fold belt (Fig. 21a) (e.g., Vendeville and Jackson, 1992; Letouzey et al., 1995; Rowan et al., 2004; Hudec and Jackson, 2007; Morley et al., 2011; Jackson and Hudec, 2017). Our case deviates from this scenario because the salt layer was originally deposited horizontally in the deep oceanic domain of the margin (Fig. 21b). We have documented how under this initial configuration, plate convergence promoted shortening by moderate subduction and overthrusting along the Algerian margin, nucleated along the OCT domain (e.g., Auzemery et al., 2021). This thick-skinned shortening linked upward to the salt detachment, originating a fold belt close to the proximal salt pinch-out (Fig. 21c).

(insert here Fig. 21)

Fig. 21. *Configuration and processes in salt continental margins, illustrating the case of deformations affecting a salt layer that was deposited after rifting.* ***(a)*** *Continental margin with a continuous and gently dipping salt layer. Gravity gliding and sliding generate suprasalt updip basinward extension and a linked, deepwater fold belt with salt inflation and local salt withdrawal in synclines (e.g.,*

Rowan et al., 2004; Jackson and Hudec, 2017). ***(b)*** *Continental margin with a deep and subhorizontal salt layer, with an inland pinch out situated close to the continent–oceanic transition (OCT). A suprasalt wedge prograding from the continental shelf above the salt layer generates an expulsion rollover and a broad salt folded belt in the deepwater region, which could affect the sequences lying above the oceanic crust (e.g., Vendeville, 2005; Zucker et al., 2020).* ***(c)*** *Possible configuration of a deep salt continental margin (case shown in [b]) after a moderate inversion by horizontal compression, which also generates an incipient subduction of the oceanic crust and pervasive shearing around the OCT domain. Initial position of the top of salt is marked in all the cases with a dotted purple line.*

8. Conclusions

1. The Messinian evaporites (including salt) in the westernmost Mediterranean Sea were deposited during the MSC between ~6.0 and ~5.55 Ma over oceanic crust flooring the deep Algerian Basin.

2. Along the Iberian margin, the upper (postsalt) Messinian sediments (possibly equivalent to the UU unit) onlap and thin progressively above several rotated extensional blocks, shaping a series of perched basins deepening progressively towards the oceanic Algerian Basin.

3. Listric normal faults merging towards the deep crust, accommodated crustal thinning of the Iberian margin and affect here the offshore continuation of the Internal Betics. Syn-extensional presalt (Middle Miocene to Tortonian) half-grabens, together with the geometry of the crustal listric faults, suggest that the Iberian margin was severely stretched southward beginning in the Middle Miocene and during the MSC.

4. Crustal thinning also occurred in the Alboran margin through basinwards (eastward) low-angle normal faults and extensional duplexes, which supporting presalt half-grabens filled with probable Middle Miocene to Tortonian sediments. Continent–oceanic transition (OCT) in this margin is accompanied by abundant Neogene–Quaternary volcanism and crustal necking. Salt and suprasalt sequences thin westward, documenting the existence of a differential subsidence between the continental East Alboran Basin and the oceanic Algerian Basin since at least the MSC.

5. Since the deposition of the MSC evaporites, the Messinian salt layer served as a detachment during the ongoing plate convergence between the African and Iberian (Eurasia) plates. North-northwest-directed overthrusting of continental crust over the oceanic domain in the Algerian margin tilted the continent seaward, produced limited

northward gliding along the salt layer, and shortened the suprasalt section, developing tighter and higher structures close to the ocean–continent boundary.

6. The Messinian salt layer constituted an effective decoupling level during deformation, promoting synsedimentary shortening in the suprasalt sequence, which is detached from partially inverted presalt half-grabens filled by Middle Miocene–Tortonian sediments.
7. The general scenario of the Algerian Basin and its contrasting margins constitutes a valuable example of a deep salt basin deformed after salt deposition by convergence-induced overthrusting of the continental crust in the southern margin. Shortening propagated along the basal detachment formed by the Messinian salt layer, causing synsedimentary folding of the suprasalt sequences.

Acknowledgments

This contribution has been benefited from the detailed reviews made by Joan F. Flinch, Franz Peltz, and Webster Mohriak. We acknowledge their numerous suggestions as well as the editorial management of Gabor Tari. JIS is indebted to continuous support and advise received from Albert W. Bally since our first meeting in 1989. Serve this contribution as recognition and gratitude to his guide. We thank Nancy Cottington and Pablo Ruiz for initial figure drafting. The support of Enrique Hernández and Juan Klimowitz in Gessal, as well as Susana Jiménez of ATH has been essential for this research. Travis Hobbs is acknowledged by his detailed edition of the manuscript. The project was funded by the Applied Geodynamics Laboratory (AGL) Industrial Associates program, comprising the following companies: BHP Billiton, BP, Chevron, Condor, EMGS, Eni, ExxonMobil, Hess, Ion, Murphy, OXY, Petrobras, Petronas, PGS, Repsol, RIPED, Rockfield, Shell, Talos Energy, TGS, and TotalEnergies (https://www.beg.utexas.edu/agl/sponsors). JD is indebted to the research team SPIRAL ("Sismique Profonde et Investigations Régionales en ALgérie") and acknowledges the funding and support by Brest University (UBO-IUEM) with a Leave for Research and Thematic Transition (CRCT) in Granada during spring 2017. Publication authorized by the Director, Bureau of Economic Geology, The University of Texas at Austin.

9. References

Acosta, J., Muñoz, A., Herranz, P., Palomo, C., Ballesteros, M., Vaquero, M., Uchupi, E., 2001. Geodynamics of the Emile Baudot Escarpment and the Balearic Promontory, Western Mediterranean. Marine and Petroleum Geology 18, 349–369. https://doi.org/10.1016/S0264-8172(01)00003-4.

Aïdi, C., Beslier, M.-O., Yelles-Chaouche, A.K., Klingelhoefer, F., Bracene, R., Galve, A., Bounife, A., Schenini, L., Hamai, L., Schnurle, P., Djellit, H., Sage, F., Charvis, P., Déverchère, J., 2018. Deep structure of the continental margin and basin off Greater Kabylia, Algeria – New insights from wide-angle seismic data modeling and multichannel seismic interpretation. Tectonophysics 728–729, 1–22. https://doi.org/10.1016/j.tecto.2018.01.007.

Alfaro, P., Delgado, J., Estévez, A., Soria, J.M., Yébenes, A., 2002. Onshore and offshore compressional tectonics in the eastern Betic Cordillera (SE Spain). Marine Geology 186, 337–349. https://doi.org/10.1016/S0025-3227(02)00336-5.

Andreetto, F., Aloisi, G., Raad, F., Heida, H., Flecker, R., Agiadi, K., Lofi, J., Blondel, S., Bulian, F., Camerlenghi, A., Caruso, A., Ebner, R., Garcia-Castellanos, D., Gaullier, V., Guibourdenche, L., Gvirtzman, Z., Hoyle, T.M., Meijer, P.T., Moneron, J., Sierro, F.J., Travan, G., Tzevahirtzian, A., Vasiliev, I., Krijgsman, W., 2021. Freshening of the Mediterranean Salt Giant: Controversies and certainties around the terminal (Upper Gypsum and Lago-Mare) phases of the Messinian Salinity Crisis. Earth Science-Reviews 216, 103577. https://doi.org/10.1016/j.earscirev.2021.103577.

Ansberque, C., 2011. Etude tectonique, structurale et sédimentaire de la région du plateau de Mostaganem (marge ouest-algérienne)—Mise en évidence d'une zone de relais transpressive. Master Thesis, SML GéoscienceS Océan, UBO (Brest University), 34 pp.

Aoudia, A., Vaccari, F., Suhadolc, P., Meghraoui, M., 2000. Seismogenic potential and earthquake hazard assessment in the Tell Atlas of Algeria. Journal of Seismolology 4, 79–98. https://doi.org/10.1023/A:1009848714019.

Arab, M., Rabineau, M., Déverchère, J., Bracène, R., Belhai, D., Roure, F., Marok, A., Bouyahiaoui, B., Granjeon, D., Andriessen, P., Sage, F., 2016. Tectonostratigraphic evolution of the eastern Algerian margin and basin from seismic data and onshore-offshore correlation. Marine and Petroleum Geology 77, 1355–1375. https://doi.org/10.1016/j.marpetgeo.2016.08.021.

[ATH] Archivo Técnico de Hidrocarburos, 2020. Ministerio para la Transición Ecológica y el Reto Demográfico, Gobierno de España. https://geoportal.minetur.gob.es/ATHv2/welcome.do (accessed 2018–2021).

Auzemery, A., Willingshofer, E., Sokoutis, D., Brun, J.P., Cloetingh, S.A.P.L., 2021. Passive margin inversion controlled by stability of the mantle lithosphere. Tectonophysics 817, 229042. https://doi.org/10.1016/j.tecto.2021.229042.

Auzende, J.-M., Bonnin, J., Olivet, J.-L., 1975. La marge nord-africaine considérée comme marge active. Bulletin de la Société géologique de France S7-XVII, 486–495. https://doi.org/10.2113/gssgfbull.S7-XVII.4.486.

Bache, F., Olivet, J.L., Gorini, C., Rabineau, M., Baztan, J., Aslanian, D., Suc, J.-P., 2009. Messinian erosional and salinity crises: View from the Provence Basin (Gulf of Lions, Western Mediterranean). Earth and Planetary Science Letters 286, 139–157. https://doi.org/10.1016/j.epsl.2009.06.021.

Bache, F., Popescu, S.M., Rabineau, M., Gorini, C., Suc, J.-P., Clauzon, G., Olivet, J.-L., Rubino, J.-L., Melinte-Dobrinescu, M.C., Estrada, F., Londeix, L., Armijo, R., Meyer, B., Jolivet, L., Jouannic, G., Leroux, E., Aslanian, D., Tadeu Dos Reis, A., Mocochain, L., Dumurdzanov, N., Zagorchev, I., Lesic, V., Tornic, D., Cagatay, M.N., Brun, J.P., Sokoutis, D., Csato, I., Ucarkus, G., Çakır, Z., 2012. A two-step process for the reflooding of the Mediterranean after the Messinian Salinity Crisis. Basin Research 24, 125–153. https://doi.org/10.1111/j.1365-2117.2011.00521.x.

Badji, R., 2014. Structure profonde de la croûte et potentiel pétrolier des bassins Sédimentaires à l'ouest de l'Algérie. Ph.D. Thesis, Université Nice–Sophia Antipolis, Nice, France, 160 pp.

Badji, R., Charvis, P., Bracene, R., Galve, A., Badsi, M., Ribodetti, A., Benaissa, Z., Klingelhoefer, F., Medaouri, M., Beslier, M.-O., 2015. Geophysical evidence for a transform margin offshore Western Algeria: A witness of a subduction-transform edge propagator? Geophysical Journal International 200, 1029–1045. https://doi.org/10.1093/gji/ggu454.

Bayer, R., Le Mouel, J.L., Le Pichon, X., 1973. Magnetic anomaly pattern in the western Mediterranean. Earth and Planetary Science Letters 19, 168–176. https://doi.org/10.1016/0012-821X(73)90111-8.

Bellucci, M., Aslanian, D., Moulin, M., Rabineau, M., Leroux, E., Pellen, R., Poort, J., Del Ben, A., Gorini, C., Camerlenghi, A., 2021. Salt morphologies and crustal segmentation relationship: New insights from the Western Mediterranean Sea. Earth-Science Reviews 222, 103818. https://doi.org/10.1016/j.earscirev.2021.103818.

Biju-Duval, B., Letouzey, J., Montadert, L., 1978. Structure and evolution of the Mediterranean Basins, in: Hsü, K.J., Montadert, L., Bernoulli, D., Bizon, G., Cita, M., Erickson, A., Fabricius, F., Garrison, R.E., Kidd, R.B., Mélières, F., Müller, C., Wright, R.C. (Eds.), Deep Sea Drilling Project, Initial Reports 42, part 1, 951–984. https://doi.org/10.2973/dsdp.proc.42-1.150.1978.

Booth-Rea, G., Ranero, C.R., Grevemeyer, I., 2018. The Alboran volcanic-arc modulated the Messinian faunal exchange and salinity crisis. Scientific Reports 8, 13015. https://doi.org/10.1038/s41598-018-31307-7.

Booth-Rea, G., Ranero, C.R., Martínez-Martínez, J.M., Grevemeyer, I., 2007. Crustal types and tertiary tectonic evolution of the Alborán sea, western Mediterranean. Geochemistry, Geophysics, Geosystems 8, Q10005. https://doi.org/10.1029/2007GC001639.

Bouillin, J.P., Durand-Delga, M., Olivier, P., 1986. Betic-Rifian and Tyrrhenian arcs: Distinctive features, genesis and development stages, in: Wezel, F.-C. (Ed.), Elsevier, Developments in Geotectonics 21, 281–304. https://doi.org/10.1016/B978-0-444-42688-8.50017-5.

Bouyahiaoui, B., Sage, F., Abtout, A., Klingelhoefer, F., Yelles-Chaouche, K., Schnürle, P., Marok, A., Déverchère, J., Arab, M., Galve, A., Collot, J.Y., 2015. Crustal structure of the eastern Algerian continental margin and adjacent deep basin: Implications for late Cenozoic geodynamic evolution of the western Mediterranean. Geophysical Journal International 201, 1912–1938. https://doi.org/10.1093/gji/ggv102.

Bougrine, A., Yelles-Chaouche, A.K., Calais, E., 2019.Active deformation in Algeria from continuous GPS measurements. Geophysical Journal International 217, 572–588. https://doi.org/10.1093/gji/ggz035.

Burollet, P.F., Said, A., Trouve, Ph., 1978. Slim holes drilled on the Algerian shelf, in: Ross, D.A., Neprochnov, Y.P., Hsü, K.S., Staffers, P., Supko, P., Trimonis, E.S., Percival, S.F., Erickson, A.J., Degens, E.T., Hunt, J.M., Manheim, F.T., Senalp, Traverse, A. (Eds.), Deep Sea Drilling Project, Initial Reports, part 2, 1181–1183. https://doi.org/10.2973/dsdp.proc.42-2.158.1978.

Camerlenghi, A., Accettella, D., Costa, S., Lastras, G., Acosta, J., Canals, M., Wardell, N., 2009. Morphogenesis of the SW Balearic continental slope and adjacent abyssal plain, Western Mediterranean Sea. International Journal of Earth Sciences 98, 735–750. https://doi.org/10.1007/s00531-008-0354-8.

Capitanio, F.A., Goes, S., 2006. Mesozoic spreading kinematics: Consequences for Cenozoic Central and Western Mediterranean subduction. Geophysical Journal International 165, 804–816. https://doi.org/10.1111/j.1365-246X.2006.02892.x.

Carlson, R., Raskin, G., 1984. Density of the ocean crust. Nature 311, 555–558. https://doi.org/10.1038/311555a0.

Carminati, E., Lustrino, M., Doglioni, C., 2012. Geodynamic evolution of the central and western Mediterranean: Tectonics vs. igneous petrology constraints. Tectonophysics 579, 173–192. https://doi.org/10.1016/j.tecto.2012.01.026.

Chalouan, A., Michard, A., El Kadiri, Kh., Negro, F., Frizon de Lamotte, D., Soto, J.I., Saddiqi, O., 2008. The Rif Belt, in: Michard, A., Chalouan, A., Saddiqi, O., Frizon de Lamotte, D. (Eds.), Continental Evolution: The Geology of Morocco. Structure, Stratigraphy, and Tectonics of the Africa-Atlantic-Mediterranean Triple Junction. Springer-Verlag, Berlin Heidelberg, Lecture Notes in Earth Sciences 116, 203–302.

Chenin, P., Schmalholz, S.M., Manatschal, G., Karner, G.D., 2018. Necking of the lithosphere: A reappraisal of basic concepts with thermo-mechanical numerical modeling. Journal of Geophysical Research: Solid Earth 123, 5279–5299. https://doi.org/10.1029/2017JB014155.

Christensen, N.I., Mooney, W.D., 1995. Seismic velocity structure and composition of the continental crust: A global view. Journal of Geophysical Research 100, 9761–9788. https://doi.org/10.1029/95JB00259.

Comas, M., Ivanov, M., Marro, G., Sánchez-Gómez, M., Fernández-Ibáñez, F., Marro, G., García, M., Román-Alpiste, M., Mhammdi, N., Vanneste, H., 2006a. Eastern Alboran margin: The transition between the Alboran and the Balearic-Algerian Basins, in: Kenyon, N.H., Ivanov, M.K., Akhmetzhanov, A.M., Kozlova, E.V. (Eds.), Interdisciplinary geoscience studies of the Gulf of Cadiz and Western Mediterranean basins. Preliminary results of investigations during the TTR-14 cruise of RV Professor Logachev (July-September, 2004), Intergovernmental Oceanographic Commission Technical Series 70, 48–52.

Comas, M., Ivanov, M., Marro, G., Sánchez-Gómez, M., Fernández-Ibáñez, F., García, M., Román-Alpiste, M., Mhammdi, N., Vanneste, H., 2006b. The Palomares and Cartagena margins, in: Kenyon, N.H., Ivanov, M.K., Akhmetzhanov, A.M., Kozlova, E.V. (Eds.), Interdisciplinary geoscience studies of the Gulf of Cadiz and Western Mediterranean basins. Preliminary results of investigations during the TTR- 14 cruise of RV Professor Logachev (July-September, 2004), Intergovernmental Oceanographic Commission Technical Series 70, 55–61.

Comas, M., Talukder, A., Woodside, J., Volkonskaya, A. 2000. South Balearic Basin: The Palomares and Mazarrón margins. Seismic Data, in: Kenyon, N.H., Ivanov, M.K., Akhmetzhanov, A.M., Akhmanov, G.G. (Eds.), Multidisciplinary Study of Geological Processes on the North East Atlantic and Western Mediterranean Margins. Preliminary results of geological and geophysical investigations during the TTR-9 cruise of R/V Professor Logachev (June-July, 1999), Intergovernmental Oceanographic Commission Technical Series 56, 91–95.

Comas, M.C., Dañobeitia, J.J., Álvarez-Marrón, J., Soto, J.I., 1997. Crustal reflections and structure in the Alboran Basin: Preliminary results of the ESCI-Alboran Survey. Revista de la Sociedad Geológica de España 8, 529–542.

Comas, M.C., García-Dueñas, V., Jurado, M.J., 1992. Neogene tectonic evolution of the Alboran Basin from MCS data. Geo-Marine Letters 12, 157–164. https://doi.org/10.1007/BF02084927.

Comas, M.C., Platt, J.P., Soto, J.I., Watts, A.B., 1999. The origin and tectonic history of the Alboran basin: Insights from Leg 161 results, in: Zahn, R., Comas, M. C., Klaus, A., et al. (Eds.), Proceedings of the Ocean Drilling Program, Scientific Results 161, 555–580. https://doi.org/10.2973/odp.proc.sr.161.262.1999.

Comas, M.C., Soto, J.I., Talukder, A.R., TTR-12 Leg 3, MARSIBAL 1 Scientific Party, 2003. Discovering active mud volcanoes in the Alboran Sea, western Mediterranean, in: Marani, M., Akhmanov, G., Suzyumov, A. (Eds.), Geological and Biological Processes at Deep-Sea European Margins and Oceanic Basins. Intergovernmental Oceanographic Commission, Workshop Report 187, 14–16.

Dal Cin, M., Ben, A., Mocnik, A., Accaino, F., Geletti, R., Wardell, N., Zgur, F., Camerlenghi, A, 2016. Seismic imaging of Late Miocene (Messinian) evaporites from Western Mediterranean backarc basins. Petroleum Geoscience 22, 297–308. https://doi.org/10.1144/petgeo2015-096.

Dale, M.S., Marín-Moreno, H., Falcon-Suarez, I.H., Grattoni, C., Bull, J.M., McNeill, L.C., 2021. The Messinian Salinity Crisis as a trigger for high pore pressure development in the Western Mediterranean. Basin Research 33, 2202–2228. https://doi.org/10.1111/bre.12554.

DeMets, C., Gordon, R.G., Argus, D.F., Stein, S., 1994. Effect of recent revisions to the geomagnetic reversal time scale on estimates of current plate motions. Geophysical Research Letters 21, 2191–2194. https://doi.org/10.1029/94GL02118.

DeMets, C., Iaffaldano, G., Merkouriev, S., 2015. High-resolution Neogene and Quaternary estimates of Nubia-Eurasia-North America plate motion. Geophysical Journal International 203, 416–427. https://doi.org/10.1093/gji/ggv277.

Déverchère, J., Yelles, K., Domzig, A., Mercier de Lépinay, B., Bouillin, J.-P., Gaullier, V., Bracène, R., Calais, E., Savoye, B., Kherroubi, A., Le Roy, P., Pauc, H., Dan, G., 2005. Active thrust faulting offshore Boumerdes, Algeria, and its relations to the 2003 M_w 6.9 earthquake. Geophysical Research Letters. 32, L04311. https://doi.org/10.1029/2004gl021646.

Dewey, J.F., Helman, M.L., Turco, E., Hutton, D.W.H., Knott, S.D., 1989. Kinematics of the western Mediterranean, in: Coward, M.P., Dietrich, D., Park, R.G. (Eds.), Alpine Tectonics, Geological Society, London, Special Publication 45, 265–283. https://doi.org/10.1144/GSL.SP.1989.045.01.15.

Do Couto, D., Gorini, C., Jolivet, L., Lebret, N., Augier, R., Gumiaux, C., d'Acremont, E., Ammar, A., Jabour, H., Auxietre, J.-L., 2016. Tectonic and stratigraphic evolution of the Western Alboran Sea Basin in the last 25 Myrs. Tectonophysics 677–678, 280–311. https://doi.org/10.1016/j.tecto.2016.03.020.

Domzig, A., Gaullier, V., Giresse, P., Pauc, H., Déverchère, J., Yelles, K., 2009. Deposition processes from echo-character mapping along the western Algerian margin, Oran–Tenes), Western Mediterranean. Marine and Petroleum Geology 26, 673–694. https://doi.org/10.1016/j.marpetgeo.2008.05.006.

Domzig, A., Yelles, K., Le Roy, Ch., Déverchère, J., Bouillin, J.-P., Bracène, R., Mercier de Lépinay, B., Le Roy, P., Calais, E., Kherroubi, A., Gaullier, V., Savoye, B., Pauc, H., 2006. Searching for the Africa–Eurasia Miocene boundary offshore western Algeria (MARADJA’03 cruise). Comptes Rendus Geoscience 338, 80–91. https://doi.org/10.1016/j.crte.2005.11.009.

Driussi, O., Briais, A., Maillard, A., 2015b. Evidence for transform motion along the South Balearic margin and implications for the kinematics of opening of the Algerian basin. Bulletin de la Société Géologique de France 186, 353–370. https://doi.org/10.2113/gssgfbull.186.4-5.353.

Driussi, O., Maillard, A., Ochoa, D., Lofi, J., Chanier, F., Gaullier, V., Briais, A., Sage, F., Sierro, F., García, M., 2015a. Messinian Salinity Crisis deposits widespread over the Balearic Promontory: Insights from new high-resolution seismic data. Marine and Petroleum Geology 66, 41–54. https://doi.org/10.1016/j.marpetgeo.2014.09.008.

Duggen, S., Hoernle, K., Van den Bogaard, P., Harris, C., 2004. Magmatic evolution of the Alboran region: The role of subduction in forming the western Mediterranean and causing the Messinian salinity crisis. Earth and Planetary Science Letters 218, 91–108. https://doi.org/10.1016/S0012-821x(03)00632-0.

Duggen, S., Hoernle, K., van den Bogaard, P., Rupke, L., Morgan, J.P., 2003. Deep roots of the Messinian salinity crisis. Nature 422, 602–606. https://doi.org/10.1038/Nature01553.

[ENIEPSA] Empresa Nacional de Investigación y Explotación de Petróleo, S.A., 1979. Informe final del sondeo Torrevieja Marino C-1, 75 pp.

ESSO Exploration Spain, 1981. Muchamiel-1, final well report. ESSO Exploration Spain, Inc., 87 pp.

Estrada, F., Ercilla, G., Gorini, C., Alonso, B., Vazquez, J.T., García-Castellanos, D., Juan, C., Maldonado, A., Ammar, A., Elabbassi, M., 2011. Impact of pulsed Atlantic water inflow into the Alboran Basin at the time of the Zanclean flooding. Geo-Marine Letters 31, 361–376. https://doi.org/10.1007/s00367-011-0249-8.

Fernandes, R.M.S., Ambrosius, B.A.C., Noomen, R., Bastos, L., Wortel, M.J.R., Spakman, W., Govers, R., 2003. The relative motion between Africa and Eurasia as derived from ITRF2000 and GPS data. Geophysics Research Letters 30, 1828. https://doi.org/10.1029/2003GL017089.

Fernández-Ibáñez, F., Soto, J.I., 2017. Pore pressure and stress regime in a thick extensional basin with active shale diapirism, Western Mediterranean. AAPG Bulletin 101, 233–264. https://doi.org/10.1306/07131615228.

Fernández-Ibáñez, F., Soto, J.I., Zoback, M.D., Morales, J., 2007. Present-day stress field in the Gibraltar Arc, Western Mediterranean. Journal of Geophysical Research, Solid Earth 112, no. B08404. https://doi.org/10.1029/2006JB004683.

Fernández-Puga, M.C., Vázquez, J.T., Somoza, L., Díaz del Rio, V., Medialdea, T., Mata, M.P., León, R., 2007. Gas-related morphologies and diapirism in the Gulf of Cádiz. Geo-Marine Letters 27, 213–221. https://doi.org/10.1007/s00367-007-0076-0.

Fernández Soler, J., Martínez-Ruiz, F., Akhmanov, G., Akhmetzhanov, A., Stadnitskaya, A., Kozlova, E., Sautkin, A., Mazurenko, L., Ovsyannikov, D., Sadekov, A., Belenkaya, I., Suslova, E., Goncharov, D., 2000. South Balearic Basin: The Palomares and Mazarrón margins–Bottom sampling results, in: Kenyon, N.H., Ivanov, M.K., Akhmetzhanov, A.M., Akhmanov, G.G. (Eds.), Multidisciplinary Study of Geological Processes on the North East Atlantic and Western Mediterranean Margins. Preliminary Results of Geological and Geophysical Investigations During the TTR-9 Cruise of R/V Professor Logachev (June-July, 1999). Intergovernmental Oceanographic Commission Technical Series 56,98–99.

Flecker, R., Krijgsman, W., Capella, W., de Castro Martíns, C., Dmitrieva, E., Mayser, J.P., Marzocchi, A., Modestu, S., Ochoa, D., Simon, D., Tulbure, M., van den Berg, B., van der Schee, M., de Lange, G., Ellam, R., Govers, R., Gutjahr, M., Hilgen, F., Kouwenhoven, T., Lofi, J., Meijer, P., Sierro, F.J., Bachiri, N., Barhoun, N., Alami, A. C., Chacon, B., Flores, J.A., Gregory, J., Howard, J., Lunt, D., Ochoa, M., Pancost, R., Vincent, S., Yousfi, M.Z., 2015. Evolution of the late Miocene Mediterranean-Atlantic gateways and their impact on regional and global environmental change. Earth-Science Reviews 150, 365–392. https://doi.org/10.1016/j.earscirev.2015.08.007.

Flinch, J.F., 1993. Tectonic evolution of the Gibraltar Arc. Ph.D. Thesis, Rice University, Houston, Texas, 381 pp.

Flinch, J.F., 1996. Accretion and extensional collapse of the External Western Rif, Northern Morocco, in: Ziegler, A., Horvath, F. (Eds.), Peri-Tethys Memoir 2, Structure and Prospects of Alpine Basins and Forelands. Muséum National d'Histoire Naturelle, Mémoires 170, 61–85.

Flinch, J.F., Soto, J.I., 2017. Allochthonous Triassic and salt tectonic processes in the Betic-Rif Orogenic Arc, in: Soto, J.I., Flinch, J.F., Tari, G. (Eds.), Permo-Triassic Salt Provinces of Europe, North Africa and the Atlantic Margins. Elsevier,417–446. http://dx.doi.org/10.1016/B978-0-12-809417-4.00020-3.

Frasca, G., Manatschal, G., Cadenas, P., Miró, J., Lescoutre, R., 2021. A kinematic reconstruction of Iberia using intracontinental strike- slip corridors. Terra Nova 33, 573–581. https://doi.org/10.1111/ter.12549.

Frizon de Lamotte, D., Saint Bezar, B., Bracène, R., Mercier, E., 2000. The two main steps of the Atlas building and geodynamics of the western Mediterranean. Tectonics 19, 740–761. https://doi.org/10.1029/2000TC900003.

Galdeano, A., Rossignol, J.C., 1977. Assemblage à altitude constante de cartes d'anomalies magnétiques couvrant l'ensemble du bassin occidental de la Méditerranée. Bulletin de la Société Géologique de France 7, 461–468.

Gallart, J., Vidal, N., Estévez, A., Pous, J., Sàbat, F., Santisteban, C., Suriñach, E., ESCI-València Trough group, 1997. The ESCI-València Trough vertical reflection experiment: A seismic image of the crust from the NE Iberian Peninsula to the Western Mediterranean. Revista de la Sociedad Geológica de España 8, 401–415.

Garcia-Castellanos, D., Estrada, F., Jiménez-Munt, I., Gorini, C., Fernàndez, M., Vergés, J., De Vicente, G., 2009. Catastrophic flood of the Mediterranean after the Messinian salinity crisis. Nature 462, 778–781. https://doi.org/10.1038/nature08555.

Garcia-Castellanos, D., Villaseñor, A., 2011. Messinian salinity crisis regulated by competing tectonics and erosion at the Gibraltar Arc. Nature 480, 359–363. https://doi.org/10.1038/nature10651.

García-Dueñas, V., Balanyá, J.C., Martínez-Martínez, J.M., 1992. Miocene extensional detachments in the outcropping basement of the northern Alboran Basin (Betics) and their tectonic implications. Geo-Marine Letters 12, 88–95. https://doi.org/10.1007/BF02084917.

García‐ Veigas, J., Gibert, L., Cendón, D.I., Artiaga, D., Corbí, H., Soria, J.M., Lowenstein, T.K., Sanz, E., 2020. Late Miocene evaporite geochemistry of Lorca and Fortuna basins (Eastern Betics, SE Spain): Evidence of restriction and continentalization. Basin Research 32, 916–948. https://doi.org/10.1111/bre.12408.

Gaullier, V., Chanier, F., Lymer, G., Vendeville, B., Maillard, A., Thinon, I., Lofi, J., Sage, F., Loncke, L., 2014. Salt tectonics and crustal tectonics along the Eastern Sardinian margin, Western Tyrrhenian: New insights from the "METYSS 1" cruise. Tectonophysics 615–616, 69–84. https://doi.org/10.1016/j.tecto.2013.12.015.

[GEBCO] Global Bathymetric Chart of the Oceans-Bathymetric Compilation Group 2019, 2019. The GEBCO_2019 Grid - a continuous terrain model of the global oceans and land. British Oceanographic Data Centre, National Oceanography Centre, NERC, UK. https://doi.org/10.5285/836f016a-33be-6ddc-e053-6c86abc0788.

Geletti, R., Zgur, F., Del Ben, A., Buriola, F., Fais, S., Fedi, M., Forte, E., Mocnik, A., Paoletti, V., Pipan, M., Ramella, R., Romeo, R., Romi, A., 2014. The Messinian Salinity Crisis: New seismic evidence in the West-Sardinian Margin and Eastern Sardo-Provençal Basin (West Mediterranean Sea). Marine Geology 351, 76–90. https://doi.org/10.1016/j.margeo.2014.03.019.

Giaconia, F., Booth-Rea, G., Ranero, C.R., Gràcia, E., Bartolome, R., Calahorrano, A., Lo Iacono, C., Vendrell, M.G., Cameselle, A.L., Costa, S., Gómez de la Peña, L., Martínez-Loriente, S., Perea, H., Viñas, M., 2015. Compressional tectonic inversion of the Algero-Balearic basin: Latemost Miocene to present oblique convergence at the Palomares margin, Western Mediterranean. Tectonics 34, 1516–1543. https://doi.org/10.1002/2015TC003861.

Gómez de la Peña, L., Grevemeyer, I., Kopp, H., Díaz, J., Gallart, J., Booth‐ Rea, G., Gràcia, E., Ranero, C., 2020. The lithospheric structure of the Gibraltar Arc System from wide‐ angle seismic data. Journal of Geophysical Research: Solid Earth 125, e2020JB019854. https://doi.org/10.1029/2020JB019854.

Gómez de la Peña, L., Ranero, C.R., Gràcia, E., 2018. The crustal domains of the Alboran Basin (western Mediterranean). Tectonics 37, 3352–3377. https://doi.org/10.1029/2017TC004946.

Gómez de la Peña, L., Ranero, C. R., Gràcia, E., Booth-Rea, G., 2021. The evolution of the westernmost Mediterranean basins. Earth-Science Reviews 214, 103445. https://doi.org/10.1016/j.earscirev.2020.103445.

Gorini, C., Montadert, L., Rabineau, M., 2015. New imaging of the salinity crisis: Dual Messinian lowstand megasequences recorded in the deep basin of both the eastern and western Mediterranean. Marine and Petroleum Geology 66, 278–294. https://doi.org/10.1016/j.marpetgeo.2015.01.009.

Gràcia, E., Bartolome, R., Lo Iacono, C., Moreno, X., Stich, D., Martínez-Diaz, J.J., Bozzano, G., Martínez-Loriente, S., Perea, H., Diez, S., Masana, E., Dañobeitia, J.J., Tello, O., Sanz, J.L., Carreño, E., EVENT-SHELF Team, 2012. Acoustic and seismic imaging of the Adra Fault, NE Alboran Sea. In search of the source of the 1910 Adra earthquake. Natural Hazards and Earth System Sciences 12, 3255–3267. https://doi.org/10.5194/nhess-12-3255-2012.

Gràcia, E., Pallàs, R., Soto, J.I., Comas, M.C., Moreno, X., Masana, E., Santanach, P., Dieza, S., García, M., Dañobeitia, J.J., HITS Scientific Party, 2006. Active faulting offshore SE Spain, Alboran Sea. Implications for earthquake hazard assessment in the Southern Iberian Margin. Earth and Planetary Science Letters 241, 734–749. https://doi.org/10.1016/j.epsl.2005.11.009.

Gueguen, E., Doglioni, C., Fernàndez, M., 1998. On the post 25 Ma geodynamic evolution of the western Mediterranean. Tectonophysics 298, 259–269. https://doi.org/10.1016/S0040-1951(98)00189-9.

Haidar, S., Déverchère, J., Graindorge, D., Arab, M., Medaouri, M., Klingelhoefer, F., 2022. Back-arc dynamics controlled by slab rollback and tearing: A reappraisal of seafloor spreading and kinematic evolution of the Eastern Algero-Balearic basin (western Mediterranean) in the Middle-Late Miocene. Tectonics 41, e2021TC006877. https://doi.org/10.1029/2021TC006877.

Hamai, L., Petit, C., Abtout, A., Yelles-Chaouche, A., Déverchère, J., 2015. Flexural behaviour of the north Algerian margin and tectonic implications. Geophysical Journal International 201, 1426–1436. https://doi.org/10.1093/gji/ggv098.

Hamai, L., Petit, C., Le Pourhiet, L., Yelles-Chaouche, A., Déverchère, J., Beslier, M.O., Abtout, A., 2018. Towards subduction inception along the inverted North African margin of Algeria? Insights from thermo-mechanical models. Earth and Planetary Science Letters, 501, 13–23. https://doi.org/10.1016/j.epsl.2018.08.028.

Handy, M.R., Schmid, S.M., Bousquet, R., Kissling, E., Bernoulli, D., 2010. Reconciling plate-tectonic reconstructions of Alpine Tethys with the geological–geophysical record of spreading and subduction in the Alps. Earth-Science Reviews 102, 121–158. https://doi.org/10.1016/j.earscirev.2010.06.002.

Haq, B., Gorini, C., Baur, J., Moneron, J., Rubino, J.-L., 2020. Deep Mediterranean's Messinian evaporite giant: How much salt? Global and Planetary Change 184, 103052. https://doi.org/10.1016/j.gloplacha.2019.103052.

Hatzfeld, D., The Working Group for Deep Seismic Sounding in the Alboran Sea 1974, 1978. Crustal seismic profiles in the Alboran Sea — Preliminary results. Pure and Applied Geophysics 116, 167–180. https://doi.org/10.1007/BF00878991.

Hinz, K., 1973. Crustal structure of the Balearic sea. Tectonophysics 20, 295–302. https://doi.org/10.1016/0040-1951(73)90118-2.

Hosseinpour, M., Williams, S., Seton, M., Barnett-Moore, N., Dietmar Müller, R., 2016. Tectonic evolution of Western Tethys from Jurassic to present day: Coupling geological and geophysical data with seismic tomography models. International Geology Review 58, 1616–1645. https://doi.org/10.1080/00206814.2016.1183146.

Hsü, K.J., Montadert, L., Bernoulli, D., Cita, M.B., Erikson, A., Garrison, R.E., Kidd, R.B., Melieres, F., Muller, C., Wright, R.H., 1977. History of the Mediterranean salinity crisis. Nature 267, 399–403. https://doi.org/10.1038/267399a0.

Hudec, M.R., Jackson, M.P.A., 2007. Terra infirma: Understanding salt tectonics. Earth-Science Reviews 82, 1–28. https://doi.org/10.1016/j.earscirev.2007.01.001.

Jackson, M.P.A., Hudec, M.R., 2017. Salt Tectonics—Principles and Practice. Cambridge University Press, 498 pp. https://doi.org/10.1017/9781139003988.

Jolivet, L., Baudin, T., Calassou, S., Chevrot, S., Ford, M., Issautier, B., Lasseur, E., Masini, E., Manatschal, G., Mouthereau, F., Thinon, I., Vidal, O., 2021a. Geodynamic evolution of a wide plate boundary in the Western Mediterranean, near-field versus far-field interactions. Bulletin de la Société Géologique de France 192, 48. https://doi.org/10.1051/bsgf/2021043.

Jolivet, L., Menant, A., Roche, V., Le Pourhiet, L., Maillard, A., Augier, R., Do Couto, D., Gorini, C., Thinon, I., Canva, A., 2021b. Transfer zones in Mediterranean back-arc regions and tear faults. Bulletin de la Société Géologique de France 192, 11. https://doi.org/10.1051/bsgf/2021006.

Jolivet, L., Faccenna, C., Agard, P., Frizon de Lamotte, D., Menant, A., Sternai, P., Guillocheau, F., 2015. Neo-Tethys geodynamics and mantle convection: from extension to compression in Africa and a conceptual model for obduction. Canadian Journal of Earth Sciences 53, 1190–1204. https://doi.org/10.1139/cjes-2015-0118.

Just, J., Hübscher, C., Betzler, C., Lüdmann, T., Reicherter, K., 2011. Erosion of continental margins in the Western Mediterranean due to sea-level stagnancy during the Messinian Salinity Crisis. Geo-Marine Letters 31, 51–64. https://doi.org/10.1007/s00367-010-0213-z.

Kherroubi, A., Déverchère, J., Yelles, A., Mercier de Lépinay, B., Domzig, A., Cattaneo, A., Bracène, R., Gaullier, V., Graindorge, D., 2009. Recent and active deformation pattern off the easternmost Algerian margin, Western Mediterranean Sea: New evidence for contractional tectonic reactivation. Marine Geology 261, 17–32. https://doi.org/10.1016/j.margeo.2008.05.016.

Kherroubi, A., Yelles-Chaouche, A., Koulakov, I., Déverchère, J., Beldjoudi, H., Haned, A., Semmane, F., Aidi, C., 2017. Full aftershock sequence of the M_w 6.9 2003 Boumerdes earthquake, Algeria: Space–time distribution, local tomography and seismotectonic implications. Pure and Applied Geophysics 174, 2495–2521. https://doi.org/10.1007/s00024-017-1571-5.

Kirkham, C., Bertoni, C., Cartwright, J., Lensky, N.G., Sirota, I., Rodriguez, K., Hodgson, N., 2020. The demise of a “salt giant” driven by uplift and thermal dissolution. Earth and Planetary Science Letters 531, 115933. https://doi.org/10.1016/j.epsl.2019.115933.

Klingelhoefer, F., Déverchère, J., Graindorge, D., Aïdi, C., Badji, A., Bouyahiaoui, B., Leprêtre, A., Mihoubi, A., Beslier, M.-O., Charvis, Ph., Schnurle, Ph., Sage, F., Medaouri, M., Arab, M., Bracene, R., Yelles-Chaouche, K., Badsi, M., Galvé, A., Géli, L., 2022. Formation, segmentation and deep crustal structure variations along the Algerian margin from the SPIRAL seismic experiment. Journal of African Earth Sciences 186, 104433. https://doi.org/10.1016/j.jafrearsci.2021.104433.

Krijgsman, W., Capella, W., Simon, D., Hilgen, F.J., Kouwenhoven, T.J., Meijer, P.Th., Sierro, F.J., Tulbure, M.A., van den Berg, B.C.J., van der Schee, M., Flecker, R., 2018. The Gibraltar Corridor: watergate of the Messinian Salinity Crisis. Marine Geology 403, 238–246. https://doi.org/10.1016/j.margeo.2018.06.008.

Krijgsman, W., Garcés, M., Agustí, J., Raffi, I., Taberner, C., Zachariasse, W.J., 2000. The 'Tortonian salinity crisis' of the eastern Betics (Spain). Earth and Planetary Science Letters 181, 497–511. https://doi.org/10.1016/S0012-821X(00)00224-7.

Krijgsman, W., Hilgen, F.J., Raffi, I., Sierro, F.J., Wilson, D.S., 1999. Chronology, causes and progression of the Messinian salinity crisis. Nature 400, 652–655. https://doi.org/10.1038/23231.

Kumar, A., Fernàndez, M., Vergés, J., Torne, M., Jiménez-Munt, I., 2021. Opposite symmetry in the lithospheric structure of the Alboran and Algerian basins and their margins (Western Mediterranean): Geodynamic implications. Journal of Geophysical Research: Solid Earth, 126, e2020JB021388. https://doi.org/10.1029/2020JB021388.

Lastras, G., Canals, M., Broennimann, C., 2006. Balearic Basin. The Eivissa Channel area, in: Kenyon, N.H., Ivanov, M.K., Akhmetzhanov, A.M., Kozlova, E.V. (Eds.), Interdisciplinary Geoscience Studies of the Gulf of Cádiz and Western Mediterranean Basins. Preliminary Results of Investigations During the TTR-14 Cruise of RV Professor Logachev (July-September, 2004). Intergovernmental Oceanographic Commission Technical Series 70, 61–67.

Lastras, G., Canals, M., Urgeles, R., Hughes-Clarke, J.E., Acosta, J., 2004. Shallow slides and pockmark swarms in the Eivissa Channel, western Mediterranean Sea. Sedimentology 51, 837–850. https://doi.org/10.1111/j.1365-3091.2004.00654.x.

Leffondré, P., Déverchère, J., Medaouri, M., Klingelhoefer, F., Graindorge, D., Arab, M., 2021. Ongoing inversion of a passive margin: Spatial variability of strain markers along the Algerian margin and basin, Mediterranean Sea) and seismotectonic implications. Frontiers in Earth Science 9, 365. https://doi.org/10.3389/feart.2021.674584.

Le Pichon, X., Francheteau, J., Bonnin, J., 1973. Plate tectonics. Developments in Geotectonics 6, Elsevier Scientific Pub. Co., 300 pp.

Leprêtre, R., Frizon de Lamotte, D., Combier, V., Gimeno-Vives, O., Mohn, G., Eschard, R., 2018. The Tell-Rif orogenic system, Morocco, Algeria, Tunisia and the structural heritage of the southern Tethys margin. Bulletin de la Société Géologique de France 189, 10. https://doi.org/10.1051/bsgf/2018009.

Leprêtre, A., Klingelhoefer, F., Graindorge, D., Schnurle, P., Yelles, K., Déverchère, J., Bracene, R., 2013. Multiphased tectonic evolution of the Central Algerian margin from combined wide-angle and reflection seismic data off Tipaza, Algeria. Journal of Geophysical Ressearch, Solid Earth 118, 3899–3916. https://doi.org/10.1002/jgrb.50318.

Leroux, E., Aslanian, D., Rabineau, M., Gorini, C., Rubino, J.-L., Poort, J., Suc, J.-P., Bache, F., Blanpied, C., 2019. Atlas of the stratigraphic markers in the western Mediterranean with focus on the Messinian, Pliocene and Pleistocene of the Gulf of Lion. Commision for the Geological Map of the World, 73 pp. https://doi.org/10.14682/2019GULFLIONATL.

Letouzey, J., Colletta, B., Vially, R., Chermette, J.C., 1995. Evolution of salt-related structures in compressional settings, in: Jackson, M.P.A., Roberts, D.G., Snelson, S. (Eds.), Salt Tectonics: A Global Perspective. American Association of Petroleum Geologists, Memoir 65, 41–60.

Lofi, J., 2018. Seismic atlas of the Messinian Salinity Crisis Markers in the Mediterranean Sea. Volume 2. Commission for the Geological Map of the World and Société Géologique de France, Mémoires de la Société Géologique de France 181, 72 pp.

Lofi, J., Déverchère, J., Gaullier, V., Gillet, H., Gorini, C., Guennoc, P., Loncke, L., Maillard, A., Sage, F., Thinon, I., 2011. Seismic atlas of the "Messinian Salinity Crisis" markers in the Mediterranean and Black Seas. Commission for the Geological Map of the World and Société Géologie de France, Mémoires de la Société Géologique de France 179, 72 pp.

Lofi, J., Maillard, A., Madof, A., Amadori, C., Camerlenghi, A., Del Ben, A., Do Couto, D., Estrada, F., Gaullier, V., Lymer, G., Saule, M., 2018. Maps and legend: Extension map of the MSC seismic markers, in: Lofi, J. (Coord.), Seismic Atlas of the Messinian Salinity Crisis Markers in the Mediterranean Sea, Vol. 2. Commission for the Geological Map of the World (CGMW) and Mémoires de la Société Géologique de France 181, 72 pp.

Lofi, J., Sage, F., Déverchère, J., Loncke, L., Maillard, A., Gaullier, V., Thinon, I., Gillet, H., Guennoc, P., Gorini, C., 2011b. Refining our knowledge of the Messinian salinity crisis records in the offshore domain through multi-site seismic analysis. Bulletin de la Société Géologique de France 182, 163–180. https://doi.org/10.2113/gssgfbull.182.2.163.

Macchiavelli, C., Vergés, J., Schettino, A., Fernàndez, M., Turco, E., Casciello, E., Torné, M., Pierantoni, P.P., Tunini, L., 2017. A new southern North Atlantic isochron map: Insights into the drift of the Iberian plate since the Late Cretaceous. Journal of Geophysical Research: Solid Earth 122, 9603–9626. https://doi.org/10.1002/2017JB014769.

Maillard, A., Driussi, O., Lofi, J., Briais, A., Chanier, F., Hübscher, H. Gaullier, V., 2014. Record of the Messinian Salinity Crisis in the SW Mallorca area (Balearic promontory, Spain). Marine Geology 357, 304–320. https://doi.org/10.1016/j.margeo.2014.10.001.

Maillard, A., Mauffret, A., 2013. Structure and present-day compression in the offshore area between Alicante and Ibiza Island, Eastern Iberian Margin. Tectonophysics 591, 116–130. https://doi.org/10.1016/j.tecto.2011.07.007.

Martínez del Olmo, W., 2011a. El arrecife messiniense del sondeo Torrevieja Marino C-1 desde las líneas sísmicas (SE. de España). Revista de la Sociedad Geológica de España 24, 173–186.

Martínez del Olmo, W., 2011b. El Messiniense en el Golfo de Valencia y el Mar de Alborán: Implicaciones paleogeográficas y paleoceanográficas. Revista de la Sociedad Geológica de España 24, 237–253.

Martínez-García, P., 2012. Recent tectonic evolution of the Alboran Ridge and Yusuf regions. Ph.D. Thesis, Granada University, Spain, 277 pp.

Martínez-García, P., Comas, M., Soto, J.I., Lonergan, L., Watts, A.W., 2013. Strike-slip tectonics and basin inversion in the Western Mediterranean: The post-Messinian evolution of the Alboran Sea. Basin Research 25, 1–27. https://doi.org/10.1111/bre.12005.

Martínez-García, P., Soto, J.I., Comas, M., 2011. Recent structures in the Alboran Ridge and Yusuf fault zones based on swath bathymetry and sub-bottom profiling: evidence of active tectonics. Geo-Marine Letters 31, 19–36. https://doi.org/10.1007/s00367-010-0212-0.

Mauffret, A., 2007. The Northwestern (Maghreb) boundary of the Nubia (Africa) Plate. Tectonophysics 429, 21–44. https://doi.org/10.1016/j.tecto.2006.09.007.

Mauffret, A., Frizon de Lamotte, D., Lallemant, S., Gorini, C., Maillard, A., 2004. E-W opening of the Algerian Basin (Western-Mediterranean). Terra Nova 16, 257–264. https://doi.org/10.1111/j.1365-3121.2004.00559.x.

Mauffret, A., Maldonado, A., Campillo, A.C., 1992. Tectonic framework of the eastern Alboran and western Algerian basins (Western Mediterranean). Geo-Marine Letters 12, 104–110. https://doi.org/10.1007/BF02084919.

Mazzini, A., Martínez-Ruiz, F., Rodríguez-Tovar, F., Akhmanov, G., Akhmetzhanov, A., Kozlova, E., Torlov, V., Samoilov, A., Sarantsev, E., Sadekov, A., Poludetnika, E., Barvalina, O., Bileva, E., Blinova, V., Jiménez Espejo, F.J., 2003. The Almeria margin: Main results–Bottom sampling, in: Kenyon, N.H., Ivanov, M.K., Akhmetzhanov, A.M., Akhmanov, G.G. (Eds.), Interdisciplinary Geoscience Research on the North East Atlantic Margin, Mediterranean Sea and Mid-Atlantic Ridge–Preliminary Results of Geological and Geophysical Investigations During the TTR-12 Cruise of R/V Professor Logachev (June-August, 2002), Intergovernmental Oceanographic Commission Technical Series 56, 68–71.

Mazzoli, S., Helman, M., 1994. Neogene patterns of relative plate motion for Africa–Europe: Some implications for recent central Mediterranean tectonics. Geologische Rundschau 83, 464–468.

Medaouri, M., 2014. Origine de la segmentation de la marge Algérienne et implication sur l'évolution géodynamique et les ressources pétrolières. Ph.D. Thesis. Université de Bretagne Occidentale, Brest, France, 254 pp.

Medaouri, M., Bracene, R., Déverchère, J., Graindorge, D., Ouabadi, A., Yelles-Chaouche, A., 2012. Structural styles and Neogene petroleum system around the Yusuf-Habibas ridge, Alboran basin, Mediterranean Sea. Leading Edge 31, 776–785. https://doi.org/10.1190/tle31070776.1.

Medaouri, M., Déverchère, J., Graindorge, D., Bracène, R., Badji, R., Ouabadi, A., Yelles-Chaouche, K., Bendiab, G., 2014. The transition from Alboran to Algerian basins, Western Mediterranean Sea): Chronostratigraphy, deep crustal structure and tectonic evolution at the rear of a narrow slab rollback system. Journal of Geodynamics 77, 186–205. https://doi.org/10.1016/j.jog.2014.01.003.

Medialdea, T., Somoza, L., Pinheiro, L., Fernández-Puga, M.C., Vázquez, J.T., León, R., Ivanov, M.K., Magalhaes, Díaz-del-Río, V., Vegas, R., 2009. Tectonics and mud volcano development in the Gulf of Cádiz. Marine Geology 261, 48–63. https://doi.org/10.1016/j.margeo.2008.10.007.

Medialdea, T., Vegas, R., Somoza, L., Vázquez, J.T., Maldonado, A., Díaz-del-Río, V., Maestro, A., Córdoba, D., Fernández-Puga, M.C., 2004. Structure and evolution of the "Olistostrome" complex of the Gibraltar Arc in the Gulf of Cádiz, eastern Central Atlantic: Evidence from two long seismic cross-sections. Marine Geology 209, 173–198. https://doi.org/10.1016/j.margeo.2004.05.029.

Meijer, P.Th., Krijgsman, W., 2005. A quantitative analysis of the desiccation and re-filling of the Mediterranean during the Messinian Salinity Crisis. Earth and Planetary Science Letters 240, 510–520. https://doi.org/10.1016/j.epsl.2005.09.029.

Meilijson, A., Hilgen, F., Sepúlveda, J., Steinberg, J., Fairbank, V., Flecker, R., Waldmann, N.D., Spaulding, S.A., Bialik, O.M., Boudinot, F.G., Illner, P., Makovsky, Y., 2019. Chronology with a pinch of salt: Integrated stratigraphy of Messinian evaporites in the deep Eastern Mediterranean reveals long-lasting halite deposition during Atlantic connectivity. Earth-Science Reviews 194, 374–398. https://doi.org/10.1016/j.earscirev.2019.05.011.

Mihoubi, A., Schnürle, P., Benaissa, Z., Badsi, M., Bracene, R., Djelit, H., Geli, L., Sage, F., Agoudjil, A., Klingelhoefer, F., 2014. Seismic imaging of the eastern Algerian margin off Jijel: Integrating wide-angle seismic modelling and multichannel seismic pre-stack depth migration. Geophysical Journal International 198, 1486–1503. https://doi.org/10.1093/gji/ggu179.

Montadert, L., Letouzey, J., Mauffret, A. 1978. Messinian event: Seismic evidence, in: Hsü, K.J., Montadert, L., Bernoulli, D., Bizon, G., Cita, M., Erickson, A., Fabricius, F., Garrison, R.E., Kidd, R.B., Mélières, F., Müller, C., Wright, R.C. (Eds.), DSDP Initial Reports 42, pp. 1037–1050. https://doi.org/10.2973/dsdp.proc.42-1.154.1978.

Morley, C.K., King, R., Hillis, R., Tingay, M., Backe, G., 2011. Deepwater fold and thrust belt classification, tectonics, structure and hydrocarbon prospectivity: A review. Earth-Science Reviews 104, 41–91. https://doi.org/10.1016/j.earscirev.2010.09.010.

Obone-Zue-Obame, E.M., 2009. Tectonic and sedimentary consequences of the Messinian Salinity Crisis in Western Mediterranean. Ph.D. Thesis, University of Perpignan, France, 247 pp.

Obone-Zue-Obame, E.M., Gaullier, V., Sage, F., Maillard, A., Lofi, J., Vendeville, B., Thinon, I., Réhault, J.-P., MAURESC Shipboard Scientific Party, 2011. The sedimentary markers of the Messinian Salinity Crisis and their relation with salt tectonics on the Provençal margin (Western Mediterranean): Results from the "MAURESC" cruise. Bulletin de la Société Géologique de France 182, 181–196. https://doi.org/10.2113/gssgfbull.182.2.181.

Ochoa, D., Sierro, F.J., Lofi, J., Maillard, A., Flores, J.-A., Suárez, M., 2015. Synchronous onset of the Messinian evaporite precipitation: First Mediterranean offshore evidence. Earth and Planetary Science Letters 427, 112–124. https://doi.org/10.1016/j.epsl.2015.06.059.

Ortí, F., Rosell, L., Gibert, L., Moragas, M., Playà, E., Inglès, M., Rouchy, J.M., Calvo, J.P., Gimeno, D., 2014. Evaporite sedimentation in a tectonically active basin: The lacustrine Las Minas Gypsum unit (Late Tortonian, SE Spain). Sedimentary Geology 311, 17–42. https://doi.org/10.1016/j.sedgeo.2014.06.004.

Ousadou, F., Bezzeghoud, M., 2019. Seismicity of the Algerian Tell Atlas and the impacts of major earthquakes, in: Bendaoud, A., Hamimi, Z., Hamoudi, M., Djemai, S., Zoheir, B. (Eds.), The Geology of the Arab World—An Overview. Springer Geology, pp. 401–426. https://doi.org/10.1007/978-3-319-96794-3_11.

Pellen, R., Aslanian, D., Rabineau, M., Leroux, E., Gorini, C., Silenziario, C., Blanpied, C., Rubino, J.-P., 2016. The Minorca Basin: A buffer zone between the Valencia and Liguro-Provençal Basins (NW Mediterranean Sea). Terra Nova 28, 245–256. https://doi.org/10.1111/ter.12215.

Péron-Pinvidic, G., Manatschal, G., 2009. The final rifting evolution at deep magma-poor passive margins from Iberia-Newfoundland: A new point of view. International Journal of Earth Sciences 98, 1581–1597. https://doi.org/10.1007/s00531-008-0337-9.

Platt, J.P., Behr, W.M., Johanesen, K., Williams, J.R., 2013. The Betic-Rif Arc and its orogenic hinterland: A review. Annual Review of Earth and Planetary Sciences 41, 313–357. https://doi.org/10.1146/annurev-earth-050212-123951.

Platt, J.P., Soto, J.I., Whitehouse, M.J., Hurford, A.J., Kelley, S.P., 1998. Thermal evolution, rate of exhumation, and tectonic significance of metamorphic rocks from the floor of the Alboran extensional basin, western Mediterranean. Tectonics 17, 671-689. https://doi.org/10.1029/98TC02204.

Polyak, B.G., Fernandez, M., Khutorskoy, M.D., Soto, J.I., Basov, I.A., Comas, M.C., Khain, V.Y., Alonso, B., Agapova, G.V., Mazurova, I.S., Negredo, A., Tochitsky, V.O., de la Linde, J., Bogdanov, N.A., Banda, E., 1996. Heat flow in the Alboran Sea, western Mediterranean. Tectonophysics 263, 191–218. https://doi.org/10.1016/0040-1951(95)00178-6.

Poort, J., Lucazeau, F., Le Gal, V., Dal Cin, M., Leroux, E., Bouzid, A., Rabineau, M., Palomino, D., Battani, A., Akhmanov, G.G., Ferrante, G.M., Gafurova, D.R., Bachir, R.S., Koptev, A., Tremblin, M., Bellucci, M., Pellen, R., Camerlenghi, A., Migeon, S., Alonso, B., Ercilla, G., Yelles-Chaouche, A.-K., Khlystov, O.M., 2020. Heat flow in the Western Mediterranean: Thermal anomalies on the margins, the seafloor and the transfer zones. Tectonophysics 419, 106064. https://doi.org/10.1016/j.margeo.2019.106064.

Raad, F., Lofi, J., Maillard, A., Tzevahirtzian, A., Caruso, A., 2021. The Messinian Salinity Crisis deposits in the Balearic Promontory: An undeformed analog of the MSC Sicilian basins?? Marine and Petroleum Geology 124, 104777. https://doi.org/10.1016/j.marpetgeo.2020.104777.

Recanati, A., Missenard, Y., Leprêtre, R., Gautheron, C., Barbarand, J., Abbassene, F., Abdallah, N., Ouabadi, A., El Messaoud Derder, M., Boukari, C., Pinna-Jamme, R., Haurine, F., 2019. A Tortonian onset for the Algerian margin inversion: Evidence from low-temperature thermochronology. Terra Nova 31, 39–48. https://doi.org/10.1111/ter.12367.

Rehault, J.-P., Boillot, G., Mauffret, A., 1984. The Western Mediterranean Basin geological evolution. Marine Geology 55, 447–477. https://doi.org/10.1016/0025-3227(84)90081-1.

Roca, E., Frizon de Lamotte, D., Mauffret, A., Bracène, R., Vergés, J., Benaouali, N., Fernàndez, M., Muñoz, J.A., Zeyen, H., 2004. Transmed, Transect II: Aquitaine Basin - Pyrenees - Ebro Basin - Catalan Range - Valencia Trough Balearic Block - Algerian Basin - Kabylies - Atlas -Saharan Platform, in: Cavazza, W., Roure, F., Spakman, W., Stampfli, G.M., Ziegler, P.A. (Eds.), The TRANSMED Atlas–The Mediterranean Region From Crust to Mantle. Geological and Geophysical Framework of the Mediterranean and the Surrounding Areas. Springer.

Rodríguez Fernández, L.R., López Olmedo, F., Oliveira, J. T., Medialdea, T., Terrinha, P., Matas, J., Martín-Serrano, A., Martín Parra, L.M., Rubio, F., Marín, C., Montes, M., Nozal, F., 2015. Mapa Geológico de España y Portugal, escala 1:1.000.000, edición 2015. Instituto Geológico y Minero de España y Laboratorio Nacional de Energía y Geología de Portugal.

Roest, E.R., Srivastava, S.P., 1991. Kinematics of the plate boundaries between Eurasia, Iberia, and Africa in the North Atlantic from the Late Cretaceous to the present. Geology 19, 613–616. https://doi.org/10.1130/0091-7613(1991)019<0613:KOTPBB>2.3.CO;2.

Romagny, A., Jolivet, L., Menant, A., Bessière, E., Maillard, A., Canva, A., Gorini, C., Augier, R., 2020. Detailed tectonic reconstructions of the Western Mediterranean region for the last 35 Ma, insights on driving mechanisms. Bulletin de la Société Géologique de France 191, 37. https://doi.org/10.1051/bsgf/2020040.

Rosenbaum, G., Lister, G.S., Duboz, C., 2002. Relative motions of Africa, Iberia and Europe during Alpine orogeny. Tectonophysics 359, 117–129. https://doi.org/10.1016/S0040-1951(02)00442-0.

Rouchy, J.M., Caruso, A., 2006. The Messinian Salinity Crisis in the Mediterranean basin: A reassessment of the data and an integrated scenario. Sedimentary Geology 188–189, 35–67. https://doi.org/10.1016/j.sedgeo.2006.02.00.

Rouchy, J.M., Caruso, A., Pierre, C., Blanc-Valleron, M.-M., Bassetti, M.A., 2007. The end of the Messinian salinity crisis: Evidences from the Chelif Basin (Algeria). Palaeogeography, Palaeoclimatology, Palaeoecology 254, 386–417. https://doi.org/10.1016/j.palaeo.2007.06.015.

Roveri, M., Flecker, R., Krijgsman, W., Lofi, J., Lugli, S., Manzi, V., Sierro, F.J., Bertini, A., Camerlenghi, A., De Lange, G., Govers, R., Hilgen, F.J., Hübscher, C., Meijer, P.Th., Stoica, M., 2014. The Messinian salinity crisis: Past and future of a great challenge for marine sciences. Marine Geology 349, 113–125. https://doi.org/10.1016/j.margeo.2014.02.002.

Roveri, M., Gennari, R., Ligi, M., Lugli, S., Manzi, V., Reghizzi, M., 2019. The synthetic seismic expression of the Messinian salinity crisis from onshore records: Implications for shallow-to deep-water correlations. Basin Research 31, 1121–1152. https://doi.org/10.1111/bre.12361.

Rowan, M.G., Peel, F.J., Vendeville, B.C., 2004. Gravity-driven fold belts on passive margins, in: McClay, K.R. (Ed.), Thrust Tectonics and Hydrocarbon Systems. American Association of Petroleum Geologists, Memoir 82, 157–182.

Rowan, M.G., Ratliff, R.A., 2012. Cross-section restoration of salt-related deformation: Best practices and potential pitfalls. Journal of Structural Geology 41, 24–37. https://doi.org/10.1016/j.jsg.2011.12.012.

Ryan, W.B.F., 2008. Modeling the magnitude and timing of evaporative drawdown during the Messinian Salinity Crisis. Stratigraphy 5, 227–243.

Ryan, W.B.F., Cita, M.B., 1978. The nature and distribution of Messinian erosional surfaces—Indicators of a several-kilometer-deep Mediterranean in the Miocene. Marine Geology 27, 193–230. https://doi.org/10.1016/0025-3227(78)90032-4.

Sàbat, F., Roca, E., Muñoz, J.A., Vergés, J., Sans, M., Masana, E., Santanach, P., Estévez, A., Santisteban, C., 1997. Role of extension and compression in the evolution of the eastern margin of Iberia: The ESCI-València Trough seismic profile. Revista de la Sociedad Geológica de España 8, 401–415.

Sandwell, D.T., Garcia, E., Soofi, K., Wessel, P., Smith, W.H.F., 2013. Toward 1 mGal Global Marine Gravity from CryoSat-2, Envisat, and Jason-1. The Leading Edge 32, 892–899. https://doi.org/10.1190/tle32080892.1.

Sandwell, D.T., Müller, R.D., Smith, W.H.F., Garcia, E., Francis, R., 2014. New global marine gravity model from CryoSat-2 and Jason-1 reveals buried tectonic structure. Science 346, 65–67. https://doi.org/10.1126/science.1258213.

Sautkin, A., Talukder, A.R., Comas, M.C., Soto, J.I., Alekseev, A., 2003. Mud volcanoes in the Alboran Sea: Evidence from micropaleontological and geophysical data. Marine Geology 195, 237–261. https://doi.org/10.1016/S0025-3227(02)00691-6.

Savelli, C., 2002. Time–space distribution of magmatic activity in the western Mediterranean and peripheral orogens during the past 30 Ma (a stimulus to geodynamic considerations). Journal of Geodynamics 34, 99–126. https://doi.org/10.1016/S0264-3707(02)00026-1.

Schettino, A., Turco, E. 2006. Plate kinematics of the Western Mediterranean region during the Oligocene and Early Miocene. Geophysical Journal International 166, 1398–1423. https://doi.org/10.1111/j.1365-246X.2006.02997.

Schettino, A., Turco, E. 2009. Breakup of Pangaea and plate kinematics of the central Atlantic and Atlas regions. Geophysical Journal International 178, 1078–1097. https://doi.org/1010.1111/j.1365-1246X.2009.04186.x.

Sclater, J.G., Christie, P.A.F., 1980. Continental stretching: An explanation of the post-mid-Cretaceous subsidence of the Central North Sea. Journal of Geophysical Research 85, 3711–3739. https://doi.org/10.1029/JB085iB07p03711.

Somoza, L., Diaz-del-Rio, R. Leon, R., Ivanov, M., Fernández-Puga, M.C., Gardner, J.M., Hernández-Molina, F.J., Pinheiro, L.M., Rodero, J., Lobato, A., Maestro, A., Vazquez, J.T., Medialdea, T., Fernández-Salas, L.M., 2003. Seabed morphology and hydrocarbon seepage in the Gulf of Cadiz mud volcano area: Acoustic imagery, multibeam and ultrahigh resolution seismic data. Marine Geology 195, 153–176. https://doi.org/10.1016/S0025-3227(02)00686-2.

Somoza, L., Medialdea, T., León, R., Ercilla, G., Vázquez, J.T., Farran, M., Hernández-Molina, J., González, J., Juan, C., Fernández-Puga, M.C., 2012. Structure of mud volcano systems and pockmarks in the region of the Ceuta contourite depositional system, Western Alborán Sea. Marine Geology 332–334, 4–26. https://doi.org/10.1016/j.margeo.2012.06.002.

Soto, J.I., Fernández-Ibáñez, F., Fernàndez, M., García-Casco, A., 2008. Thermal structure of the crust in the Gibraltar Arc: Influence on active tectonics in the western Mediterranean. Geochemistry, Geophysics, Geosystems 9, Q10011. https://doi.org/10.1029/2008GC002061.

Soto, J.I., Fernández-Ibáñez, F., Talukder, A.R., 2012. Recent shale tectonics and basin evolution of the NW Alboran Sea. The Leading Edge 31, 768–775. https://doi.org/10.1190/tle31070768.1.

Soto, J.I., Fernández-Ibáñez, F., Talukder, A.R., Martínez-García, P., 2010. Miocene shale tectonics in the northern Alboran Sea, Western Mediterranean, in: Wood, L. (Ed.), Shale tectonics. American Association of Petroleum Geologists, Memoir 93, 119–144. https://doi.org/10.1306/13231312M933422.

Soumaya, A., Ben Ayed, N., Rajabi, M., Meghraoui, M., Delvaux, D., Kadri, A., Ziegler, M., Maouche, S., Braham, A., 2018. Active faulting geometry and stress pattern near complex strike-slip systems along the Maghreb region: Constraints on active convergence in the western Mediterranean. Tectonics 37, 3148–3173. https://doi.org/10.1029/2018TC004983.

Spakman, W., Chertova, M.V., van den Berg, A., van Hinsbergen, D.J.J., 2018. Puzzling features of western Mediterranean tectonics explained by slab dragging. Nature Geoscience 11, 211–216. https://doi.org/10.1038/s41561-018-0066-z.

Srivastava, S.P., Roest, W.R., Kovacs, L.C., Oakey, G., Levesque, S., Verhoef, J., Macnab, R., 1990. Motion of Iberia since the Late Jurassic: Results from detailed aeromagnetic measurements in the Newfoundland Basin. Tectonophysics, 184, 229–260. https://doi.org/10.1016/0040-1951(90)90442-B.

Strzerzynski, P., Déverchère, J., Cattaneo, A., Domzig, A., Yelles, K., Mercier de Lépinay, B., Babonneau, N., Boudiaf, A., 2010. Tectonic inheritance and Pliocene-Pleistocene inversion of the Algerian margin around Algiers: Insights from multibeam and seismic reflection data. Tectonics 29, TC2008. https://doi.org/10.1029/2009tc002547.

Strzerzynski, P., Dominguez, S., Boudiaf, A., Déverchère, J., 2021. Tectonic inversion and geomorphic evolution of the Algerian margin since Messinian times: Insights from new onshore/offshore analog modeling experiments. Tectonics 40, e2020TC006369. https://doi.org/10.1029/2020TC006369.

Talukder, A.R., Comas, M.C., Soto, J.I., 2003. Pliocene to Recent mud diapirism and related mud volcanoes in the Alboran Sea, western Mediterranean, in: Van Rensbergen, P., Hills, R.R., Maltman, A., Morley, C. (Eds.), Subsurface Sediment Mobilization. Geological Society of London, Special Publications 216,443–459. https://doi.org/10.1144/GSL.SP.2003.216.01.29.

Texas Pacific Oil Co., 1975. Calpe no. 1, final well report. Texas Pacific Oil Company, Inc., 110 pp.

Texas Pacific Oil Co., 1977. Informe final del sondeo Javea-1. Texas Pacific Oil Company, Inc., 10 pp.

Torne, M., Fernàndez, M., Comas, M.C., Soto, J.I., 2000. Lithospheric structure beneath the Alboran Basin: Results from 3D gravity modeling and tectonic relevance, Journal of Geophysical Research, Solid Earth 105, 3209–3228. https://doi.org/10.1029/1999JB900281.

Tozer, B., Sandwell, D.T., Smith, W.H.F., Olson, C., Beale, J.R., Wessel, P., 2019. Global bathymetry and topography at 15 arc seconds: SRTM15+. Earth and Space Science 6, 1847–1864. https://doi.org/10.1029/2019EA000658.

Travan, G., Gaullier, V., Vendeville, B., Déverchère, J., Raad, F., Lofi, J., 2021. Gravity gliding and spreading in a compressional setting: The example of the Algerian margin. EGU General Assembly 2021, abstract no. EGU21-11948. https://doi.org/10.5194/egusphere-egu21-11948.

Upton, T.L., Young, J.B., 1984. Alicante A-1, final well report. ESSO Exploration Spain Inc., 110 pp.

van Hinsbergen, D.J.J., Torsvik, T.H., Schmid, S.M., Maţenco, L.C., Maffione, M., Vissers, R.L.M., Gürer, D., Spakman, W., 2020. Orogenic architecture of the Mediterranean region and kinematic reconstruction of its tectonic evolution since the Triassic. Gondwana Research 81, 79–229. https://doi.org/10.1016/j.gr.2019.07.009.

van Hinsbergen, D.J.J., Vissers, R.L.M., Spakman, W., 2014. Origin and consequences of western Mediterranean subduction, rollback, and slab segmentation. Tectonics 33, 393–419. https://doi.org/10.1002/2013TC003349.

Van Rensbergen, P., Depreiter, D., Pannemans, B., Moerkerke, G., van Rooij, D., Marsset, B., Akhmanov, G., Blinova, V., Ivanov, M., Rachidi, M., Magalhaes, V., Pinheiro, L., Cunha, M., Henriet, J.P., 2005. The El Arraiche mud volcano field at the Moroccan Atlantic slope, Gulf of Cadiz. Marine Geology 219, 1–17. https://doi.org/10.1016/j.margeo.2005.04.007.

Vendeville, B.C., 2005. Salt tectonics driven by sediment progradation: Part I—Mechanics and kinematics. AAPG Bulletin 89, 1071–1079. https://doi.org/10.1306/03310503063.

Vendeville, B.C., Jackson, M.P.A., 1992. The rise of diapirs during thin-skinned extension. Marine and Petroleum Geology 9, 331–354. https://doi.org/10.1016/0264-8172(92)90047-I.

Vidal, N., Gallart, J., Dañobeitia, J.J., 1998. A deep seismic crustal transect from the NE Iberian Peninsula to the western Mediterranean. Journal of Geophysical Research, Solid Earth 103, 12381–12396. https://doi.org/10.1029/98JB00076.

Vissers, R.L.M., Platt, J.P., van der Wal, D., 1995. Late orogenic extension of the Betic Cordillera and the Alboran Domain: A lithospheric view. Tectonics 14, 786–803. https://doi.org/10.1029/95TC00086.

Woodside, J., Ivanov, M., Koelewijn, R., Zeldenrust, I., Shashkin, P., 2000. South Balearic Basin: The Palomares and Mazarrón margins. Sidescan sonar data, in: Kenyon, N.H., Ivanov, M.K., Akhmetzhanov, A.M., Akhmanov, G.G. (Eds.), Multidisciplinary Study of Geological Processes on the North East Atlantic and Western Mediterranean Margins. Preliminary Results of Geological and Geophysical Investigations During the TTR-9 Cruise of R/V Professor Logachev (June-July, 1999), Intergovernmental Oceanographic Commission Technical Series 56, 95–98.

Yelles-Chaouche, A.K., Boudiaf, A., Djellit, H., Bracene, R., 2006. La tectonique active de la région nord-algérienne—Active tectonics in northern Algeria. Comptes Rendus Geoscience 338, 126–139. https://doi.org/10.1016/j.crte.2005.11.002.

Zitellini, N., Gràcia, E., Gutscher, M.-A., Matias, L., Terrinha, P., Abreu, M.A., DeAlteriis, G., Henriet, J.P., Dañobeitia, J.J., Masson, D.G., Mulder, T., Ramella, R., Somoza, L., Diez, S., 2009. The quest for the Africa-Eurasia plate boundary west of the Strait of Gibraltar. Earth and Planetary Science Letters 280, 13–50. https://doi.org/10.1016/j.epsl.2008.12.005.

Zucker, E., Gvirtzman, Z., Steinberg, J., Enzel, Y., 2020. Salt tectonics in the Eastern Mediterranean Sea: Where a giant delta meets a salt giant. Geology 48, 134–138. https://doi.org/10.1130/G47031.1.

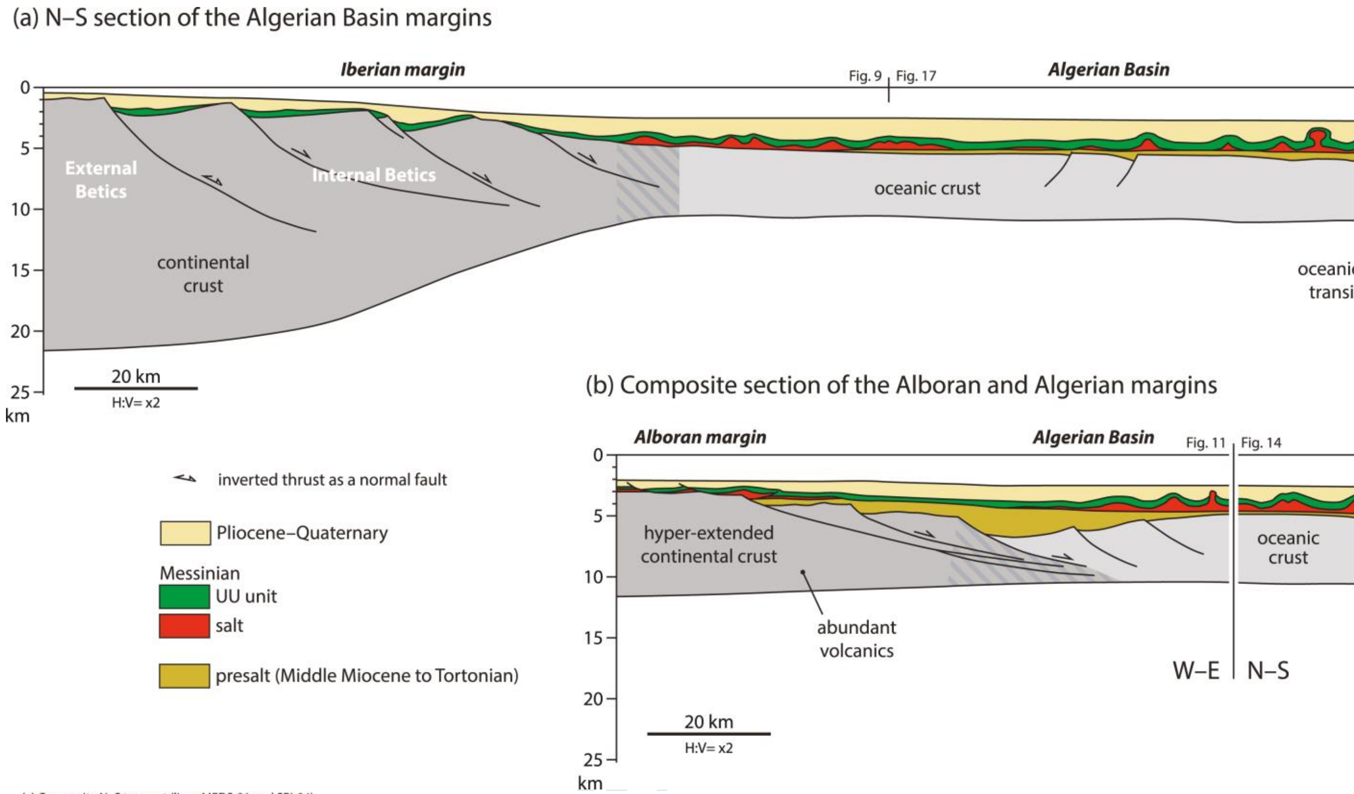
(a) N–S section of the Algerian Basin margins
Iberian margin
Fig. 9
Fig. 17
Algerian Basin
External Betics
Internal Betics
oceanic crust
continental crust
20 km
H:V= x2
km
inverted thrust as a normal fault
Pliocene–Quaternary
Messinian
UU unit
salt
presalt (Middle Miocene to Tortonian)
(b) Composite section of the Alboran and Algerian margins
Alboran margin
Algerian Basin
Fig. 11
Fig. 14
hyper-extended continental crust
oceanic crust
abundant volcanics
W–E
N–S
20 km
H:V= x2
km

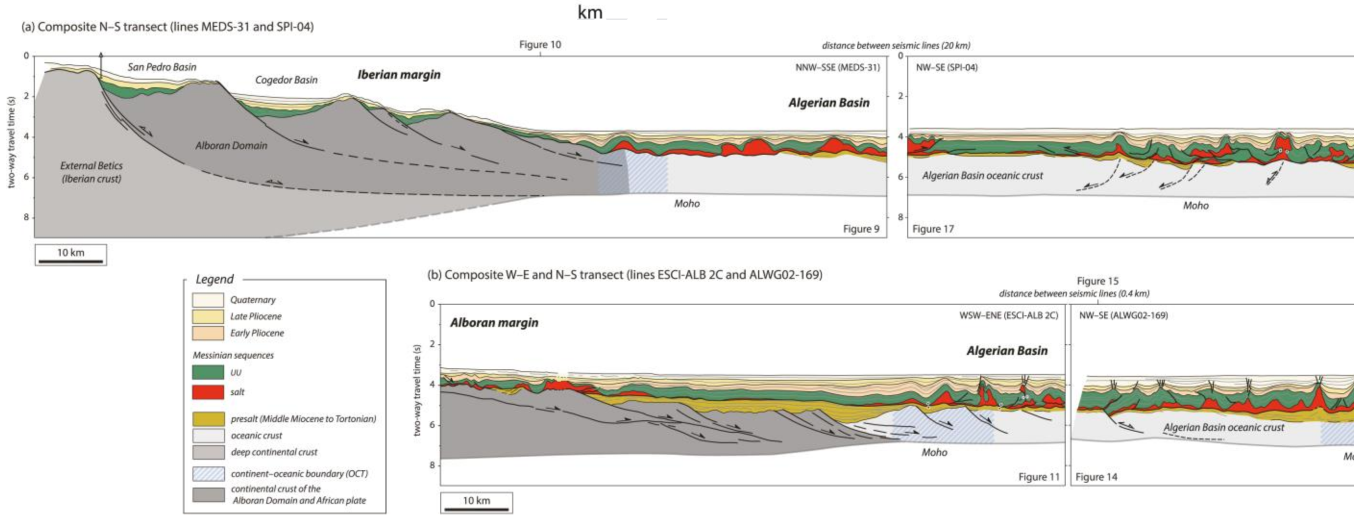
(a) Composite N–S transect (lines MEDS-31 and SPI-04)
Figure 10
distance between seismic lines (20 km)
San Pedro Basin
Cogedor Basin
Iberian margin
NNW–SSE (MEDS-31)
NW–SE (SPI-04)
Algerian Basin
two-way travel time (s)
External Betics (Iberian crust)
Alboran Domain
Algerian Basin oceanic crust
Moho
Figure 9
Figure 17
10 km
Legend
Quaternary
Late Pliocene
Early Pliocene
Messinian sequences
UU
salt
presalt (Middle Miocene to Tortonian)
oceanic crust
deep continental crust
continent–oceanic boundary (OCT)
continental crust of the Alboran Domain and African plate
(b) Composite W–E and N–S transect (lines ESCI-ALB 2C and ALWG02-169)
Figure 15
distance between seismic lines (0.4 km)
Alboran margin
WSW–ENE (ESCI-ALB 2C)
NW–SE (ALWG02-169)
Algerian Basin
Algerian Basin oceanic crust
Moho
Figure 11
Figure 14
10 km

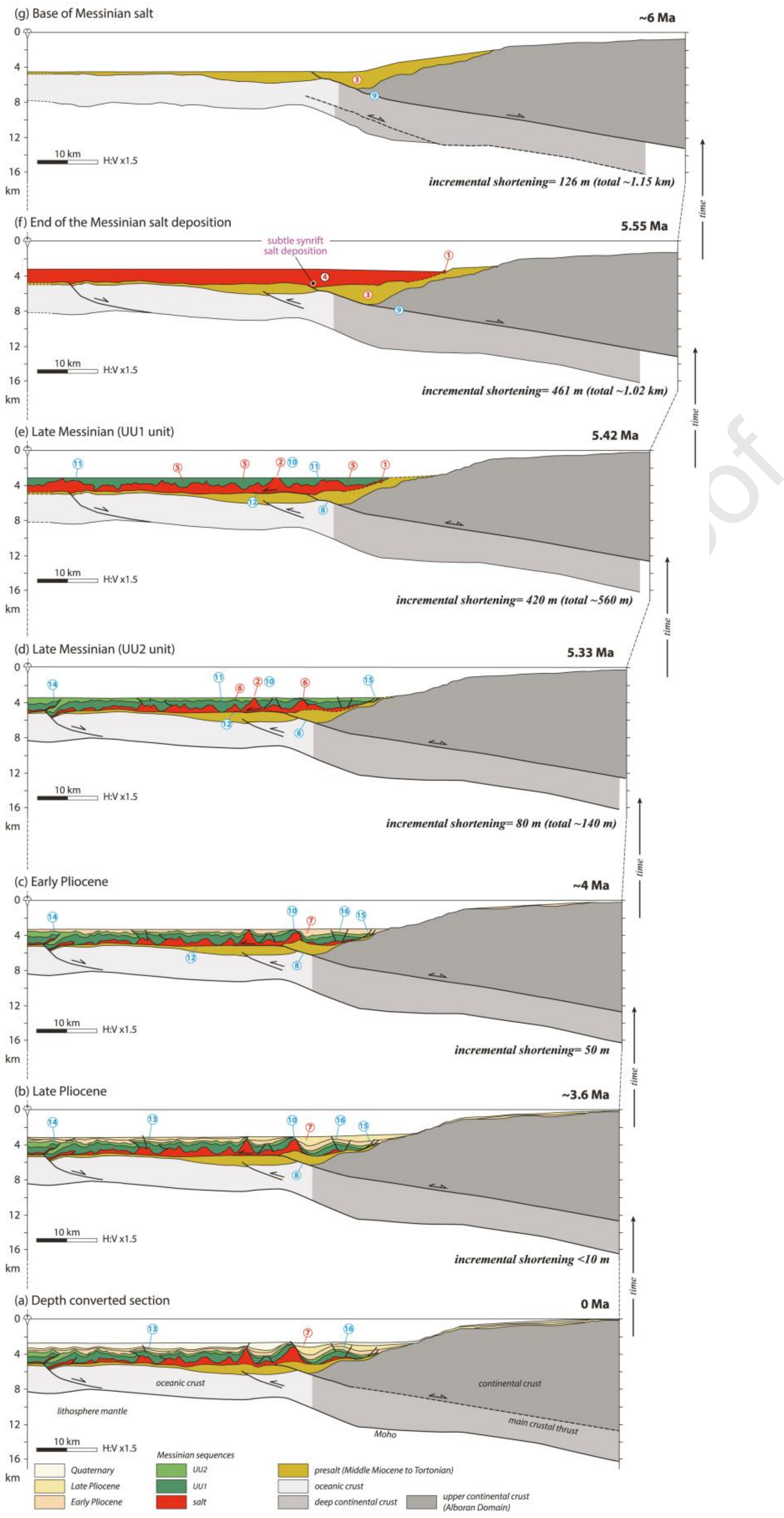
(g) Base of Messinian salt
~6 Ma
incremental shortening= 126 m (total ~1.15 km)
(f) End of the Messinian salt deposition
5.55 Ma
subtle synrift salt deposition
incremental shortening= 461 m (total ~1.02 km)
(e) Late Messinian (UU1 unit)
5.42 Ma
incremental shortening= 420 m (total ~560 m)
(d) Late Messinian (UU2 unit)
5.33 Ma
incremental shortening= 80 m (total ~140 m)
(c) Early Pliocene
~4 Ma
incremental shortening= 50 m
(b) Late Pliocene
~3.6 Ma
incremental shortening <10 m
(a) Depth converted section
0 Ma
oceanic crust
continental crust
lithosphere mantle
main crustal thrust
Moho
10 km
H:V x1.5
km
time
Quaternary
Late Pliocene
Early Pliocene
Messinian sequences
UU2
UU1
salt
presalt (Middle Miocene to Tortonian)
oceanic crust
deep continental crust
upper continental crust (Alboran Domain)

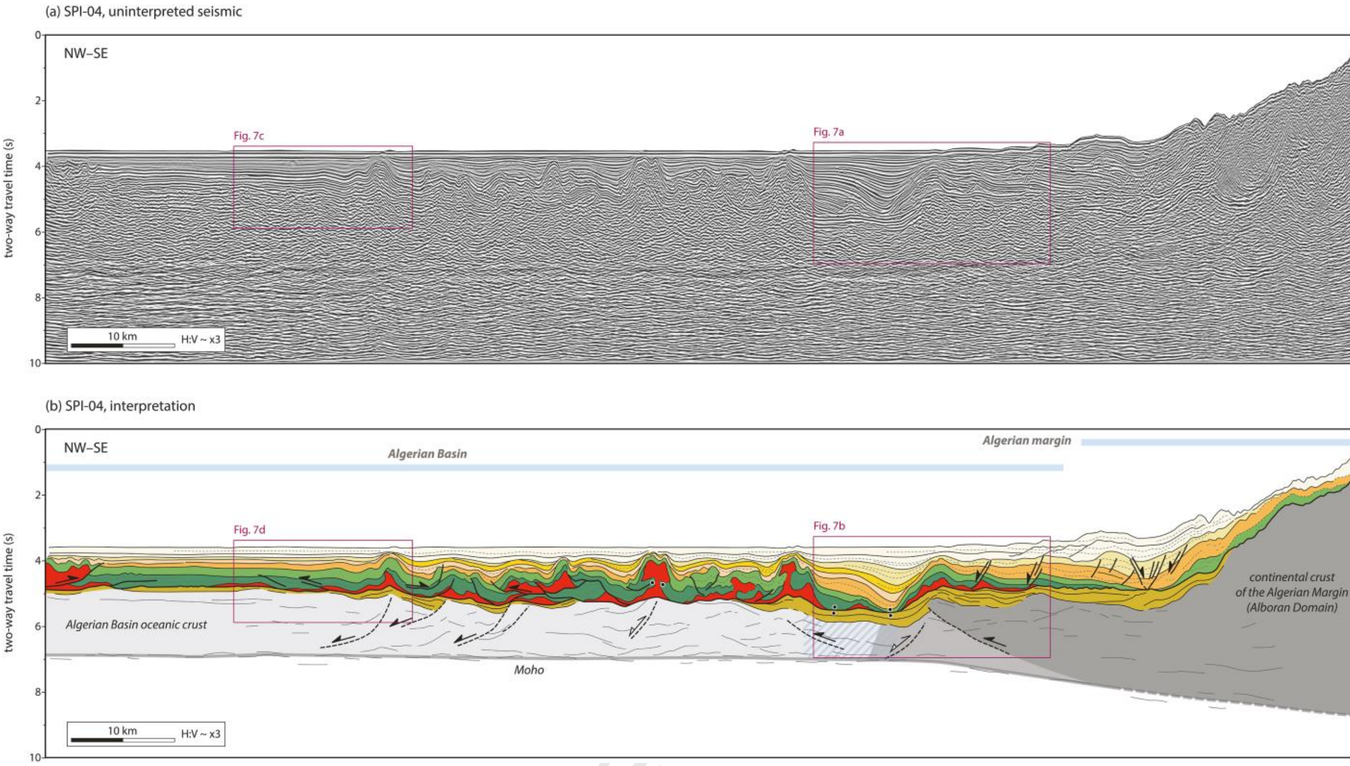
(a) SPI-04, uninterpreted seismic
NW–SE
Fig. 7c
Fig. 7a
two-way travel time (s)
10 km
H:V ~ x3
(b) SPI-04, interpretation
NW–SE
Algerian Basin
Algerian margin
Fig. 7d
Fig. 7b
Algerian Basin oceanic crust
continental crust
of the Algerian Margin
(Alboran Domain)
Moho
two-way travel time (s)
10 km
H:V ~ x3

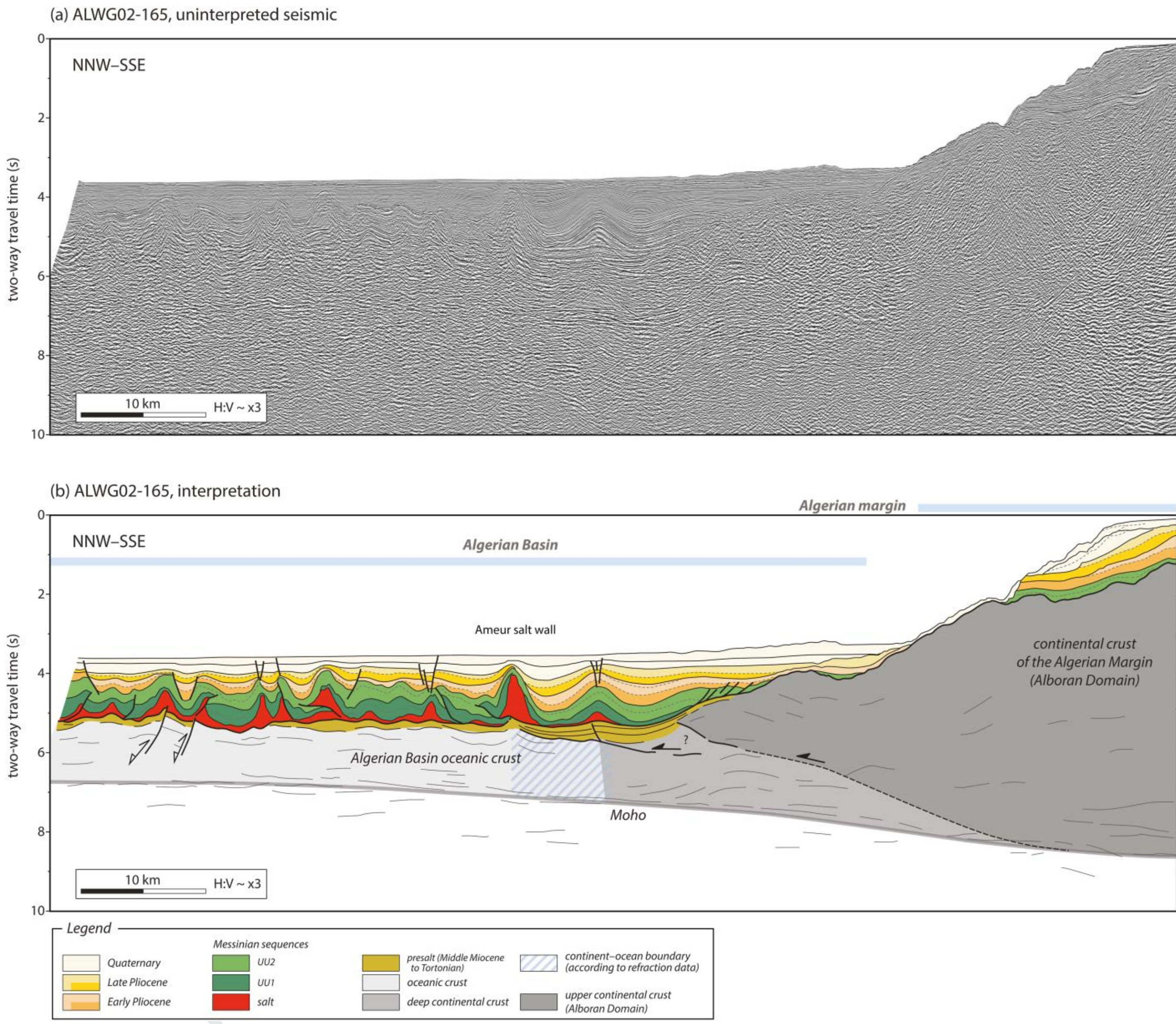
(a) ALWG02-165, uninterpreted seismic
NNW–SSE
two-way travel time (s)
0
2
4
6
8
10
10 km
H:V ~ x3
(b) ALWG02-165, interpretation
NNW–SSE
Algerian Basin
Algerian margin
Ameur salt wall
continental crust
of the Algerian Margin
(Alboran Domain)
Algerian Basin oceanic crust
Moho
Legend
Quaternary
Late Pliocene
Early Pliocene
Messinian sequences
UU2
UU1
salt
presalt (Middle Miocene to Tortonian)
oceanic crust
deep continental crust
continent–ocean boundary (according to refraction data)
upper continental crust (Alboran Domain)

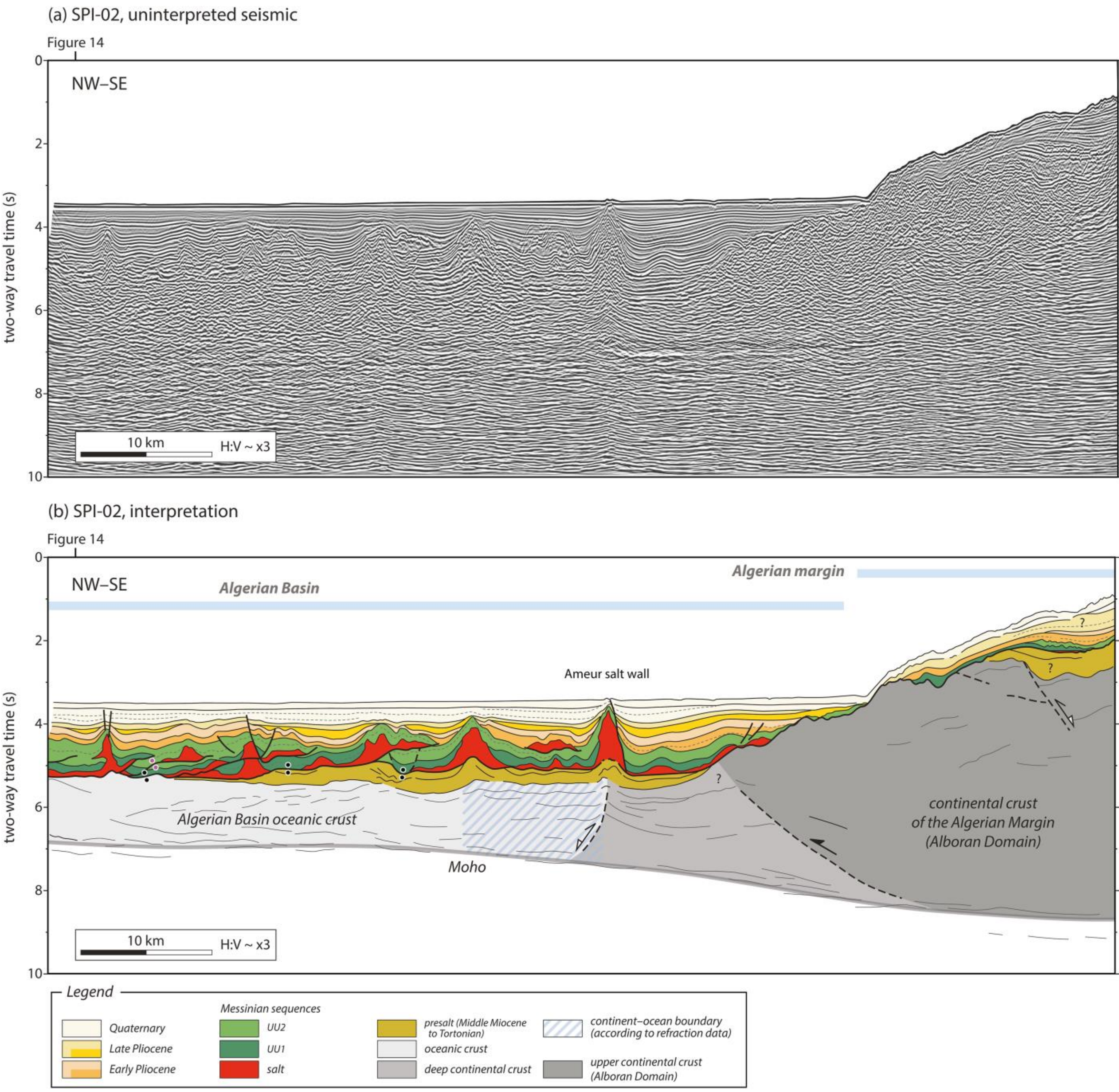

(a) SPI-02, uninterpreted seismic
Figure 14
NW–SE
two-way travel time (s)
10 km
H:V ~ x3
(b) SPI-02, interpretation
Figure 14
NW–SE
Algerian Basin
Algerian margin
Ameur salt wall
Algerian Basin oceanic crust
Moho
continental crust
of the Algerian Margin
(Alboran Domain)
10 km
H:V ~ x3
Legend
Messinian sequences
Quaternary
Late Pliocene
Early Pliocene
UU2
UU1
salt
presalt (Middle Miocene
to Tortonian)
oceanic crust
deep continental crust
continent–ocean boundary
(according to refraction data)
upper continental crust
(Alboran Domain)

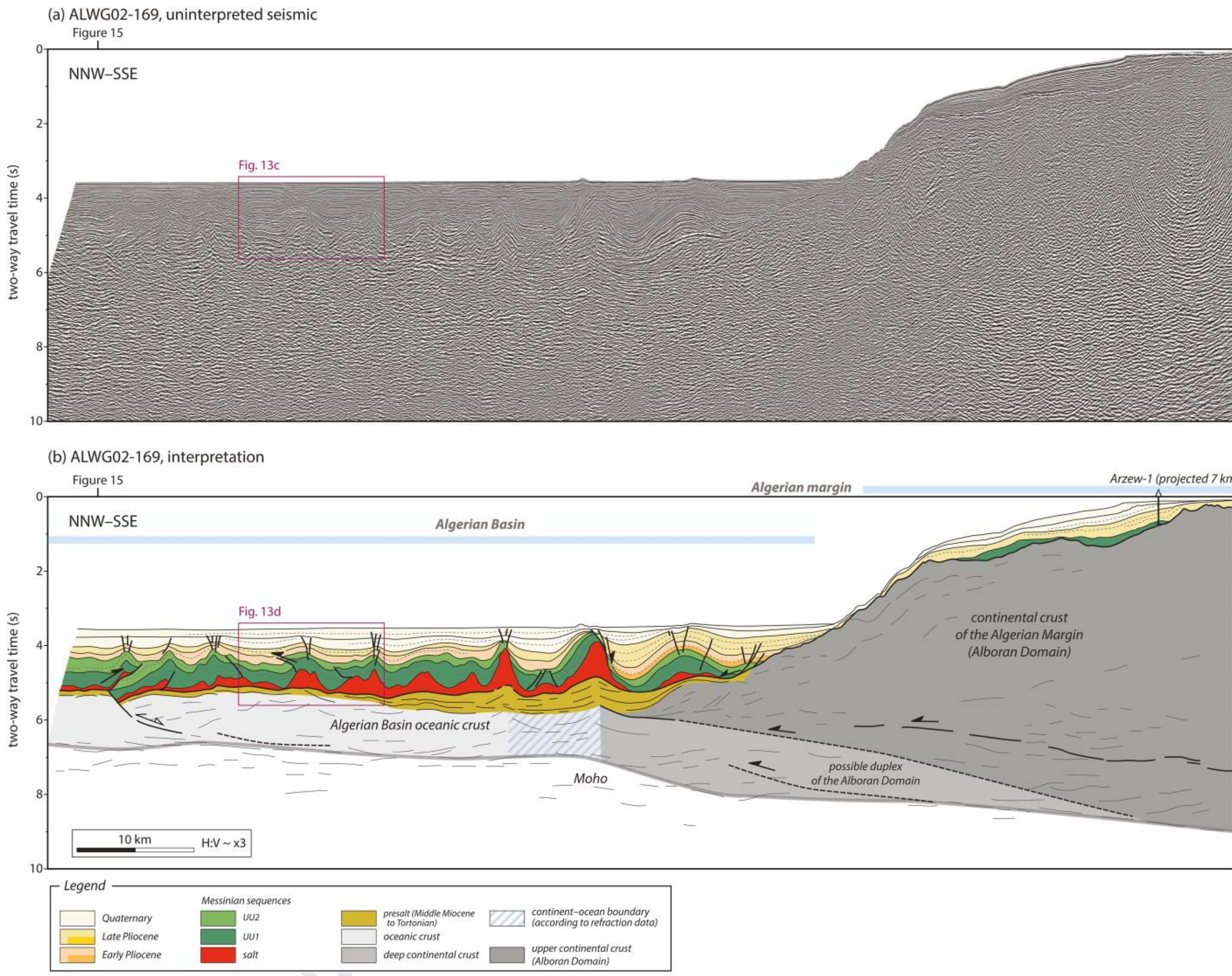

(a) ALWG02-169, uninterpreted seismic
Figure 15
NNW–SSE
Fig. 13c
two-way travel time (s)
(b) ALWG02-169, interpretation
Figure 15
Algerian margin
Arzew-1 (projected 7 km
NNW–SSE
Algerian Basin
Fig. 13d
continental crust
of the Algerian Margin
(Alboran Domain)
Algerian Basin oceanic crust
Moho
possible duplex
of the Alboran Domain
10 km
H:V ~ x3
Legend
Quaternary
Late Pliocene
Early Pliocene
Messinian sequences
UU2
UU1
salt
presalt (Middle Miocene to Tortonian)
oceanic crust
deep continental crust
continent–ocean boundary (according to refraction data)
upper continental crust (Alboran Domain)

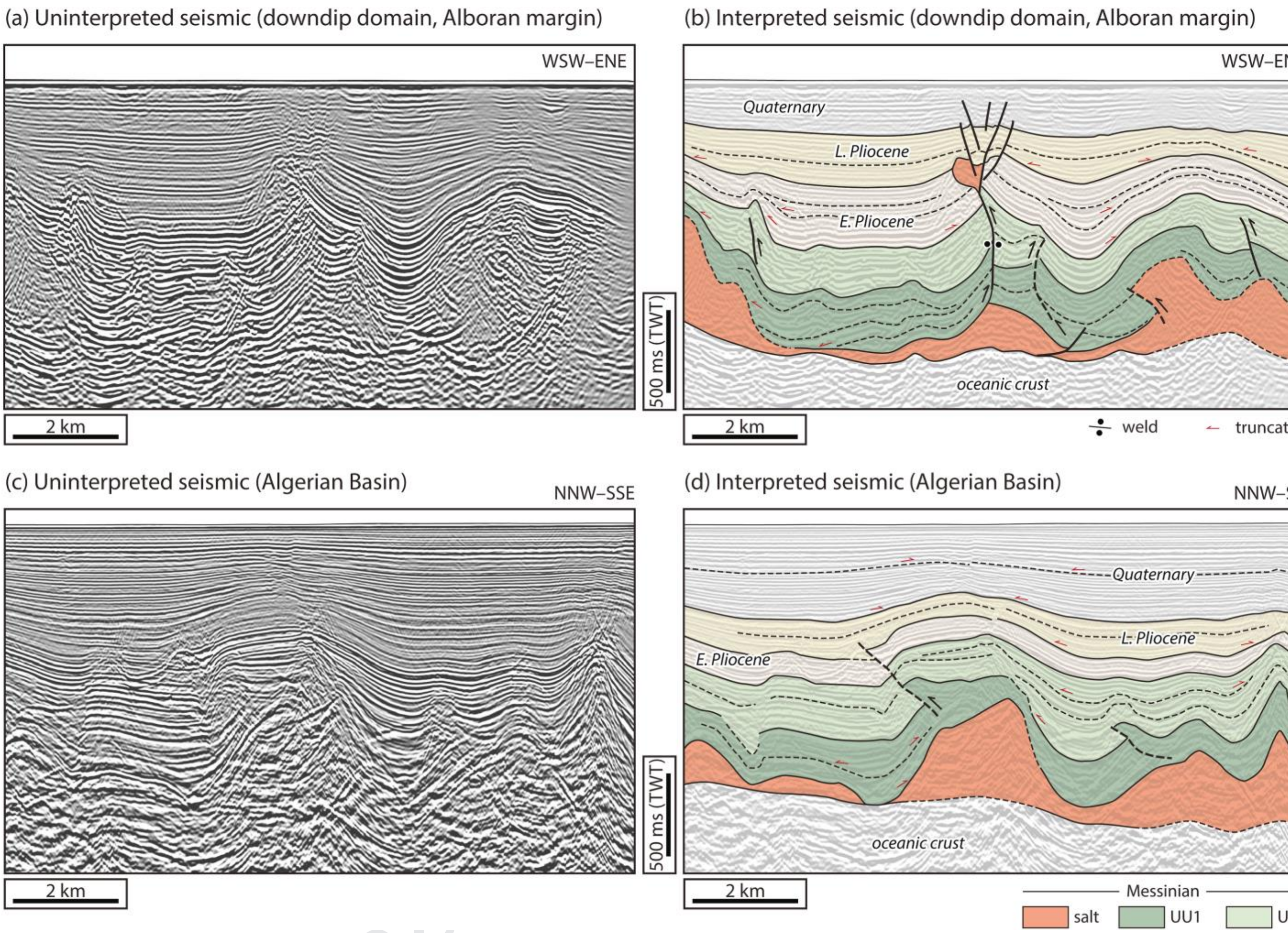

(a) Uninterpreted seismic (downdip domain, Alboran margin)
WSW–ENE
500 ms (TWT)
2 km
(b) Interpreted seismic (downdip domain, Alboran margin)
Quaternary
L. Pliocene
E. Pliocene
oceanic crust
2 km
weld
(c) Uninterpreted seismic (Algerian Basin)
NNW–SSE
500 ms (TWT)
2 km
(d) Interpreted seismic (Algerian Basin)
Quaternary
L. Pliocene
E. Pliocene
oceanic crust
2 km
Messinian
salt
UU1

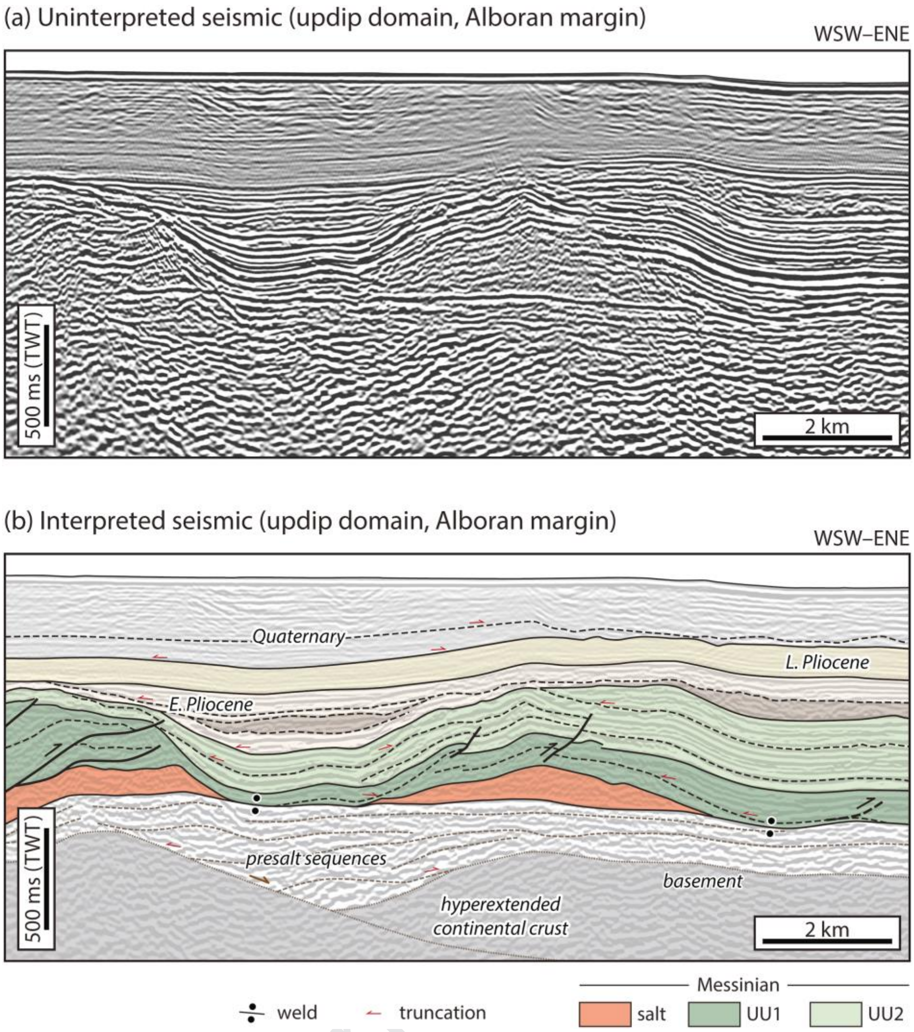
(a) Uninterpreted seismic (updip domain, Alboran margin)
WSW–ENE
500 ms (TWT)
2 km
(b) Interpreted seismic (updip domain, Alboran margin)
WSW–ENE
Quaternary
L. Pliocene
E. Pliocene
presalt sequences
basement
hyperextended continental crust
500 ms (TWT)
2 km
weld
truncation
Messinian
salt
UU1
UU2

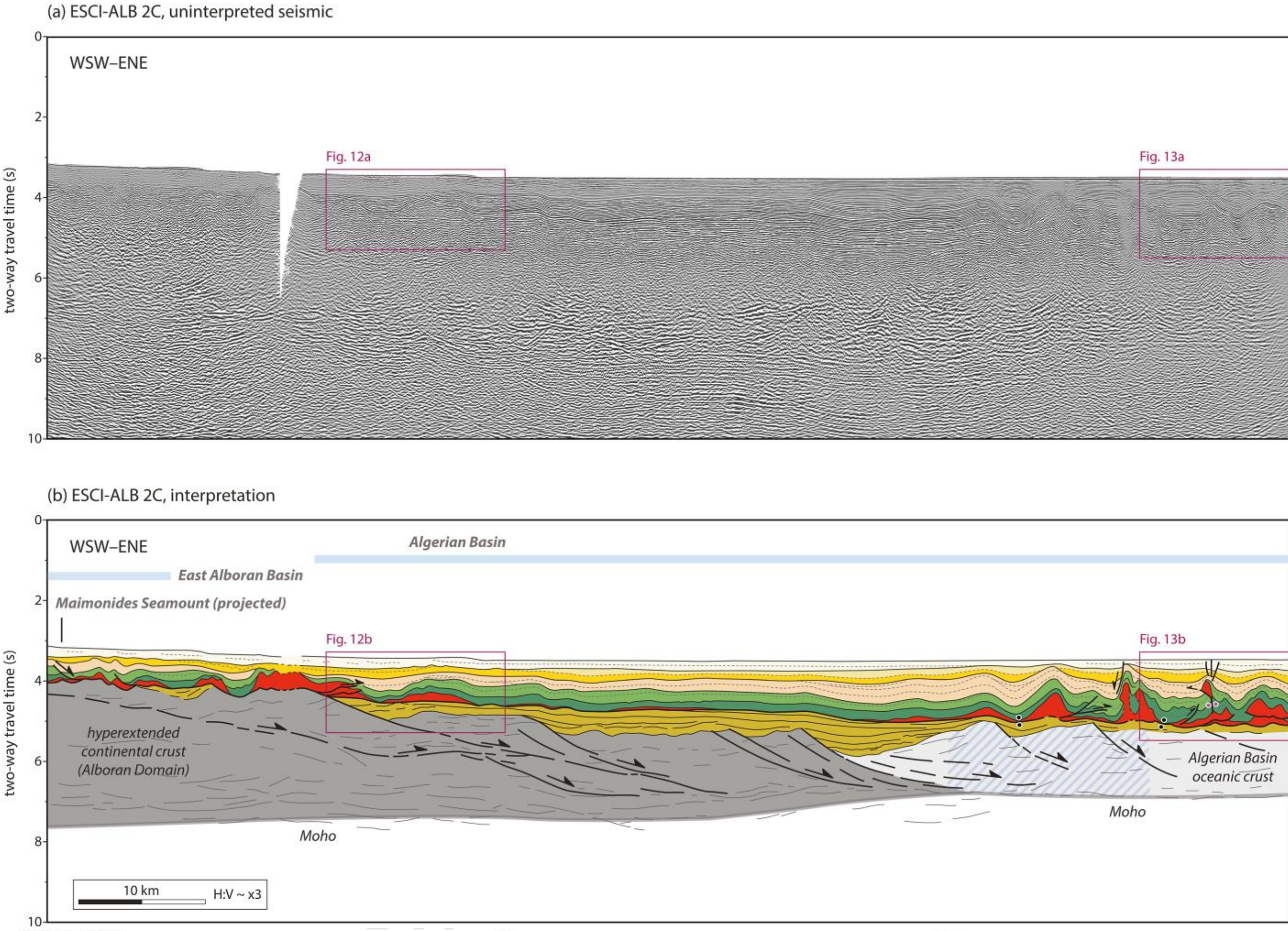
(a) ESCI-ALB 2C, uninterpreted seismic
WSW–ENE
two-way travel time (s)
0
2
4
6
8
10
Fig. 12a
Fig. 13a
(b) ESCI-ALB 2C, interpretation
WSW–ENE
Algerian Basin
East Alboran Basin
Maimonides Seamount (projected)
Fig. 12b
Fig. 13b
hyperextended continental crust (Alboran Domain)
Algerian Basin oceanic crust
Moho
Moho
10 km
H:V ~ x3

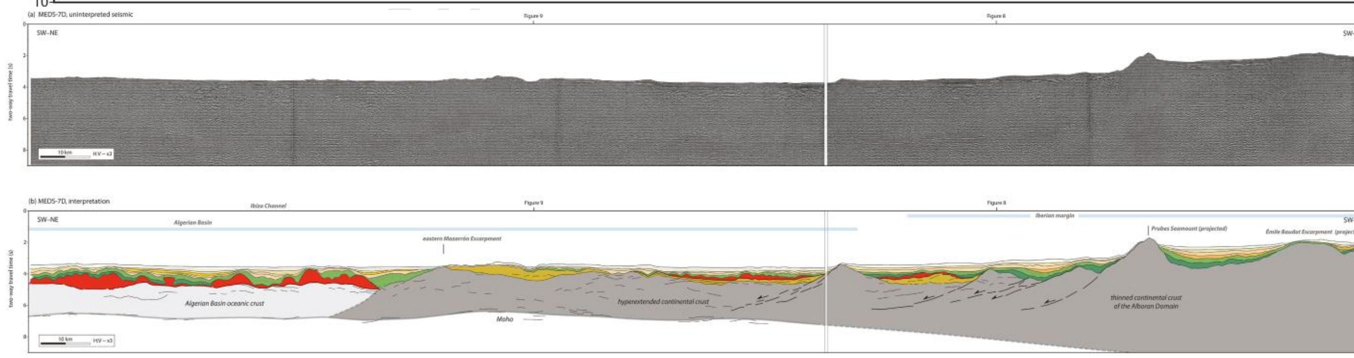
(a) MEDS-7D, uninterpreted seismic
SW–NE
(b) MEDS-7D, interpretation
SW–NE
Algerian Basin
Ibiza Channel
eastern Mazarrón Escarpment
Algerian Basin oceanic crust
hyperextended continental crust
Moho
Iberian margin
thinned continental crust of the Alboran Domain
10 km

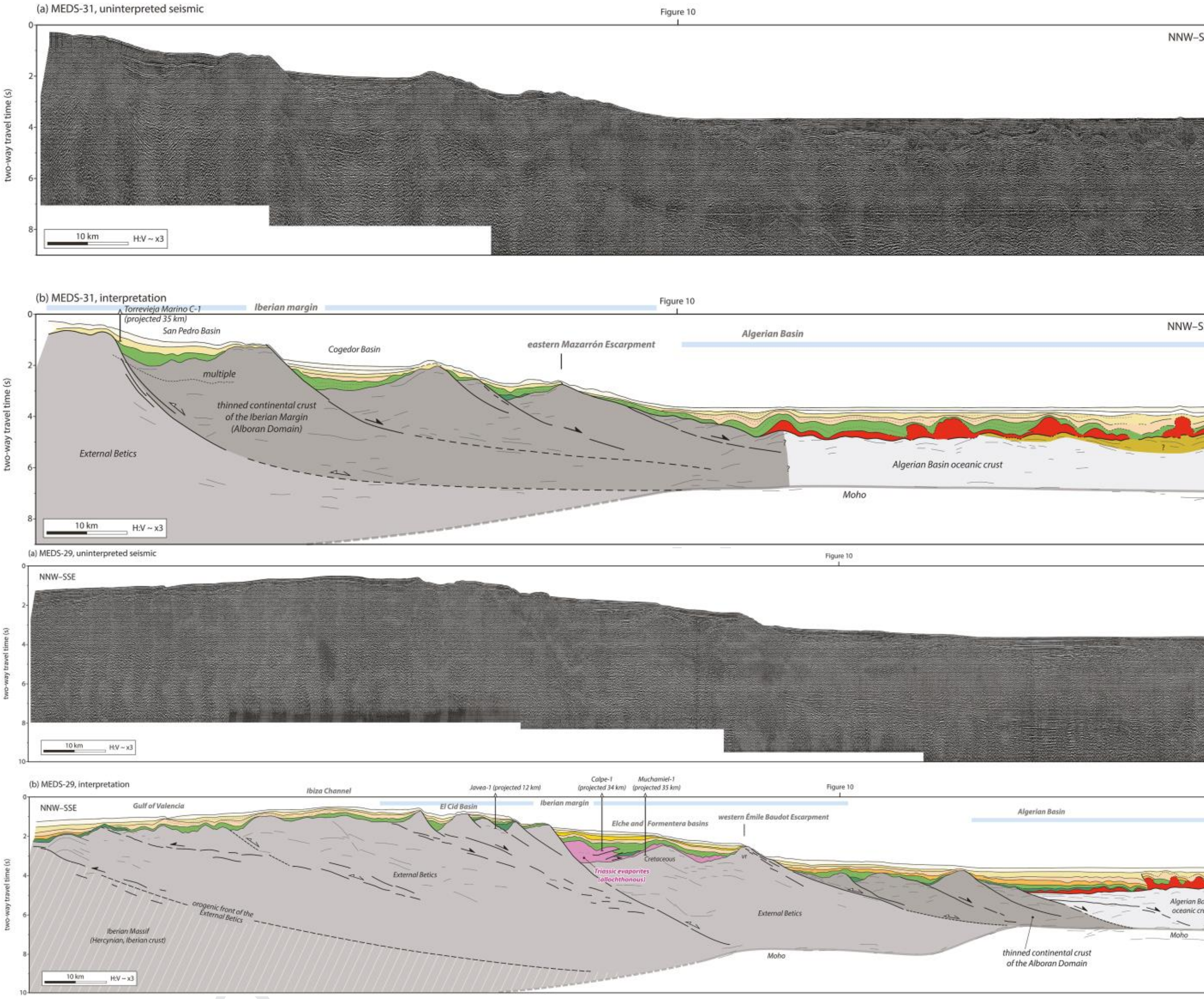
(a) MEDS-31, uninterpreted seismic
Figure 10
NNW–S
two-way travel time (s)
10 km
H:V ~ x3
(b) MEDS-31, interpretation
Iberian margin
Torrevieja Marino C-1
(projected 35 km)
San Pedro Basin
Cogedor Basin
eastern Mazarrón Escarpment
Algerian Basin
multiple
thinned continental crust
of the Iberian Margin
(Alboran Domain)
External Betics
Algerian Basin oceanic crust
Moho
(a) MEDS-29, uninterpreted seismic
NNW–SSE
(b) MEDS-29, interpretation
Gulf of Valencia
Ibiza Channel
El Cid Basin
Javea-1 (projected 12 km)
Calpe-1
(projected 34 km)
Muchamiel-1
(projected 35 km)
Elche and Formentera basins
western Émile Baudot Escarpment
Cretaceous
Triassic evaporites
(allochthonous)
orogenic front of the
External Betics
Iberian Massif
(Hercynian, Iberian crust)
thinned continental crust
of the Alboran Domain

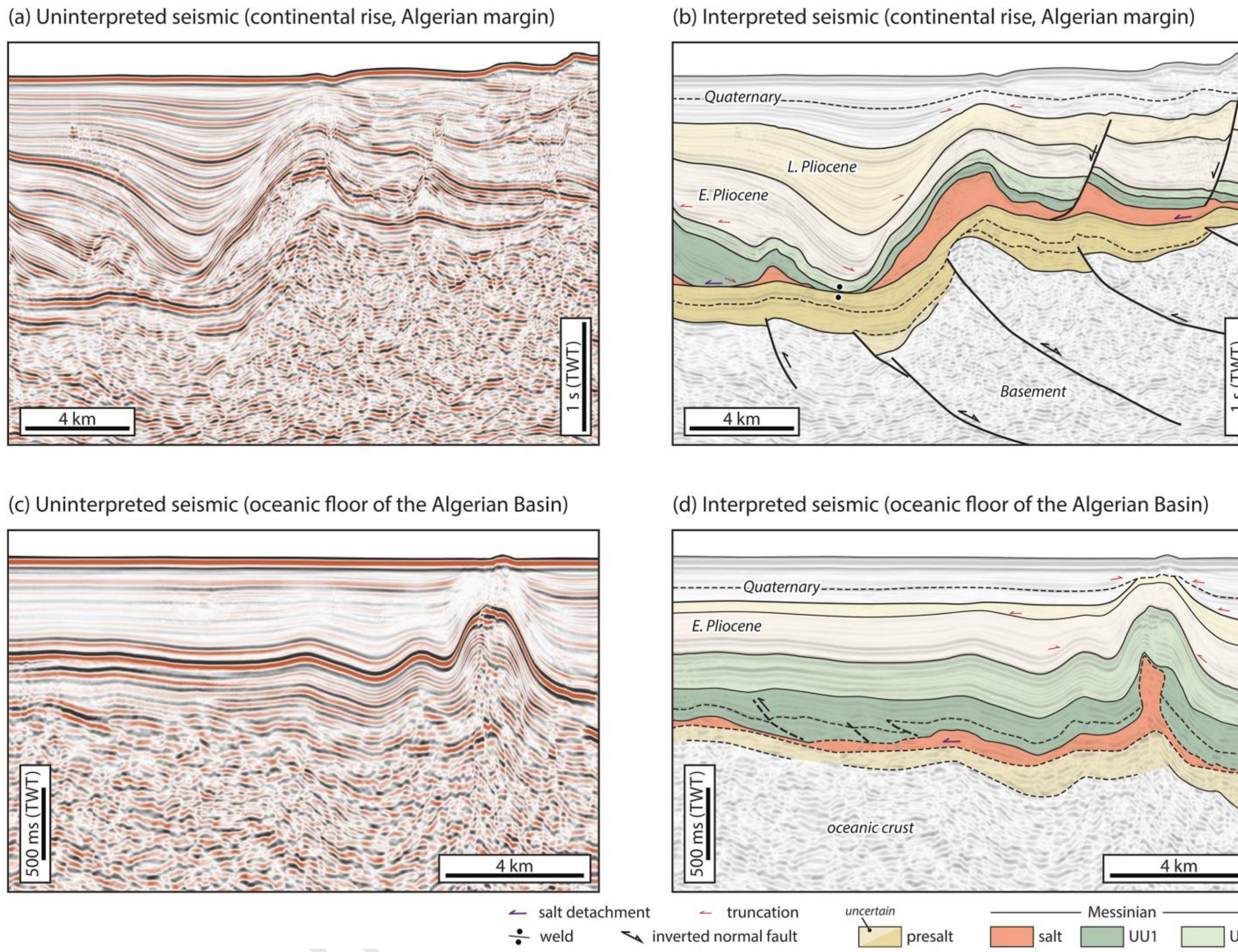

(a) Uninterpreted seismic (continental rise, Algerian margin)
1 s (TWT)
4 km
(b) Interpreted seismic (continental rise, Algerian margin)
Quaternary
L. Pliocene
E. Pliocene
Basement
4 km
(c) Uninterpreted seismic (oceanic floor of the Algerian Basin)
500 ms (TWT)
4 km
(d) Interpreted seismic (oceanic floor of the Algerian Basin)
Quaternary
E. Pliocene
oceanic crust
500 ms (TWT)
4 km
salt detachment
truncation
uncertain
Messinian
weld
inverted normal fault
presalt
salt
UU1

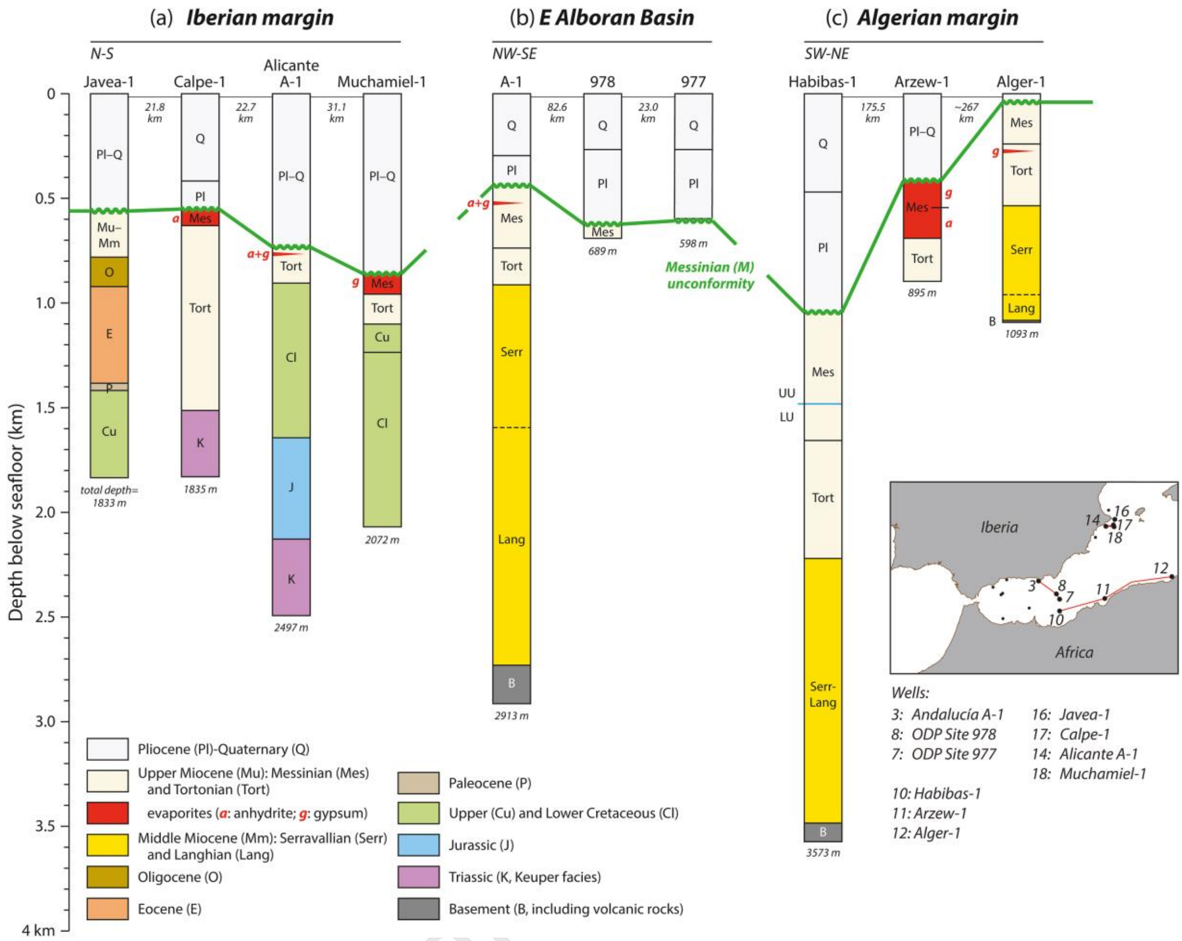

(a) Iberian margin
N-S
Javea-1
Calpe-1
Alicante A-1
Muchamiel-1
21.8 km
22.7 km
31.1 km
(b) E Alboran Basin
NW-SE
A-1
978
977
82.6 km
23.0 km
(c) Algerian margin
SW-NE
Habibas-1
Arzew-1
Alger-1
175.5 km
~267 km
Depth below seafloor (km)
Messinian (M) unconformity
total depth= 1833 m
1835 m
2497 m
2072 m
2913 m
689 m
598 m
3573 m
895 m
1093 m
Pliocene (Pl)-Quaternary (Q)
Upper Miocene (Mu): Messinian (Mes) and Tortonian (Tort)
evaporites (a: anhydrite; g: gypsum)
Middle Miocene (Mm): Serravallian (Serr) and Langhian (Lang)
Oligocene (O)
Eocene (E)
Paleocene (P)
Upper (Cu) and Lower Cretaceous (Cl)
Jurassic (J)
Triassic (K, Keuper facies)
Basement (B, including volcanic rocks)
Iberia
Africa
Wells:
3: Andalucía A-1
8: ODP Site 978
7: ODP Site 977
10: Habibas-1
11: Arzew-1
12: Alger-1
16: Javea-1
17: Calpe-1
14: Alicante A-1
18: Muchamiel-1

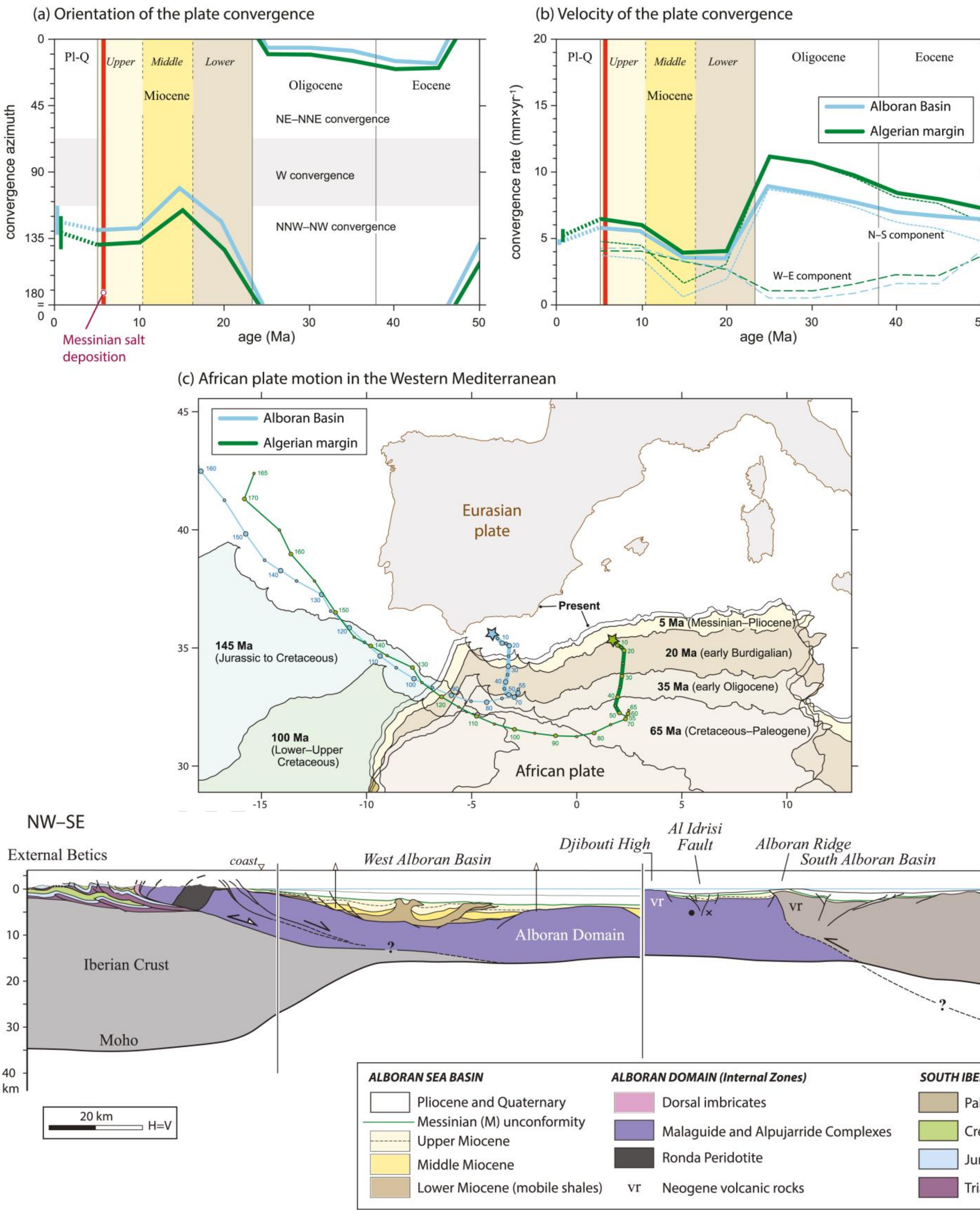
(a) Orientation of the plate convergence
(b) Velocity of the plate convergence
Pl-Q
Upper
Middle
Lower
Miocene
Oligocene
Eocene
NE–NNE convergence
W convergence
NNW–NW convergence
convergence azimuth
age (Ma)
Messinian salt deposition
convergence rate (mm×yr⁻¹)
Alboran Basin
Algerian margin
N-S component
W-E component
(c) African plate motion in the Western Mediterranean
Eurasian plate
Present
5 Ma (Messinian–Pliocene)
20 Ma (early Burdigalian)
35 Ma (early Oligocene)
65 Ma (Cretaceous–Paleogene)
145 Ma (Jurassic to Cretaceous)
100 Ma (Lower–Upper Cretaceous)
African plate
NW–SE
External Betics
coast
West Alboran Basin
Djibouti High
Al Idrisi Fault
Alboran Ridge
South Alboran Basin
Iberian Crust
Moho
Alboran Domain
km
20 km
H=V
ALBORAN SEA BASIN
Pliocene and Quaternary
Messinian (M) unconformity
Upper Miocene
Middle Miocene
Lower Miocene (mobile shales)
ALBORAN DOMAIN (Internal Zones)
Dorsal imbricates
Malaguide and Alpujarride Complexes
Ronda Peridotite
Neogene volcanic rocks

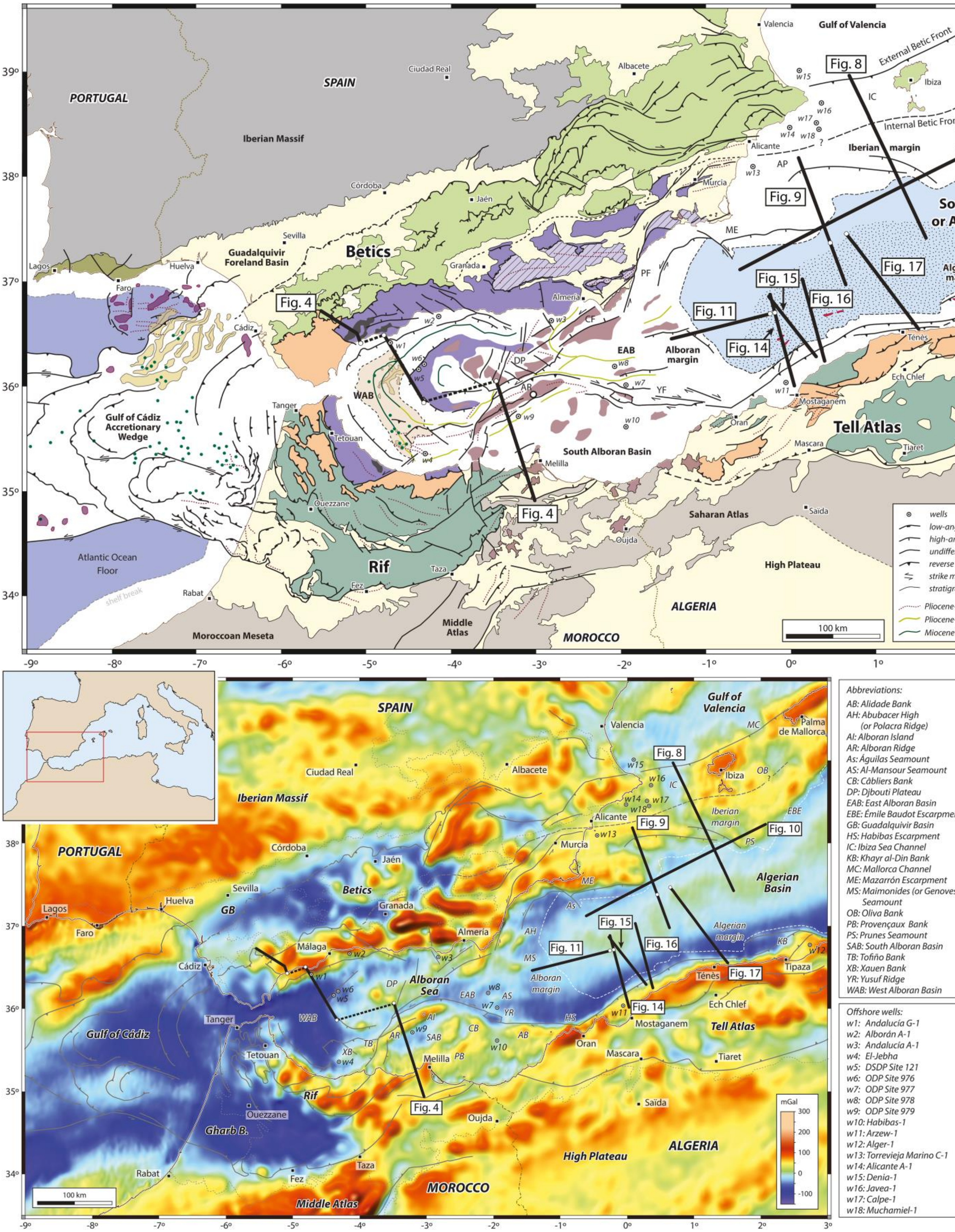
PORTUGAL
SPAIN
Iberian Massif
Ciudad Real
Albacete
Valencia
Gulf of Valencia
External Betic Front
Internal Betic Front
Fig. 8
Ibiza
IC
Iberian margin
Alicante
Murcia
AP
Córdoba
Jaén
Sevilla
Guadalquivir Foreland Basin
Betics
Granada
Lagos
Huelva
Faro
Cádiz
Fig. 4
Fig. 9
ME
PF
Almería
CF
EAB
Alboran margin
Fig. 11
Fig. 15
Fig. 16
Fig. 14
Fig. 17
DP
AR
YF
WAB
Tanger
Tetouan
Gulf of Cádiz Accretionary Wedge
South Alboran Basin
Melilla
Mostaganem
Oran
Ech Chlef
Ténès
Tell Atlas
Mascara
Tiaret
Saida
Saharan Atlas
Ouezzane
Oujda
Rif
Taza
Fez
Rabat
shelf break
Atlantic Ocean Floor
Middle Atlas
Moroccoan Meseta
MOROCCO
ALGERIA
High Plateau
100 km
wells
Pliocene
Miocene
Abbreviations:
AB: Alidade Bank
AH: Abubacer High (or Polacra Ridge)
AI: Alboran Island
AR: Alboran Ridge
As: Águilas Seamount
AS: Al-Mansour Seamount
CB: Cábliers Bank
DP: Djbouti Plateau
EAB: East Alboran Basin
GB: Guadalquivir Basin
HS: Habibas Escarpment
IC: Ibiza Sea Channel
KB: Khayr al-Din Bank
MC: Mallorca Channel
ME: Mazarrón Escarpment
OB: Oliva Bank
PB: Provençaux Bank
PS: Prunes Seamount
SAB: South Alboran Basin
TB: Tofiño Bank
XB: Xauen Bank
YR: Yusuf Ridge
WAB: West Alboran Basin
Offshore wells:
w1: Andalucía G-1
w2: Alborán A-1
w3: Andalucía A-1
w4: El-Jebha
w5: DSDP Site 121
w6: ODP Site 976
w7: ODP Site 977
w8: ODP Site 978
w9: ODP Site 979
w10: Habibas-1
w11: Arzew-1
w12: Alger-1
w13: Torrevieja Marino C-1
w14: Alicante A-1
w15: Denia-1
w16: Javea-1
w17: Calpe-1
w18: Muchamiel-1
Palma de Mallorca
Algerian Basin
Algerian margin
Fig. 10
Alboran Sea
Tipaza
Gharb B.
Gulf of Cádiz
mGal
300
200
100
0
-100
-9º
-8º
-7º
-6º
-5º
-4º
-3º
-2º
-1º
0º
1º
2º
3º
34º
35º
36º
37º
38º
39º

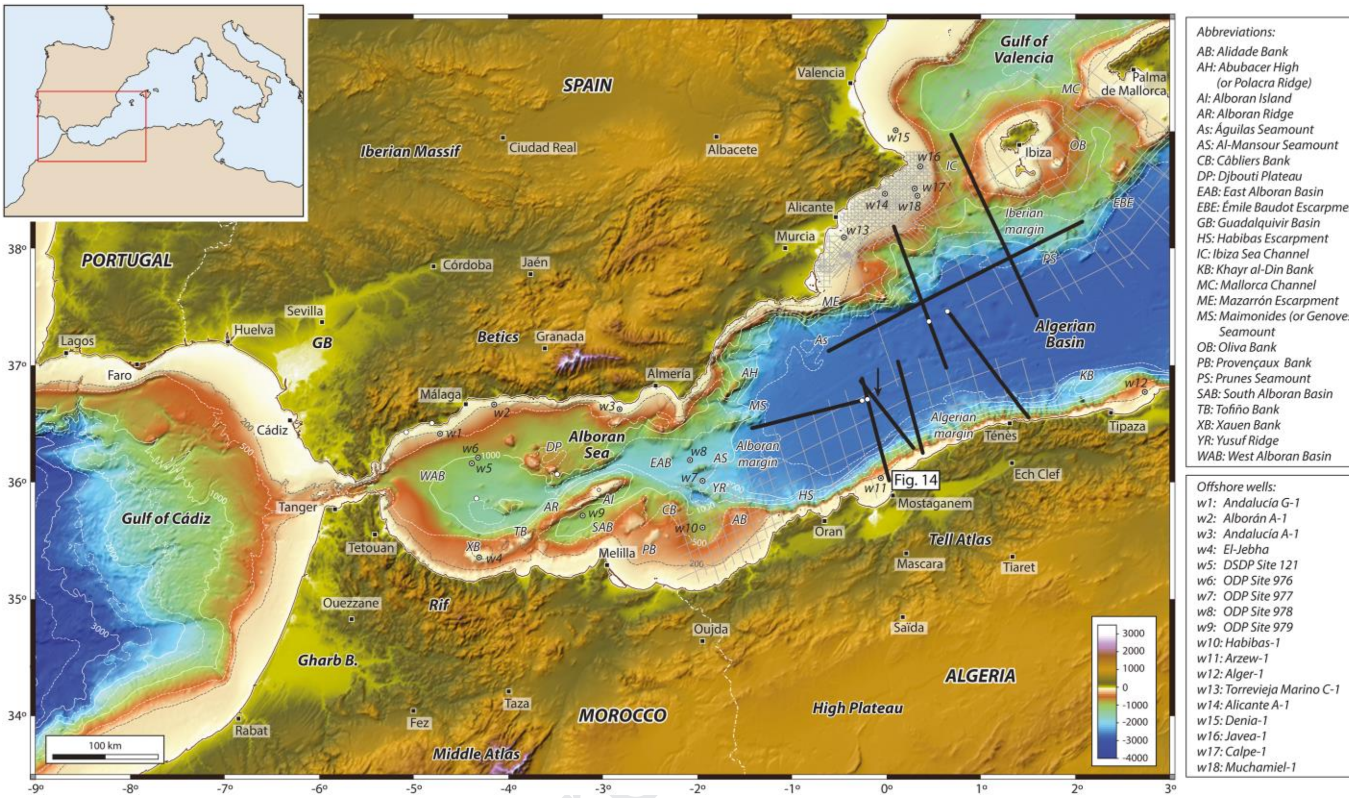

SPAIN
PORTUGAL
MOROCCO
ALGERIA
Iberian Massif
Betics
Rif
Gharb B.
Middle Atlas
Tell Atlas
High Plateau
GB
Gulf of Cádiz
Alboran Sea
Gulf of Valencia
Algerian Basin
Iberian margin
Alboran margin
Algerian margin
Fig. 14
100 km
Valencia
Ciudad Real
Albacete
Alicante
Murcia
Córdoba
Jaén
Sevilla
Huelva
Lagos
Faro
Granada
Almería
Málaga
Cádiz
Tanger
Tetouan
Ouezzane
Melilla
Oran
Mostaganem
Mascara
Tiaret
Ténès
Ech Clef
Tipaza
Ibiza
Palma de Mallorca
Oujda
Saïda
Taza
Fez
Rabat
38º
37º
36º
35º
34º
-9º
-8º
-7º
-6º
-5º
-4º
-3º
-2º
-1º
0º
1º
2º
3º
3000
2000
1000
0
-1000
-2000
-3000
-4000
Abbreviations:
AB: Alidade Bank
AH: Abubacer High (or Polacra Ridge)
AI: Alboran Island
AR: Alboran Ridge
As: Águilas Seamount
AS: Al-Mansour Seamount
CB: Cábliers Bank
DP: Djbouti Plateau
EAB: East Alboran Basin
EBE: Émile Baudot Escarpme
GB: Guadalquivir Basin
HS: Habibas Escarpment
IC: Ibiza Sea Channel
KB: Khayr al-Din Bank
MC: Mallorca Channel
ME: Mazarrón Escarpment
MS: Maimonides (or Genoves Seamount
OB: Oliva Bank
PB: Provençaux Bank
PS: Prunes Seamount
SAB: South Alboran Basin
TB: Tofiño Bank
XB: Xauen Bank
YR: Yusuf Ridge
WAB: West Alboran Basin
Offshore wells:
w1: Andalucía G-1
w2: Alborán A-1
w3: Andalucía A-1
w4: El-Jebha
w5: DSDP Site 121
w6: ODP Site 976
w7: ODP Site 977
w8: ODP Site 978
w9: ODP Site 979
w10: Habibas-1
w11: Arzew-1
w12: Alger-1
w13: Torrevieja Marino C-1
w14: Alicante A-1
w15: Denia-1
w16: Javea-1
w17: Calpe-1
w18: Muchamiel-1

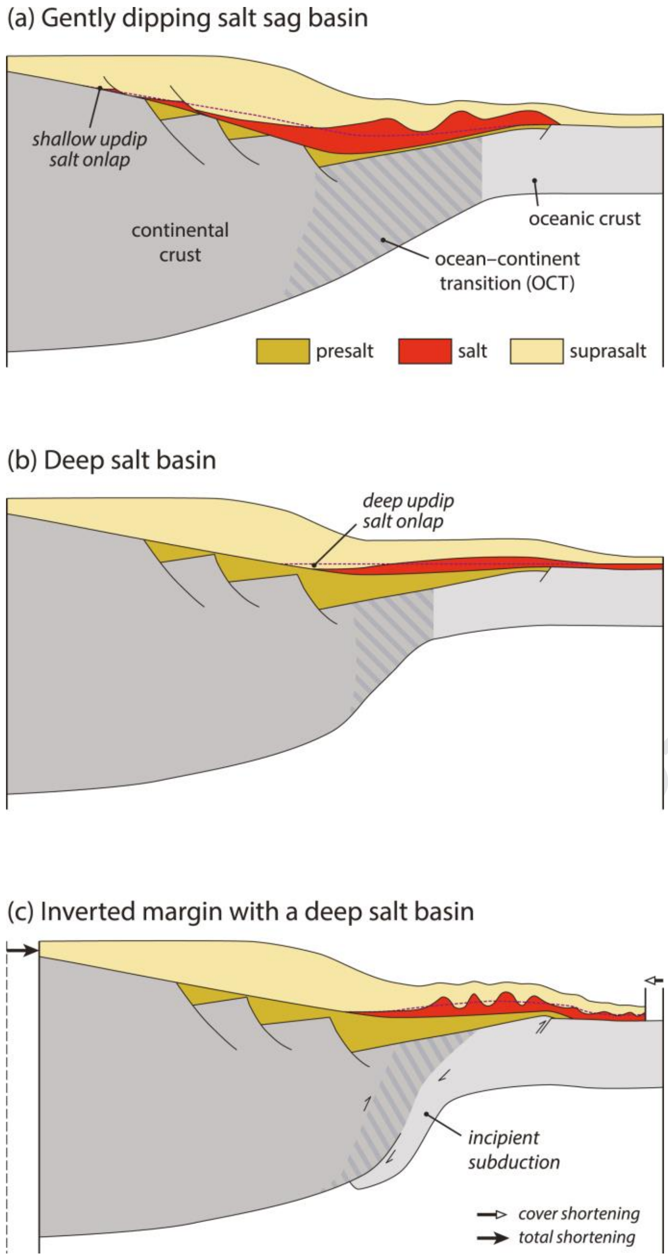
(a) Gently dipping salt sag basin
shallow updip
salt onlap
continental
crust
oceanic crust
ocean–continent
transition (OCT)
presalt
salt
suprasalt
(b) Deep salt basin
deep updip
salt onlap
(c) Inverted margin with a deep salt basin
incipient
subduction
cover shortening
total shortening

Highlights:

- Crustal structure of the W Algerian Basin is reviewed by the first time
- Seismic interpretation to unravel the crustal structures of the basin and margins
- How the Messinian salt layer is deformed in the oceanic floor of the basin
- How the deformation occurring in the margins affected the deep–seated salt layer
- Restoration to evaluate timing, magnitude, and rate of post-6 Ma deformations

Declaration of interests

☐The authors declare that they have no known competing financial interests or personal relationships that could have appeared to influence the work reported in this paper.

☒The authors declare the following financial interests/personal relationships which may be considered as potential competing interests:

Juan I. Soto reports financial support was provided by The University of Texas at Austin.